Supporting Information

$CsPbBr_3$ Perovskite Quantum Dots as Visible Light Photocatalyst for cyclisation of diamines and amino alcohols: An efficient approach to synthesize Imidazolidines, fused-imidazolidines, and Oxazolidines

Bikram Gurung, Sajan Pradhan, Debesh Sharma, Deshaj Bhujel, Siddhant Basel, Shivanand Chettri, Saragmani Rasaily, Anand Pariyar and Sudarsan Tamang*

Department of Chemistry, School of Physical Sciences, Sikkim University, Sikkim 737102, India.
*stamang@cus.ac.in

Table of Contents

1. General Information

Materials and general considerations: Cesium carbonate (Cs_2CO_3, 99.9%,), lead acetate ($Pb(OAc)_2$), oleic acid (OA, technical grade), 1-octadecene (ODE, technical grade), oleylamine (OLAM, technical grade), anhydrous toluene (99.8%,), and anhydrous hexane (95%) were all purchased from Sigma-Aldrich. Dibromoisocyanuric acid (DBI, 97%) was purchased from TCI. All of the mentioned chemical reagents were used as received without further purification. The substrates such as 1,2-diamine (**1a-i**)[1], **(3a-c)**[2], and 1,2-amino alcohol (**5a-c**)[3] for photocatalytic organic transformation were prepared by following earlier reports. Visualizations of the spots were done under a UV lamp or by blowing an I_2 stain. For purification of substrate and products, column chromatographic technique was performed using Silica gel 60–120 mesh size as eluate and the combination of ethyl acetate and petroleum ether as the eluent. Unless otherwise mentioned, all the reactions were performed in a 4 mL homeopathic vial in a pen atmosphere under the blue light considering appropriate solvents.

2. Characterization Methods

Nuclear magnetic resonance (**NMR**): ^{1}H NMR and ^{13}C NMR spectra were recorded on a Bruker ASCEND^{TM} (400 MHZ) spectrometer in $CDCl_3$ solvent. Multiplicity was indicated as follows: s (singlet), d (doublet), t (triplet), q (quartet), dd (doublet of doublet) and m (multiplet).

Blue light LED: A Kessil 160WE Tuna blue LED Light (40W) purchased from the Kessil company was used as the source of blue light. The maximum absorption wavelength and the illumination intensity of the blue LED Light are 461 nm and 0.363mW/cm^2 at a distance of 100 cm respectively.

Cyclic voltammetry (CV) measurement: The electrochemical data were collected using a BASI INC, USA/EPSILON electrochemistry workstation. The working electrode (Pt disc electrode, 1.6 mm diameter), the counter electrode (Pt wire) and the reference electrode (Ag/AgCl electrode) were used to construct a three-electrode cell employing tetrabutylammonium perchlorate (TBAP, 0.1 M) as the supporting electrolyte. Before the experiment, solution was purged with N_2 for 10 min. Experimental conditions: scan range from 1.5V to -1.5V, scan rate of 50 mV s^{-1}. The potentials obtained from CV experiments were converted to the HOMO/LUMO levels assuming the potential of ferrocene/ferrocenium (Fc/Fc^+) redox pair to be –4.80 eV as a reference from the vacuum level. The formal redox potential of Fc/Fc^+ couple (reference) *vs* Ag/AgCl in acetonitrile and 1:4 v/v mixture of acetonitrile and toluene using 0.1 M TBAP as supporting electrolyte were 0.42 and 0.48 V respectively. The energy levels (eV) were estimated from $-E_{HOMO/LUMO} = E^{redox}$ (*vs* Ag/AgCl) + 4.44 eV = E^{redox} (*vs* Fc/Fc^+) + 4.8 eV.[4–6] For model substrates, E_{HOMO} = [-e(E_{ox} -0.42 + 4.8)] eV and for photocatalyst, E_{HOMO} = [-e(E_{ox} -0.48 + 4.8)] eV; E_{LUMO} = [-e(E_{red} -0.48 + 4.8)] eV.

UV-Vis spectrophotometer: The UV-Visible absorption spectra were collected using Perkin Elmer spectrophotometer and Agilent Technologies Cary 100 UV-vis.

Vis-NIR spectrofluorometer: The PL spectra of $CsPbBr_3$ NCs were collected using a HORIBA Scientific spectrophotometer (Model: PTI-QM 510). A Fluorometer with XM- Xenon coupled monochromatic source were used to determine the quantum yield of the photochemical reaction.

Transmission electron microscopy (**TEM**): TEM images were taken in the JEOL-JEM-2100 Plus electron microscope. HRTEM images were obtained using a 200 kV electron source. Samples were prepared by drop-casting of nanocrystal solution in hexane on carbon-coated copper grid purchased from EMS, the grids were kept overnight in a vacuum desiccator. The average particle size was measured using 150 particles. The lattice plane was obtained from lattice fringes. Image J software was used for calculations.

Fourier Transform Infrared Spectroscopy (FTIR): FTIR spectra were obtained using Bruker ALPHA E, 200396.

X-ray Diffractometer Analysis: The purified **QDs** in hexane were drop-casted on a clean and dry glass slide. Powder X-ray Diffraction (PXRD) analysis of prepared sample was run under the Pananalytical X-Ray diffractometer using Cu Kα (λ= 1.54 Å) as the incident radiation (40 kV and 30 mA). Single-crystal X-Ray diffraction (SCXRD) intensity data were collected using Super Nova Agilent Technology, a single crystal diffractometer.

Inductively coupled plasma-mass-spectrometry (ICP-MS): The dissolved QDs in reaction solvent was diluted with millipore water in tube. ICP-MS technique for to determine the dissolved ions concentration were performed under Agilent 7800 ICP-MS.

X-ray Photoelectron Spectroscopy (XPS): XPS samples containing halides ions were prepared on gold foil and placed inside the petri–disc. It was degassed in a vacuum-oven at room temperature under pressure of 700 mm Hg. XPS spectra were obtained using Thermo-Scientific NEXSA spectrometer with Al Kα (1486.7 eV) X-ray source. Percentage atomic concentration (A%) of Cs, Pb, Br and N were determined from the survey data using CASA XPS. The software computes A% from the peak area after correcting the corresponding sensitivity factors. Relative sensitivity factors (RSF) used for Pb 4f, Cs 3d and Br 3p are 22.74, 40.22 and 5.03 respectively.

3. Experimental Details

Synthesis of $CsPbBr_3$ colloidal QDs: Cs-oleate solution was prepared by dissolving 0.8125 g (2.5 mmol) of Cs_2CO_3 in 20 mL ODE and 2.5 mL OA. The solution was degassed at room temperature (rt) for 15 min, followed by degassing at 120 °C under a vacuum until a clear solution was obtained. The solution was stored in N_2 atmosphere (in schlenk line) at 100 °C for further use.

0.0325 g (0.1 mmol) of lead acetate, 0.3 mL OA, 0.5 mL of OAm, 0.0834 g (0.3 mmol) of DBI and 4 mL of ODE were mixed and degassed under vacuum at RT for 30 min, followed by degassing under vacuum at 120 °C for 60 min. Subsequently, the temperature was increased to 200 °C under an inert (N_2) atmosphere. To this solution, 0.4 mL of Cs-oleate solution was quickly injected. The reaction was quenched immediately by immersing the reaction flask in icebath. The green emiting colloidal solution was formed. The crude colloidal **QDs** were purified using

centrigfucation to obtain powdered form of **QDs**. It was stored in N_2 atmosphere (in schlenk line) further use in photocatalysis.

Purification: To 4 mL of the freshly prepared **QDs** in ODE dry toluene was added [1:1 (*v/v*)] and centrifuged at 500 rotation per minute (rpm) for 2 minutes. The precipitate was discarded to remove unreacted DBI. The supernatant was further centrifuged at 6000 rpm for 10 min. The precipitate was collected and dried.

4. Temperature-dependent size-tunability

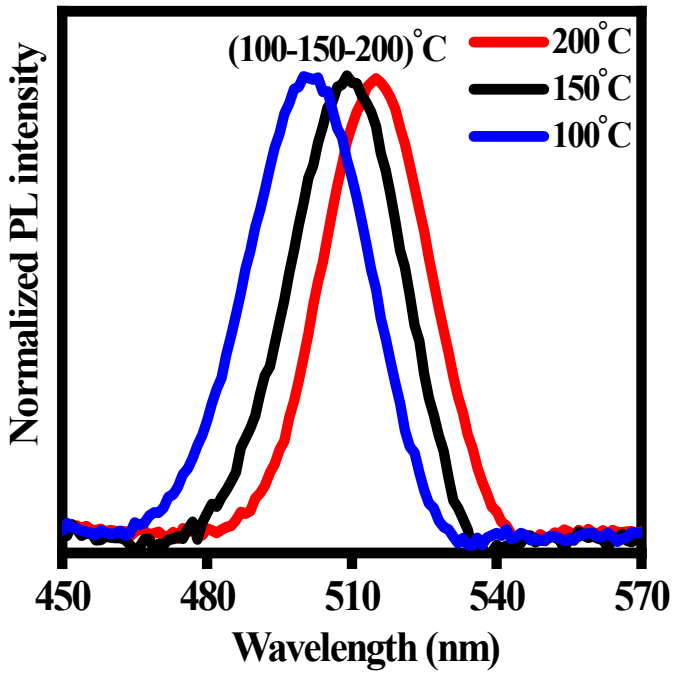

Figure S1. The size-tunable emission spectrum of **QDs** prepared at 100 ˚C (blue), 150 ˚C (red) and 200 ˚C (black) excited at 400 nm.

5. Photoluminescence Quantum Yield (PLQY) determination:

The relative PLQY of the **QDs** was determined using Rhodamine 6G as a reference compound.[7] The absorption and emission spectrum of both **QDs** and reference compound rhodamine 6G were determined at different concentrations (Figure S4). The slopes of emission intensity vs absorption (at excitation wavelength = 480 nm) were obtained and compared.

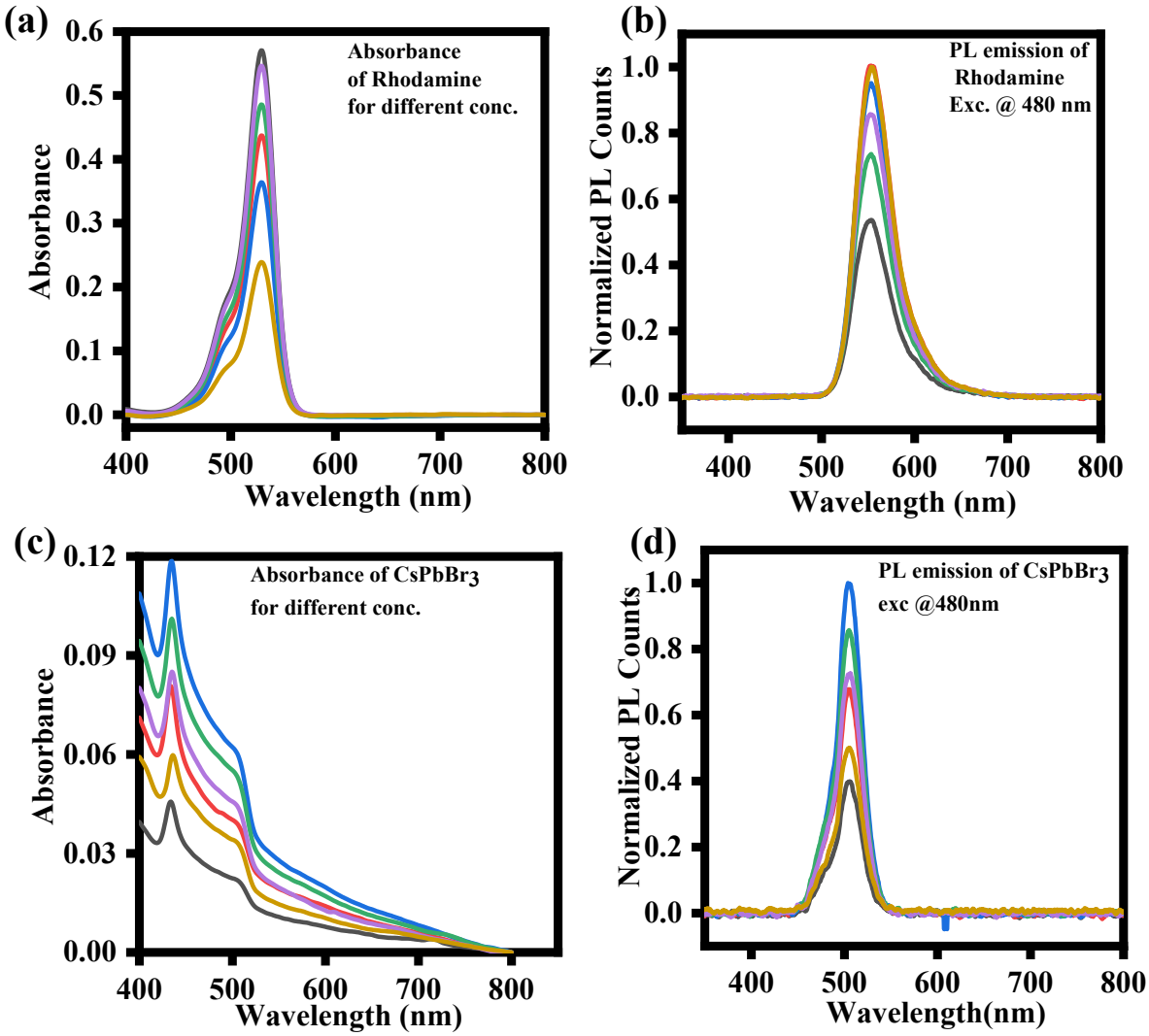

Figure S2: (a) UV-Visible spectra and (b) PL emission spectra of rhodamine 6G at different concentrations (excitation wavelength 480 nm). (c) UV-Visible spectra and (b) PL emission spectra of $CsPbBr_3$ **QDs** at different concentrations (excitation wavelength 480 nm).

PLQY was determined with the help of the following equation:

where,

$$Relative\ quantum\ yield\ (\phi) = \phi_{ref} \times \frac{m_{QDs}}{m_{ref}} \times \left(\frac{\eta_{QDs}}{\eta_{ref}}\right)^2$$

$\phi_{ref} =$ quantum yield of reference = 0.95 (in ethanol when excited at 480 nm)

$m_{QDs} =$ gradient of **QDs**

$m_{ref} =$ gradient of reference

$\eta_{QDs} =$ refractive index of solvent used to disperse **QDs**

$\eta_{ref} =$ refractive index of solvent used to dissolve reference compound

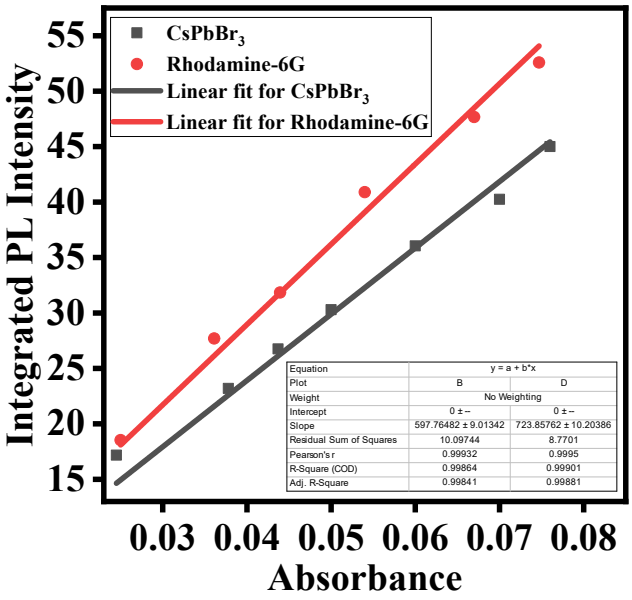

Figure S3: Linear fit of PL intensity vs absorbance (at 480 nm) of $CsPbBr_3$ **QDs** (black) and rhodamine 6G reference compound (red). The slopes of **QDs** and Rhodamine are 597.76 and 723.85 respectively.

6. Characterization of QDs:

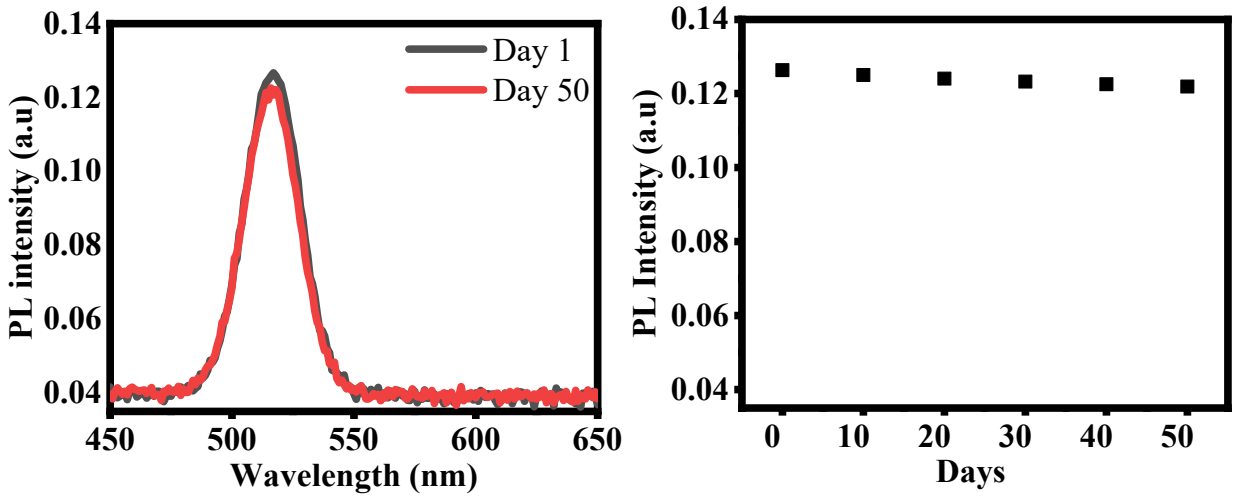

Figure S4. (a) The PL spectra of **QDs** dispersed in hexane for day 1 (black) and day 50 (red) (b) The temporal evolution of PL intensity of the QDs over 50 days.

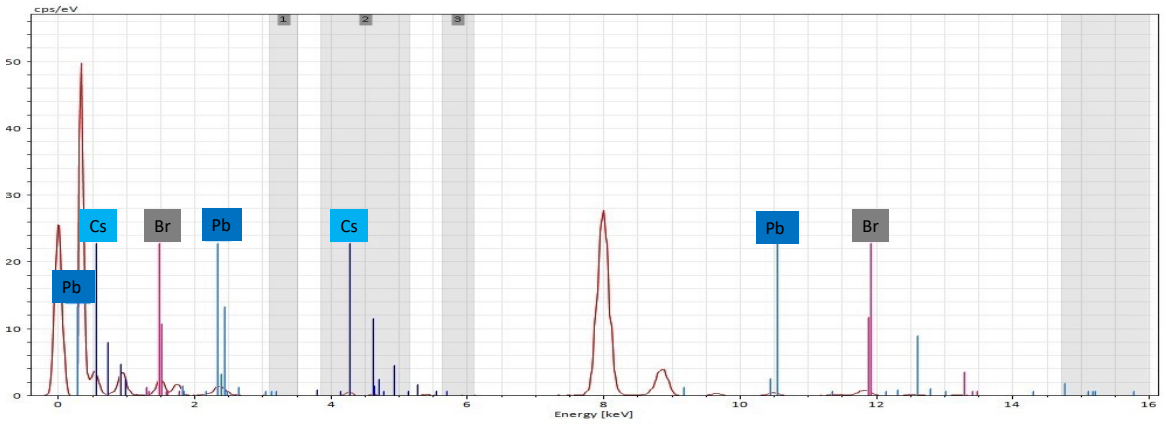

Element	At. No.	Netto	Mass [%]	Mass Norm. [%]	Atom [%]	Abs. Error [%] (1 sigma)	Rel. Error [%] (1 sigma)
Bromine	35	2444	40.94	40.94	58.66	1.54	3.77
Lead	82	1624	30.88	30.88	17.07	3.28	10.61
Cesium	55	2314	28.18	28.18	24.28	2.95	10.48
		Sum	**100.00**	**100.00**	**100.00**		

Figure S5. EDX spectrum of $CsPbBr_3$ **QDs.**

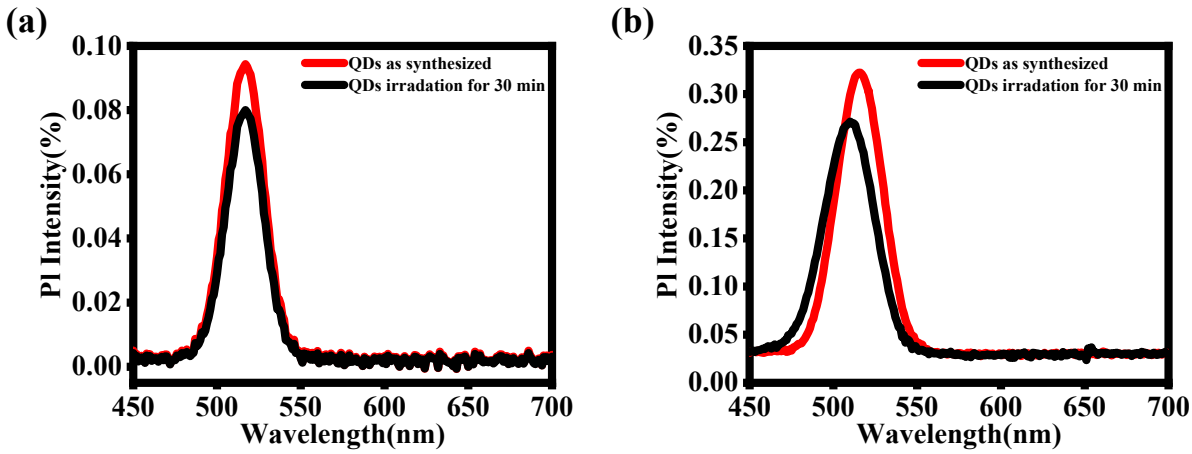

Figure S6. (**a**) PL spectra of **QDs** in DCE before (black) and after blue LED irradiation (red) for 30 min. (b) PL spectra of **QDs** in DCM before (black) and after blue LED irradiation (red) for 30 min.

7. Comparative study of photocatalytic performance of QDs with conventionally prepared CsPbBr3 QDs:

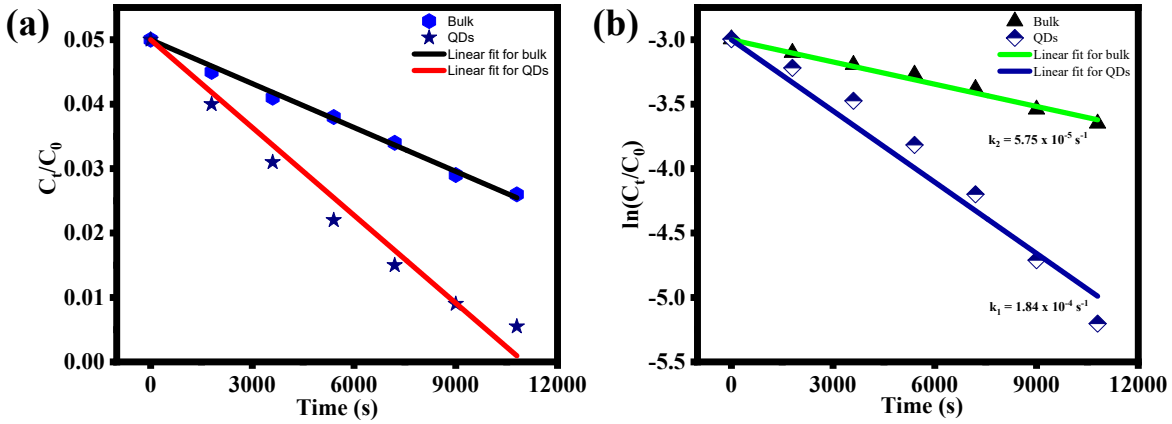

Figure S7: (a) A linear fit plot of C_t/C_0 versus reaction time (s) using photocatalyst **QDs** (red line) and conventionally prepared perovskites **QDs** (black line). (b) Rate constants of **QDs** ($k_1 = 1.84 \times 10^{-4}\, s^{-1}$) and conventionally prepared perovskites **QDs** ($k_2 = 5.75 \times 10^{-5}\, s^{-1}$) catalyzed sp^3 C-H functionalization of **3a** obtained through a plot of $\ln(C_t/C_0)$ versus time.

8. Catalyst recyclability test

The catalyst recyclability test was performed following the reported literature protocol.[8] In a 4 mL glass vial, **QDs** (1 mg), **3a** (0.1 mmol) and 3 mL 1,2-dichloroethane (DCE) were mixed together. The mixture was irradiated with the blue LED for 3 h. The distance between the LED source and the vial was 6 cm. The product yield was calculated from ^{1}H-NMR using trimethoxybenzene as an internal standard. The yield of the corresponding C-H functionalized product **4a** for the 1st cycle was 89%. For the 2nd cycle, 0.1 mmol of **3a** was added into the same glass vial (without adding extra catalyst) and irradiated with the blue light for another 3 h. The overall yield for the 2nd cycle was 82 %. The above step was repeated for the 3rd (yield 69 %) and 4th cycle (yield: 66%)

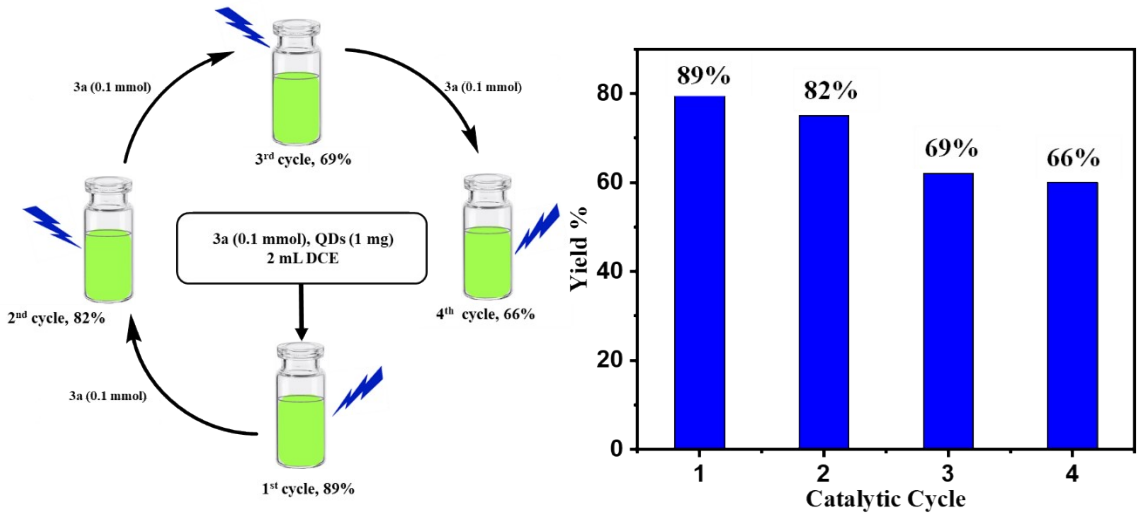

Figure S8. (a) Scheme for the recyclability test of **QDs** for the C-H amination of **3a. (b)** Yield % vs number of cycle plot.

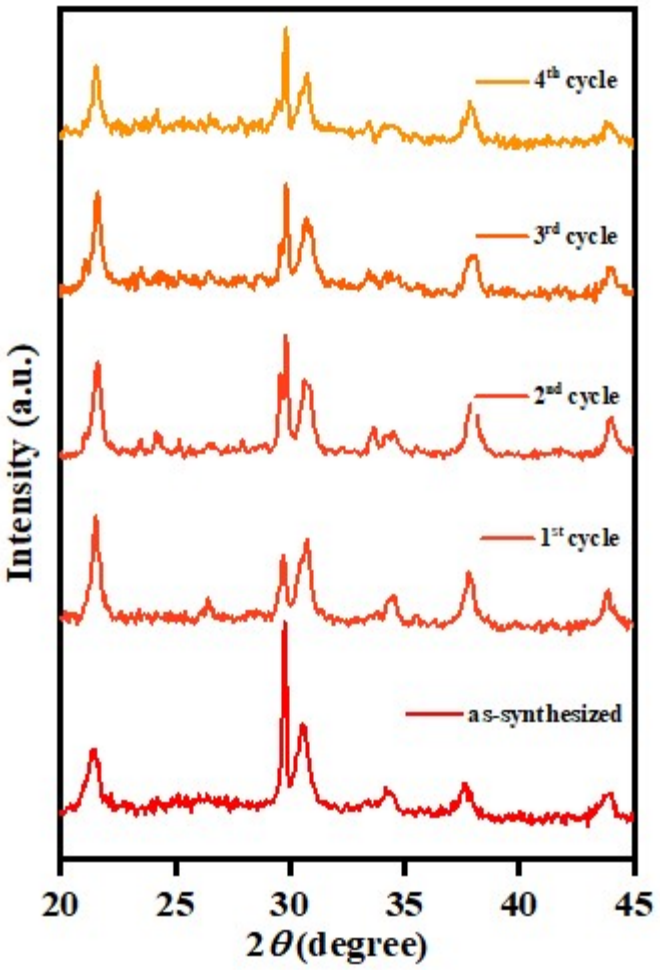

Fig S9: Powder X-ray diffraction (PXRD) patterns of $CsPbBr_3$ QDs after every catalytic cycle. It retains its orthorhombic phase in every cycle.

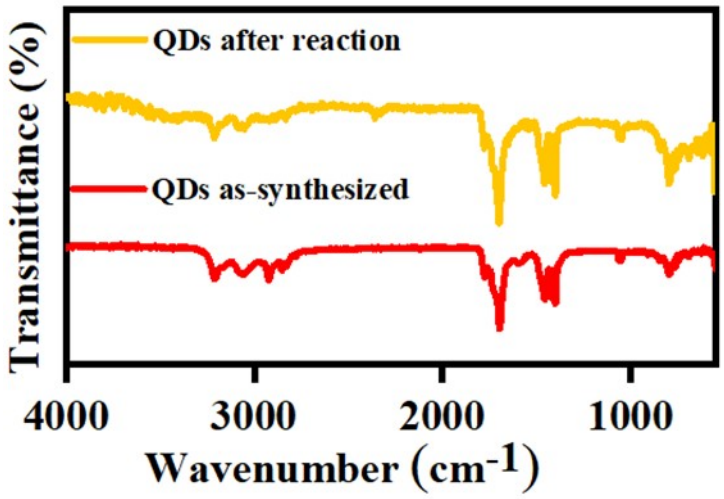

Fig S10: FTIR spectra of QDs before and after reaction.

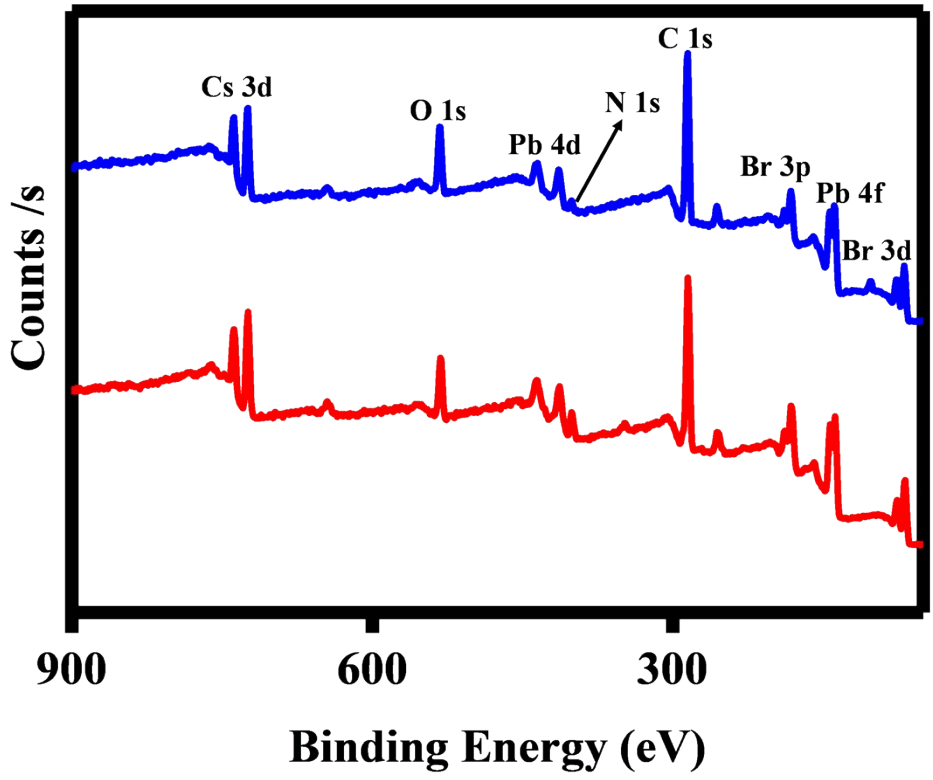

Quantitative analysis (After catalysis)	
Element	Atomic %
Cs	18.76
Pb	19.62
Br	61.63

Quantitative analysis (Pristine)	
Element	Atomic %
Cs	16.90
Pb	20.65
Br	62.45

Fig S11: XPS survey spectra of $CsPbBr_3$ **QDs** before (red) and after (blue) photocatalysis with retention of structural integrity. Inset: quantitative analysis of pristine **QDs** (red) and **QDs** after catalysis (blue).

9. Determination of catalyst digestion:

In a 4 mL glass vial, **3a** (0.1 mmol) and $CsPbBr_3$ **QDs** (1mg) were dissolved in 3 mL 1,2-dichloroethane (DCE) and stirred under the photo-irradiation of Blue LED in the air at room temperature for 3h. After the reaction, QDs were removed by centrifugation (~10000 rpm) followed by filtration (~0.22 μm). The 20 μL of the filtrate were diluted with 15 mL of water and performed ICP-MS analysis. The ICP-MS results are shown in the following Table S1, The concentrations of Pb and Cs were 0.44×10^{-5} mol/L and 0.39×10^{-5} mol/L respectively.

Table S1: ICP-MS result. Amount of QDs in the reaction mixture before the reaction was 1 mg in 3 mL.

Filtrate (μL)	**Dilution (mL)**	**Pb ion concentration after the (ppb)**	**Pb ion concentration (mol/L)**	**Cs ion concentration (ppb)**	**Cs ion concentration (mol/L)**
20	**15**	**5.9**	0.44×10^{-5}	**5.3**	0.39×10^{-5}

10. Calculation of the Turnover Number (TON):

a) For a 0.1 mmol scale reaction using 1.0 mg QDs we obtained 89%, 82%, 69%, 66% yields in 1st, 2nd, 3rd and 4th cycle respectively. The TON for conversion of **3a** to **4a** was calculated using the equation

$$TON = \frac{total\ mol\ of\ produt\ 3a\ in\ 4\ cycles}{total\ mol\ of\ catalyst\ employed}$$

$$= \frac{\{0.1\ mmol \times (0.89 + 0.82 + 0.69 + 0.66)\}}{(1.0\ mg \div 579.8\ g\ mol^{-1})} \approx 177$$

11. Procedure for gram-scale synthesis:

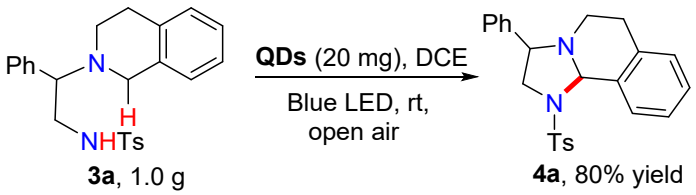

3a, 1.0 g — **4a**, 80% yield

3a (2.46 mmol, 1g) was dissolved in DCE (20 ml) with catalyst loading of 20 mg at room temperature. The reaction was set at a distance of 6 cm away from Blue LED with continuous stirring. The progress of the reaction was monitored by TLC. The product **4a** obtained was isolated using Column Chromatography (ethyl acetate: pet ether ~5:95). The isolated yield is reported.

12. Copies of Cyclic voltammogram (CV) spectra:

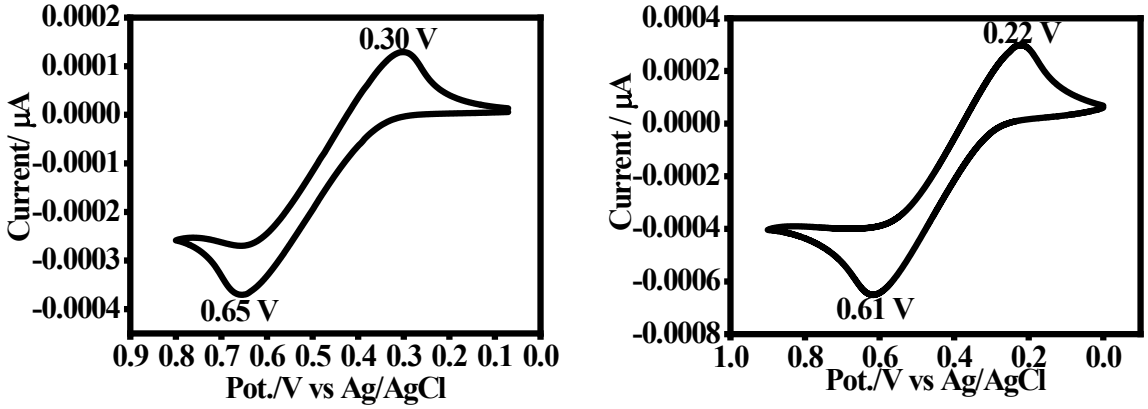

Figure S12. CV spectra of ferrocene/ferrocenium (Fc/Fc^+) redox pair using TBAP (0.1 M) as a supporting electrolyte: (a) in N_2 saturated CH_3CN (for organic substrate), E_{redox} = 0.42 V *vs* Ag/AgCl and (b) in N_2 saturated 1:4 v/v of CH_3CN and toluene (for **QDs**), E_{redox} = 0.48 V *vs* Ag/AgCl.

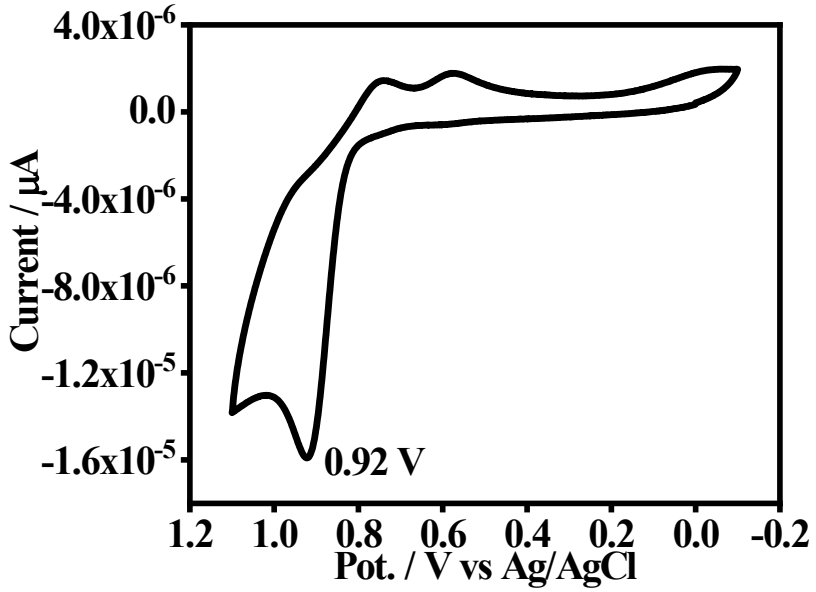

Figure S13. CV spectra of **1a** [(4-methyl-*N*-(2-(methyl(phenyl)amino)-2-phenylethyl)-benzenesulfonamide] using TBAP (0.1 M) as electrolyte in N_2-saturated CH_3CN. E_{ox} = 0.92 V *vs* Ag/AgCl.

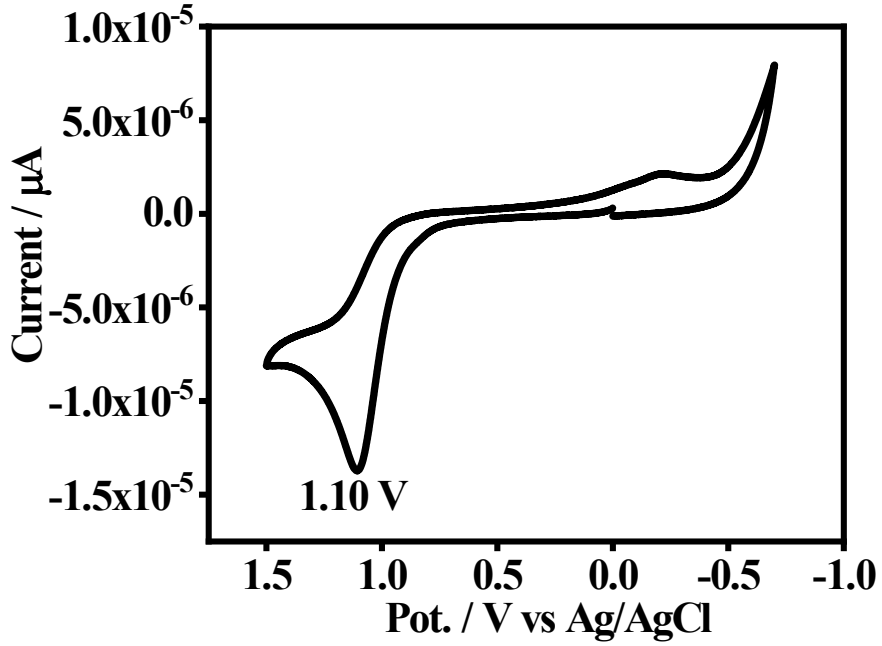

Figure S14. CV spectra of **3a** [*N*-(2-(3,4-dihydroisoquinolin-2(1*H*)-yl)-2-phenylethyl)-4-methylbenzenesulfonamide] using TBAP (0.1 M) as electrolyte in N_2-saturated CH_3CN. E_{ox} = 1.10 V *vs* Ag/AgCl.

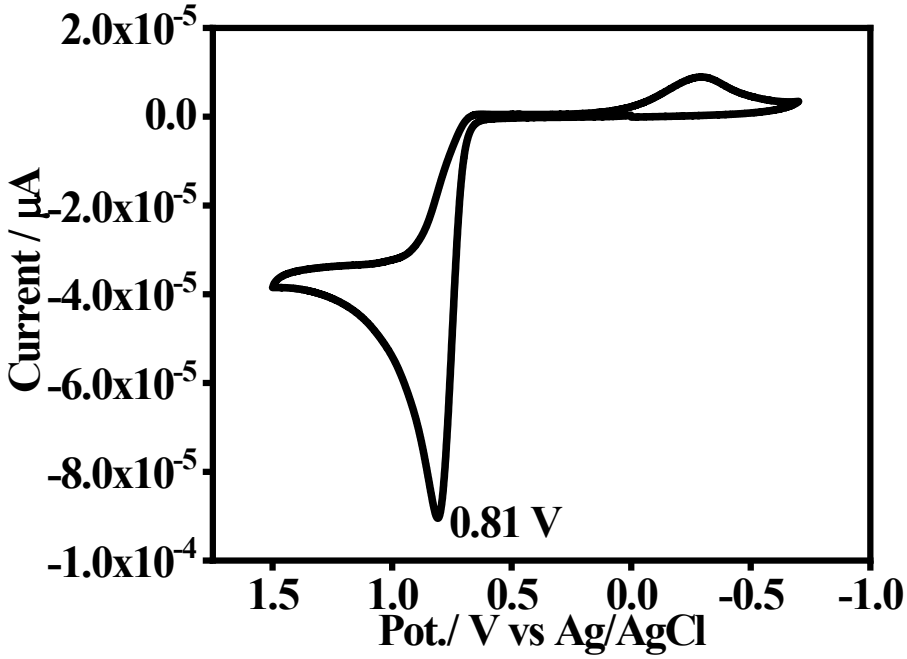

Figure S15. CV spectra of (2-(methyl(phenyl)amino)-2-phenylethan-1-ol **5(a)** using TBAP (0.1 M) in N_2 saturated CH_3CN. E_{ox} = 0.81 V *vs* Ag/AgCl.

13. Photoluminescence quenching experiment:

The hole-accepting property of the substrate was examined using the Stern-Volmer equation[9],

$$I_0/I = 1 + K_{sv}[Q]$$

where I_0 and I are the PL maxima in the absence and presence of the quencher [Q] respectively. The slope of [I_0/I - 1] vs [Q] plot gives the value of the Stern-Volmer quenching constant (K_{sv}). The quenching constant (K_{sv}) was calculated using the Stern-Volmer equation[9],

$$I_0/I = 1 + K_{sv}[Q]$$

1 mg of **QDs** was dispersed in 3 mL DCE. **1a** was progressively added and PL maxima was monitored.

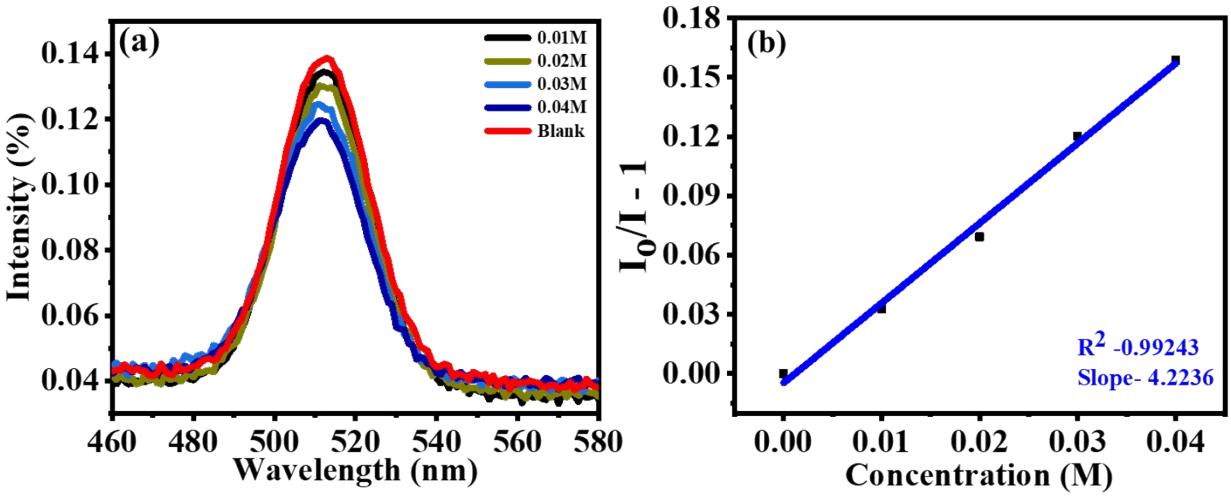

Figure S16. (a) The gradual quenching of PL of **QDs** (Excitation: 400 nm). with the increase of fluorophore **(1a)** concentration [0.01 to 0.04 M]; (b) Stern-Volmer plot (k_{sv} = 4.2236 $M^{-1}s^{-1}$).

14. Superoxide radical anion ($O_2^{\bullet-}$) detection study:

Benzoquinone (BZ) is a well-known superoxide radical anion ($O_2^{\bullet-}$) scavenger.[10–12] A controlled experiment was performed by adding benzoquinone to the optimized reaction solution. The photocatalytic reaction is significantly inhibited resulting in traces amount of product monitored by TLC.

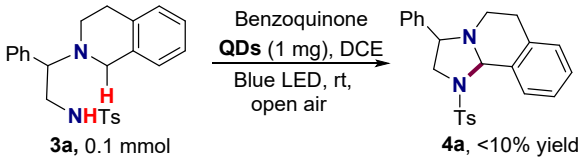

3a, 0.1 mmol **4a**, <10% yield

$O_2^{\bullet-}$ ion were detected by applying a standard analytical method in the presence of benzoquinone.[13,14] Briefly, to a solution of 5 mg benzoquinone in 3 mL DCE, $CsPbBr_3$ **QDs** (1 mg) was added. The solution was then irradiated under a blue LED with constant stirring in the open air and at room temperature. 10 mL of aliquots were added to 3mL solvent (hexane) and UV-visible absorption spectra were recorded after every 10 minutes of photo-irradiation. The *in-situ* generated $O_2^{\bullet-}$ ion in the solution reacts with benzoquinone and transformed it into hydroquinone (HQ) with the emergence of the characteristic absorption peak at 386 nm.

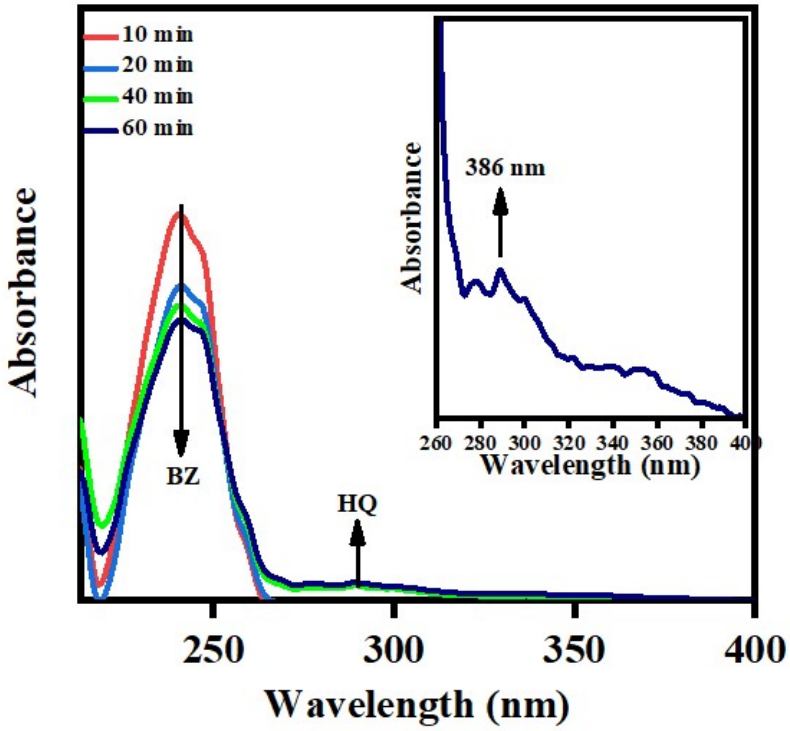

Figure S17. UV–Vis spectra for the detection of superoxide ions. The graph represents the temporal diminishing of benzoquinone (BZ) peak at 246 nm and the emergence of hydroquinone (HQ) peak at around 386 nm with reaction time (10- 60 min); Inset: UV-Vis spectra magnified around 260 nm to 350 nm depicting the formation of hydroquinone.

15. Intermediate trapping experiment:

To a vial containing 3mL DCE, 0.1 mmol of 3a, 0.2 mmol of TEMPO and 1mg of photocatalyst QDs were added. The solution was then kept under blue LED with constant stirring in open air and at room temperature. After 1h of continuous irradiation, aliquots of reaction mixture were taken out and performed ESI-MS characterization. The mass spectroscopy of TEMPO- trapped intermediate **I** *via* amino-radical was analysed in reaction solution.

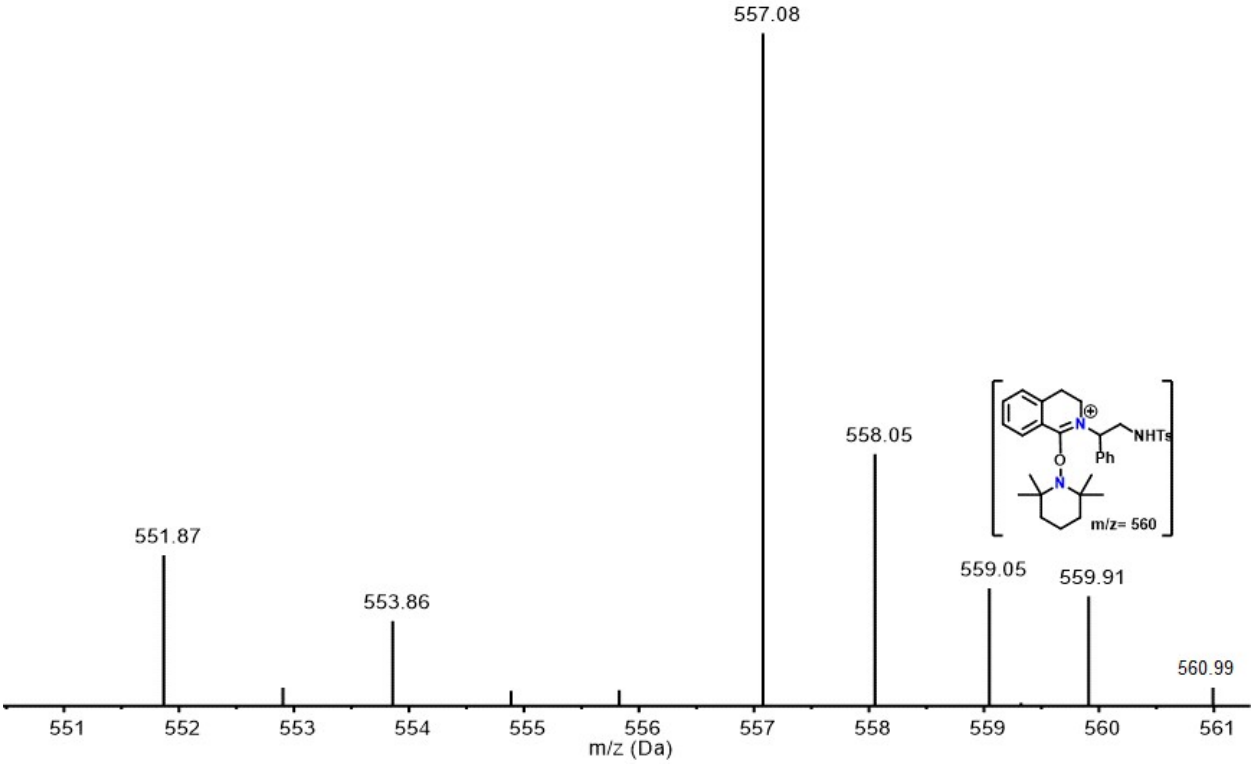

Figure S18: ESI-MS spectra of TEMPO trapped reaction mixture.

16. H_2O_2 detection study:

A saturated solution of KI was prepared in acetonitrile. 0.4 mL of the 2h reaction mixture (C-H amination of **3a)** was taken out in a clean vial. 2.6 mL of KI solution was added to it followed by a few drops of glacial acetic acid (17.4 N). The H_2O_2 present in the reaction mixture reacts with the iodide ion to generate a triiodide ion, which has a characteristic peak at 360 nm.[15] Controlled experiments were performed using blank aliquot, KI solution and KI+H_2O_2 (commercially available).

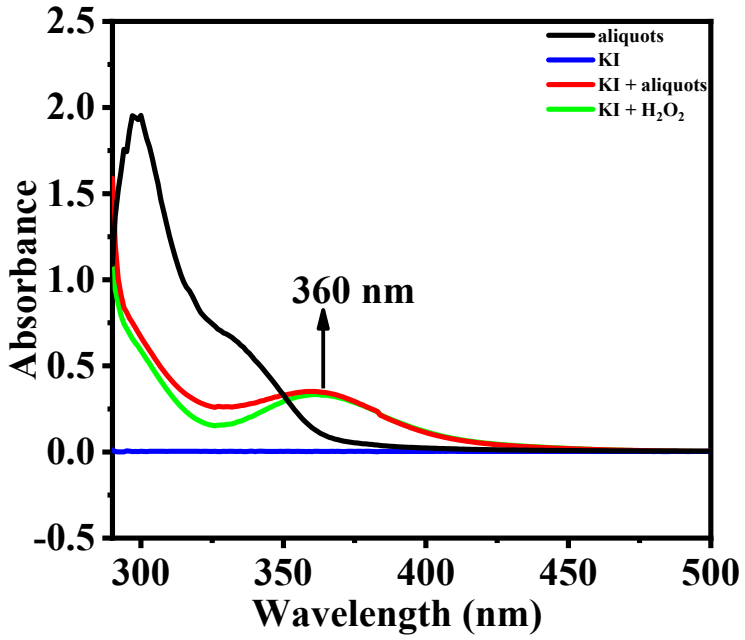

Figure S19. UV–Visible spectra for the detection of H_2O_2. Pure saturated KI solution (blue), KI solution + aliquots of reaction mixture of **3a** (red), KI + 30 % H_2O_2 (green) and aliquots of reaction mixture in solvent (CH_3CN).

17. Computational Studies:

The computational studies were performed by using Gaussian 09 software.[16,17] Dispersion corrected M06-2X DFT functional and basis set with one diffuse and two polarization functions, M06-2X/6-311+G(d,p) were used for optimization of all reactants, intermediates, transition states and product.[16] The vibrational frequencies calculation were also performed under the same functions and basis sets to verify that the transition state structures have only one imaginary frequency while the optimized intermediates and final product structures have only positive frequencies. The free energies (ΔG) were calculated using the zero-point energy corrected Gibbs free energy at 298.15 K (Sum of Thermal and Free Energies in Gaussian Output).

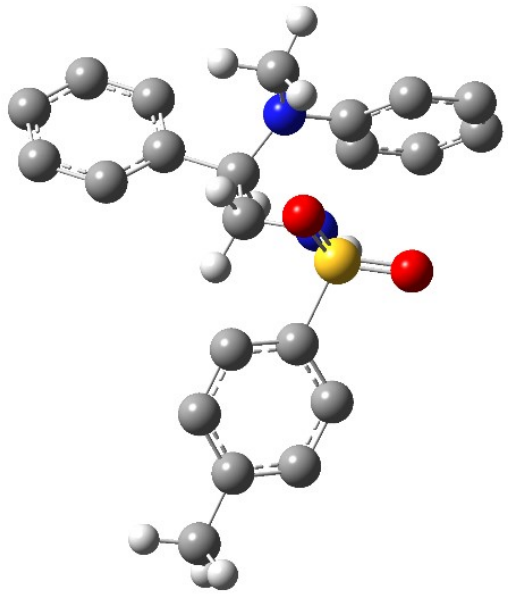

I

Center Number	Atomic Number	Atomic Type	Coordinates (Angstroms) X	Y	Z
1	6	0	6.587966	-2.193654	0.193500
2	6	0	5.308307	-1.407017	0.124498
3	6	0	5.137055	-0.418675	-0.850973
4	6	0	3.979085	0.341840	-0.905915
5	6	0	2.976450	0.098125	0.028735
6	6	0	3.117917	-0.869164	1.017385
7	6	0	4.287585	-1.617428	1.054259
8	16	0	1.471614	1.023766	-0.073589
9	8	0	0.782656	0.916003	1.203283
10	8	0	1.740975	2.298512	-0.696538
11	7	0	0.470995	0.224366	-1.155355
12	6	0	-0.287211	-0.949459	-0.751216

13	6	0	-1.786094	-0.594604	-0.632396
14	6	0	-2.717149	-1.774669	-0.421844
15	6	0	-2.256834	-3.065534	-0.171419
16	6	0	-3.163154	-4.108379	0.005474
17	6	0	-4.529322	-3.866451	-0.061394
18	6	0	-4.994607	-2.577546	-0.310311
19	6	0	-4.092019	-1.539009	-0.492074
20	7	0	-1.954880	0.395971	0.452114
21	6	0	-1.944771	1.730029	0.245596
22	6	0	-2.034492	2.617959	1.365473
23	6	0	-1.971367	3.975275	1.184593
24	6	0	-1.823660	4.515411	-0.101462
25	6	0	-1.754486	3.667919	-1.213352
26	6	0	-1.818059	2.305202	-1.059738
27	6	0	-1.957526	-0.137195	1.820077
28	1	0	7.349128	-1.624362	0.733762
29	1	0	6.444898	-3.139731	0.715386
30	1	0	6.976541	-2.400915	-0.804217
31	1	0	5.929339	-0.235353	-1.568129
32	1	0	3.859362	1.128088	-1.642348
33	1	0	2.340529	-1.007960	1.758986
34	1	0	4.415628	-2.368422	1.825548
35	1	0	0.861186	0.212387	-2.090743
36	1	0	-0.181387	-1.732386	-1.504083
37	1	0	0.086112	-1.341249	0.199062
38	1	0	-2.082815	-0.115923	-1.561961
39	1	0	-1.195810	-3.279052	-0.110646
40	1	0	-2.797055	-5.109796	0.195199

41	1	0	-5.231504	-4.679360	0.076216
42	1	0	-6.058691	-2.385021	-0.369928
43	1	0	-4.456080	-0.535648	-0.694092
44	1	0	-2.139813	2.223753	2.364719
45	1	0	-2.028597	4.631886	2.043153
46	1	0	-1.764733	5.588441	-0.234156
47	1	0	-1.638537	4.086213	-2.204627
48	1	0	-1.736976	1.683214	-1.935850
49	1	0	-1.135827	0.309433	2.377614
50	1	0	-2.917402	0.069351	2.297436
51	1	0	-1.826837	-1.214198	1.774864

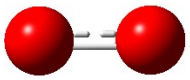

Superoxide anion ($O_2^{\bullet -}$)

Center Number	Atomic Number	Atomic Type	Coordinates (Angstroms) X	Y	Z
1	8	0	0.000000	0.000000	0.660945
2	8	0	0.000000	0.000000	-0.660945

.

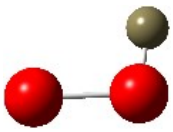

HO_2^- anion

Center Number	Atomic Number	Atomic Type	Coordinates (Angstroms) X	Y	Z
1	8	0	0.055465	0.795451	0.000000
2	8	0	0.055465	-0.687380	0.000000
3	1	0	-0.887436	-0.864569	0.000000

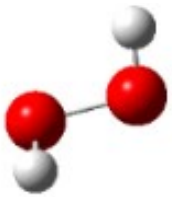

H_2O_2

Center Number	Atomic Number	Atomic Type	Coordinates (Angstroms) X	Y	Z
1	8	0	-0.701895	0.119161	-0.053213
2	1	0	-1.025353	-0.652562	0.425707
3	8	0	0.701894	-0.119162	-0.053212
4	1	0	1.025354	0.652570	0.425691

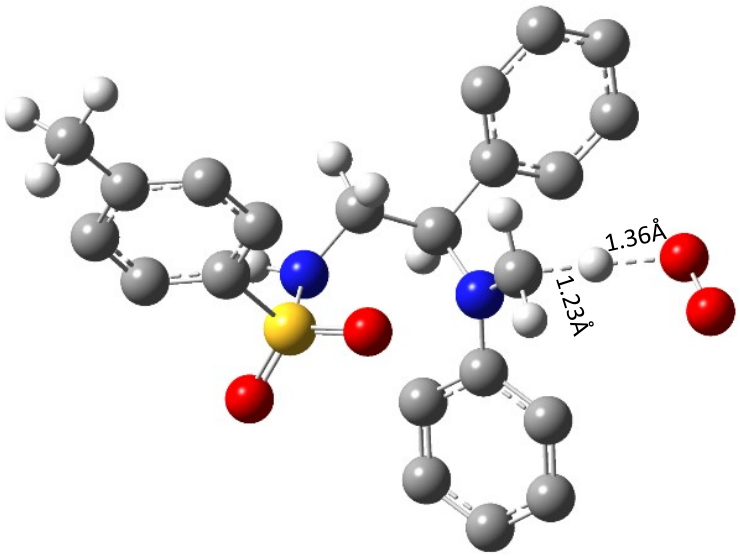

TS-I

Center Number	Atomic Number	Atomic Type	Coordinates (Angstroms) X	Y	Z
1	6	0	7.063810	-1.700498	0.714348
2	6	0	5.752634	-0.995552	0.493956
3	6	0	5.643729	0.004117	-0.483694
4	6	0	4.451971	0.688738	-0.681985
5	6	0	3.351149	0.357095	0.108916
6	6	0	3.427138	-0.622963	1.095383
7	6	0	4.632993	-1.294792	1.277424
8	16	0	1.818259	1.193142	-0.175342
9	8	0	0.962686	0.990692	0.990377
10	8	0	2.087792	2.504416	-0.729937
11	7	0	1.023437	0.368804	-1.409903
12	6	0	0.307576	-0.861827	-1.118513
13	6	0	-1.215771	-0.629156	-1.079086
14	6	0	-2.055443	-1.893310	-0.984439
15	6	0	-1.509128	-3.140985	-0.678447
16	6	0	-2.339367	-4.258106	-0.571156
17	6	0	-3.712503	-4.131572	-0.758812
18	6	0	-4.262440	-2.885213	-1.063754
19	6	0	-3.436676	-1.772797	-1.179197
20	7	0	-1.577266	0.259971	0.074539
21	6	0	-1.986907	1.585171	-0.130730
22	6	0	-2.836978	2.197239	0.814406
23	6	0	-3.208858	3.519448	0.638987

24	6	0	-2.739401	4.243081	-0.460345
25	6	0	-1.899715	3.634837	-1.396165
26	6	0	-1.529905	2.307554	-1.250982
27	6	0	-1.577803	-0.282955	1.294910
28	1	0	7.761904	-1.044801	1.244420
29	1	0	6.934695	-2.605941	1.310012
30	1	0	7.526973	-1.974258	-0.236838
31	1	0	6.511202	0.257136	-1.086573
32	1	0	4.377093	1.484779	-1.416668
33	1	0	2.569769	-0.827285	1.728665
34	1	0	4.709719	-2.053448	2.050632
35	1	0	1.553365	0.387152	-2.276369
36	1	0	0.499138	-1.589106	-1.911890
37	1	0	0.652244	-1.300794	-0.174783
38	1	0	-1.508405	-0.082610	-1.975839
39	1	0	-0.440948	-3.266008	-0.528170
40	1	0	-1.907712	-5.226045	-0.339796
41	1	0	-4.354674	-5.001460	-0.671874
42	1	0	-5.331371	-2.782642	-1.217251
43	1	0	-3.865868	-0.802717	-1.424007
44	1	0	-3.238351	1.636861	1.650975
45	1	0	-3.878006	3.983865	1.354534
46	1	0	-3.032857	5.279388	-0.589997
47	1	0	-1.518201	4.202615	-2.237137
48	1	0	-0.826893	1.864597	-1.944467
49	1	0	-1.471281	0.399431	2.143513
50	1	0	-2.732052	-0.610821	1.573824
51	1	0	-1.120714	-1.269299	1.364761
52	8	0	-3.825980	-0.726986	2.378556
53	8	0	-3.600089	0.112428	3.380653

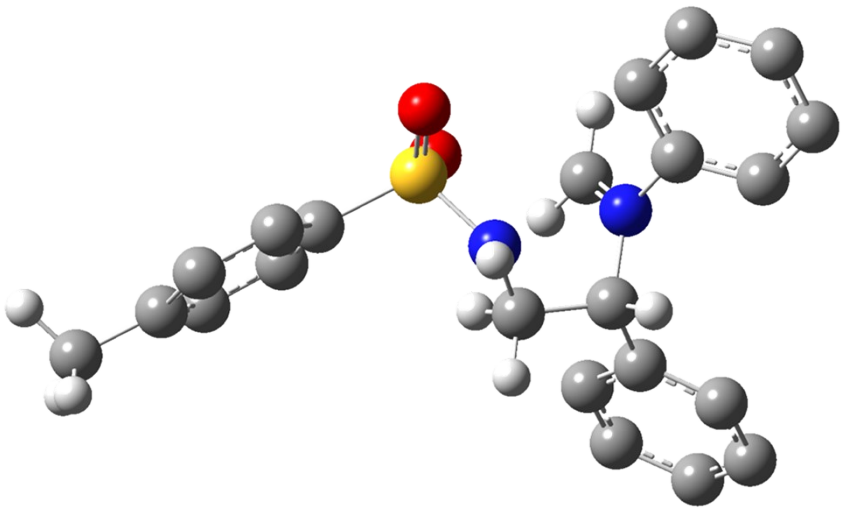

II

Center Number	Atomic Number	Atomic Type	Coordinates (Angstroms) X	Y	Z
1	6	0	-6.874566	1.348213	-0.565736
2	6	0	-5.525751	0.722990	-0.341901
3	6	0	-5.165063	-0.444065	-1.025127
4	6	0	-3.941287	-1.055422	-0.803487
5	6	0	-3.065249	-0.479423	0.113346
6	6	0	-3.395399	0.673029	0.817231
7	6	0	-4.628050	1.267543	0.578866
8	16	0	-1.483696	-1.231211	0.352486
9	8	0	-0.924319	-0.713964	1.599654
10	8	0	-1.579897	-2.649417	0.100302
11	7	0	-0.450456	-0.655278	-0.827640
12	6	0	0.057781	0.706118	-0.755631

13	6	0	1.583754	0.705156	-0.553418
14	6	0	2.184092	2.073800	-0.330292
15	6	0	1.574746	3.032782	0.482807
16	6	0	2.175471	4.271908	0.677137
17	6	0	3.383355	4.568399	0.055362
18	6	0	3.987116	3.626473	-0.770614
19	6	0	3.388571	2.387309	-0.962171
20	7	0	1.910575	-0.258957	0.565114
21	6	0	2.545053	-1.515755	0.217335
22	6	0	3.772719	-1.486071	-0.433650
23	6	0	4.385666	-2.691353	-0.749370
24	6	0	3.767278	-3.896305	-0.423878
25	6	0	2.536326	-3.902839	0.222596
26	6	0	1.910224	-2.704923	0.550431
27	6	0	1.524336	-0.040956	1.759852
28	1	0	-7.630971	0.828909	0.028838
29	1	0	-6.879882	2.397589	-0.271630
30	1	0	-7.171694	1.277540	-1.612699
31	1	0	-5.860645	-0.885095	-1.730246
32	1	0	-3.675424	-1.975887	-1.310425
33	1	0	-2.715304	1.073192	1.559257
34	1	0	-4.903426	2.160993	1.127541
35	1	0	-0.666290	-1.028611	-1.744837
36	1	0	-0.160969	1.261474	-1.669592
37	1	0	-0.433748	1.232300	0.064844
38	1	0	2.043403	0.250340	-1.430259
39	1	0	0.619797	2.842415	0.960567
40	1	0	1.693594	5.008974	1.307455

41	1	0	3.847008	5.535512	0.205443
42	1	0	4.919481	3.858036	-1.270369
43	1	0	3.855355	1.663830	-1.622716
44	1	0	4.253504	-0.541049	-0.658801
45	1	0	5.349532	-2.688927	-1.242329
46	1	0	4.248166	-4.832852	-0.677240
47	1	0	2.050511	-4.839235	0.465723
48	1	0	0.936569	-2.699395	1.027075
49	1	0	1.733675	-0.773757	2.530042
50	1	0	1.013068	0.880110	2.004485

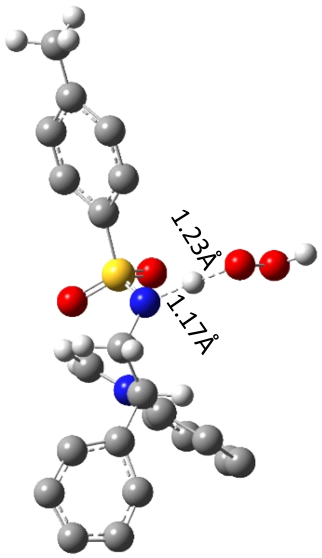

TS-II

Center Number	Atomic Number	Atomic Type	Coordinates (Angstroms) X	Y	Z
1	8	0	0.708775	-0.757140	2.903803
2	8	0	-0.673637	-0.354044	3.069788

3	1	0	-1.001464	-1.040280	3.657347
4	6	0	6.971492	1.296440	0.463935
5	6	0	5.604713	0.729671	0.181991
6	6	0	4.709309	0.479051	1.223053
7	6	0	3.456528	-0.072956	0.980592
8	6	0	3.105308	-0.373055	-0.331178
9	6	0	3.970175	-0.125913	-1.390243
10	6	0	5.216837	0.425178	-1.125046
11	16	0	1.515852	-1.124232	-0.650260
12	8	0	1.085937	-0.614386	-1.973741
13	8	0	1.632420	-2.567126	-0.513628
14	7	0	0.507163	-0.595280	0.477303
15	6	0	0.027990	0.772050	0.387524
16	6	0	-1.500030	0.725371	0.249951
17	6	0	-2.196549	2.052014	0.067306
18	6	0	-1.722242	3.026798	-0.812950
19	6	0	-2.402695	4.230351	-0.964066
20	6	0	-3.558347	4.477017	-0.230436
21	6	0	-4.026459	3.520398	0.663822
22	6	0	-3.347221	2.316372	0.811263
23	7	0	-1.825610	-0.235128	-0.871508
24	6	0	-2.556498	-1.436396	-0.523010
25	6	0	-3.899233	-1.310053	-0.188872
26	6	0	-4.608381	-2.453005	0.157477
27	6	0	-3.969609	-3.690513	0.172734
28	6	0	-2.622359	-3.789558	-0.155971
29	6	0	-1.894634	-2.655562	-0.505314
30	6	0	-1.348202	-0.085068	-2.043088

31	1	0	7.692418	0.489809	0.623512
32	1	0	7.328869	1.900767	-0.371172
33	1	0	6.963513	1.916621	1.361226
34	1	0	4.991289	0.723589	2.241450
35	1	0	2.761591	-0.247003	1.798888
36	1	0	3.658538	-0.352074	-2.402954
37	1	0	5.898352	0.626912	-1.944696
38	1	0	0.683174	-0.845811	1.608085
39	1	0	0.247107	1.297246	1.322853
40	1	0	0.486518	1.325159	-0.438436
41	1	0	-1.864172	0.228125	1.148758
42	1	0	-0.805837	2.869527	-1.371086
43	1	0	-2.022100	4.980585	-1.646641
44	1	0	-4.083653	5.417445	-0.345314
45	1	0	-4.914376	3.714691	1.253279
46	1	0	-3.697833	1.577885	1.524717
47	1	0	-4.375143	-0.336117	-0.213679
48	1	0	-5.658057	-2.376876	0.412539
49	1	0	-4.524340	-4.579011	0.448664
50	1	0	-2.121713	-4.749200	-0.128003
51	1	0	-0.832352	-2.713728	-0.717162
52	1	0	-1.537802	-0.840168	-2.795899
53	1	0	-0.784348	0.802248	-2.289312

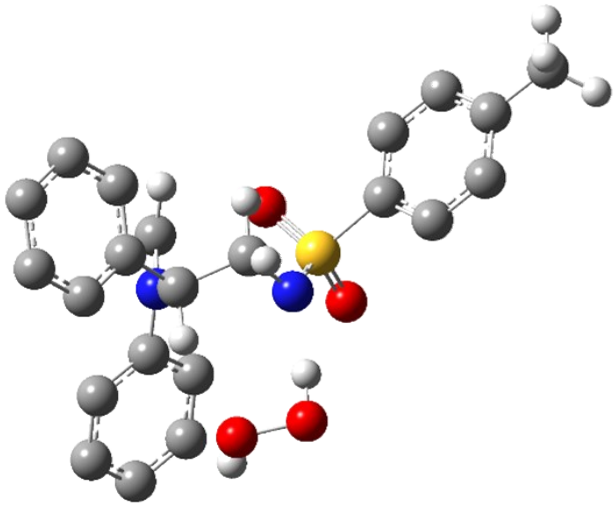

III

Center Number	Atomic Number	Atomic Type	Coordinates (Angstroms) X	Y	Z
1	8	0	-0.672958	-1.855974	2.756325
2	8	0	-2.000723	-1.620209	2.295180
3	1	0	-2.246862	-2.474511	1.917907
4	6	0	7.082099	1.176717	0.506816
5	6	0	5.689839	0.654474	0.265426
6	6	0	4.911192	0.195555	1.332021
7	6	0	3.637045	-0.311896	1.120890
8	6	0	3.133528	-0.365415	-0.174739
9	6	0	3.883434	0.087000	-1.251021
10	6	0	5.158094	0.596681	-1.022340
11	16	0	1.496782	-1.059182	-0.426313
12	8	0	1.105962	-0.535590	-1.778877

13	8	0	1.605677	-2.511273	-0.338952
14	7	0	0.553560	-0.535014	0.718601
15	6	0	0.093033	0.833185	0.625117
16	6	0	-1.417084	0.845521	0.315468
17	6	0	-2.052263	2.211152	0.195811
18	6	0	-1.467487	3.246096	-0.537588
19	6	0	-2.090130	4.486612	-0.627762
20	6	0	-3.298442	4.712102	0.023070
21	6	0	-3.877262	3.695381	0.774794
22	6	0	-3.255344	2.454898	0.860292
23	7	0	-1.643821	0.005784	-0.917519
24	6	0	-2.386253	-1.222658	-0.755852
25	6	0	-3.707701	-1.144556	-0.334276
26	6	0	-4.412447	-2.320597	-0.115523
27	6	0	-3.791496	-3.552642	-0.314276
28	6	0	-2.468375	-3.608734	-0.740511
29	6	0	-1.749053	-2.437701	-0.964337
30	6	0	-1.016861	0.244211	-2.008255
31	1	0	7.787659	0.348469	0.615537
32	1	0	7.421158	1.797432	-0.323442
33	1	0	7.126787	1.770332	1.421600
34	1	0	5.308958	0.241365	2.340498
35	1	0	3.026074	-0.658723	1.946874
36	1	0	3.463031	0.043990	-2.248057
37	1	0	5.747948	0.956490	-1.858837
38	1	0	-0.132050	-1.479109	2.010049
39	1	0	0.211904	1.344946	1.586268
40	1	0	0.638308	1.430043	-0.118684

41	1	0	-1.905062	0.279279	1.108931
42	1	0	-0.509573	3.104868	-1.025620
43	1	0	-1.624047	5.281176	-1.198025
44	1	0	-3.779486	5.680378	-0.044695
45	1	0	-4.808407	3.869474	1.300513
46	1	0	-3.695652	1.667850	1.464284
47	1	0	-4.168812	-0.176549	-0.175380
48	1	0	-5.442857	-2.275883	0.214391
49	1	0	-4.340372	-4.468613	-0.132169
50	1	0	-1.977943	-4.563836	-0.881161
51	1	0	-0.702202	-2.476786	-1.244008
52	1	0	-1.146719	-0.420085	-2.851826
53	1	0	-0.460527	1.161573	-2.120253

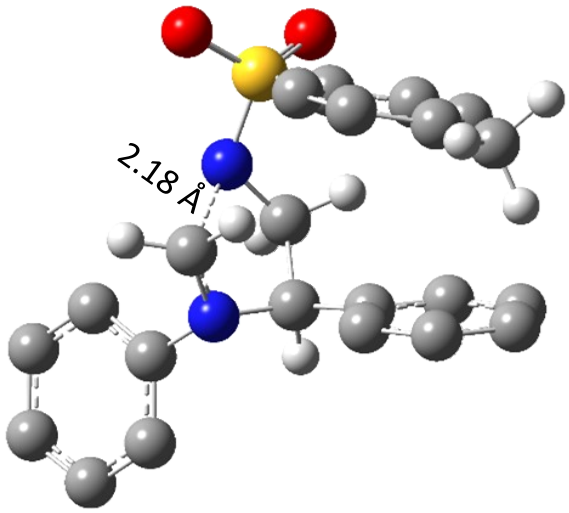

TS-III

Center Number	Atomic Number	Atomic Type	Coordinates (Angstroms) X	Y	Z
1	6	0	3.195319	-0.563991	-0.493495
2	6	0	3.889557	-1.770128	-0.565129
3	6	0	5.279834	-1.762203	-0.496911
4	6	0	5.966098	-0.554867	-0.360348
5	6	0	5.260414	0.644150	-0.282470
6	6	0	3.867008	0.648611	-0.340971
7	7	0	1.754463	-0.599262	-0.547936
8	6	0	1.131230	0.348690	-1.258149
9	7	0	0.912661	1.614434	0.500772
10	6	0	0.996198	0.542124	1.459061
11	6	0	1.098280	-0.874732	0.733897
12	6	0	-0.215618	-1.631793	0.627650
13	6	0	-0.879823	-1.947303	1.819908
14	6	0	-2.036333	-2.718394	1.811571
15	6	0	-2.557994	-3.183592	0.603975
16	6	0	-1.904645	-2.877229	-0.585052
17	6	0	-0.734403	-2.116448	-0.573222
18	16	0	-0.417760	2.562129	0.480268
19	8	0	-0.737645	2.965155	1.851093
20	8	0	-0.190767	3.556432	-0.564032
21	6	0	-1.812537	1.578419	-0.073562
22	6	0	-2.570082	0.865677	0.854556
23	6	0	-3.612115	0.061872	0.407441
24	6	0	-3.910315	-0.044709	-0.955976
25	6	0	-5.026705	-0.945008	-1.416399
26	6	0	-3.153435	0.697707	-1.866125
27	6	0	-2.110386	1.515001	-1.432295
28	1	0	3.336269	-2.697233	-0.684541
29	1	0	5.827277	-2.697008	-0.559512
30	1	0	7.050146	-0.550587	-0.311880
31	1	0	5.792004	1.582738	-0.164177
32	1	0	3.295160	1.569194	-0.245857
33	1	0	1.705772	0.909763	-1.987206
34	1	0	0.057641	0.269012	-1.381938
35	1	0	1.912362	0.662168	2.049021
36	1	0	0.148836	0.520308	2.152884
37	1	0	1.785165	-1.503275	1.308422
38	1	0	-0.478931	-1.597531	2.768526
39	1	0	-2.529428	-2.958363	2.748533

40	1	0	-3.462519	-3.784212	0.593943
41	1	0	-2.297154	-3.235510	-1.532234
42	1	0	-0.220116	-1.924257	-1.509295
43	1	0	-2.352813	0.966162	1.913788
44	1	0	-4.205094	-0.496598	1.127602
45	1	0	-5.968054	-0.689694	-0.920784
46	1	0	-5.178809	-0.872166	-2.495694
47	1	0	-4.800568	-1.989394	-1.173074
48	1	0	-3.391394	0.648297	-2.925570
49	1	0	-1.541457	2.124096	-2.129309

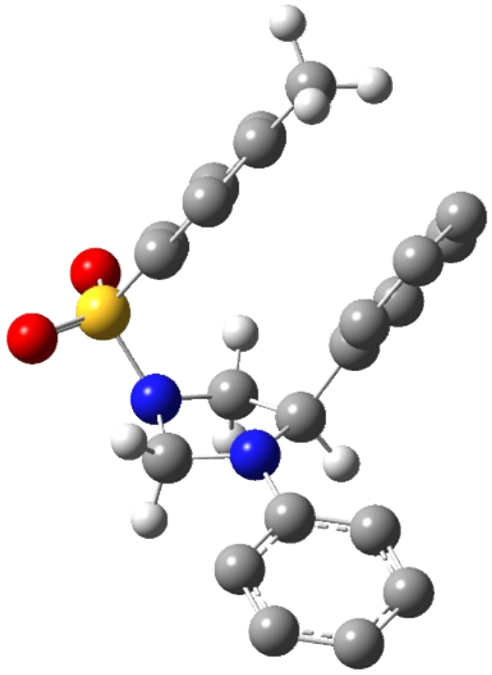

2a

Center Number	Atomic Number	Atomic Type	Coordinates (Angstroms) X	Y	Z
1	6	0	2.849185	0.032656	-0.133162
2	6	0	3.304717	-1.206699	0.346483
3	6	0	4.518145	-1.724429	-0.086484
4	6	0	5.306458	-1.035981	-1.002285

5	6	0	4.856720	0.187401	-1.485545
6	6	0	3.646428	0.721335	-1.062687
7	7	0	1.624868	0.559188	0.272057
8	6	0	1.365201	1.982098	0.055578
9	7	0	0.209446	2.273311	0.880427
10	6	0	0.233797	1.346008	2.012966
11	6	0	0.975111	0.088749	1.493358
12	6	0	0.087479	-1.129575	1.283181
13	6	0	-0.652043	-1.624033	2.360658
14	6	0	-1.425227	-2.770226	2.224655
15	6	0	-1.455521	-3.448821	1.008396
16	6	0	-0.719663	-2.962746	-0.065315
17	6	0	0.042166	-1.804833	0.067531
18	16	0	-1.252279	2.626540	0.152955
19	8	0	-2.129548	3.010006	1.238861
20	8	0	-0.924997	3.518788	-0.940046
21	6	0	-1.909353	1.129292	-0.547560
22	6	0	-2.786872	0.356518	0.208548
23	6	0	-3.293230	-0.810265	-0.340533
24	6	0	-2.937765	-1.211954	-1.631235
25	6	0	-3.501221	-2.485059	-2.201732
26	6	0	-2.061829	-0.415277	-2.367906
27	6	0	-1.543920	0.760020	-1.835416
28	1	0	2.702162	-1.778126	1.041039
29	1	0	4.846341	-2.682819	0.298906
30	1	0	6.251339	-1.446407	-1.334775
31	1	0	5.452855	0.740565	-2.201987
32	1	0	3.323140	1.673118	-1.464200
33	1	0	2.216489	2.590046	0.392528
34	1	0	1.161254	2.218378	-0.990116
35	1	0	0.794435	1.811731	2.826014
36	1	0	-0.776452	1.141221	2.365494
37	1	0	1.738231	-0.188222	2.233377
38	1	0	-0.616966	-1.113156	3.318830
39	1	0	-1.994603	-3.140237	3.069296
40	1	0	-2.046255	-4.351735	0.903718
41	1	0	-0.741109	-3.480471	-1.018151
42	1	0	0.606728	-1.422600	-0.774607
43	1	0	-3.077152	0.684166	1.199586
44	1	0	-3.970394	-1.425841	0.241954
45	1	0	-4.561509	-2.365658	-2.439191
46	1	0	-2.981366	-2.776718	-3.114983
47	1	0	-3.414718	-3.298607	-1.477232

48	1	0	-1.784384	-0.713493	-3.373062
49	1	0	-0.888023	1.397304	-2.416591

Table S2: Mullikan Charge Distribution on sp^3 C and H in intermediate-I

Sp3 C-H bond	Bond length (A)	Mulikan Charge on H atom	Mullikan Charge on sp3 carbon atom
C(27)–H(36)	1.093	0.241	-0.252
C(12)–H(32)	1.093	0.208	-0.318
C(13)–H(34)	1.089	0.167	-0.012

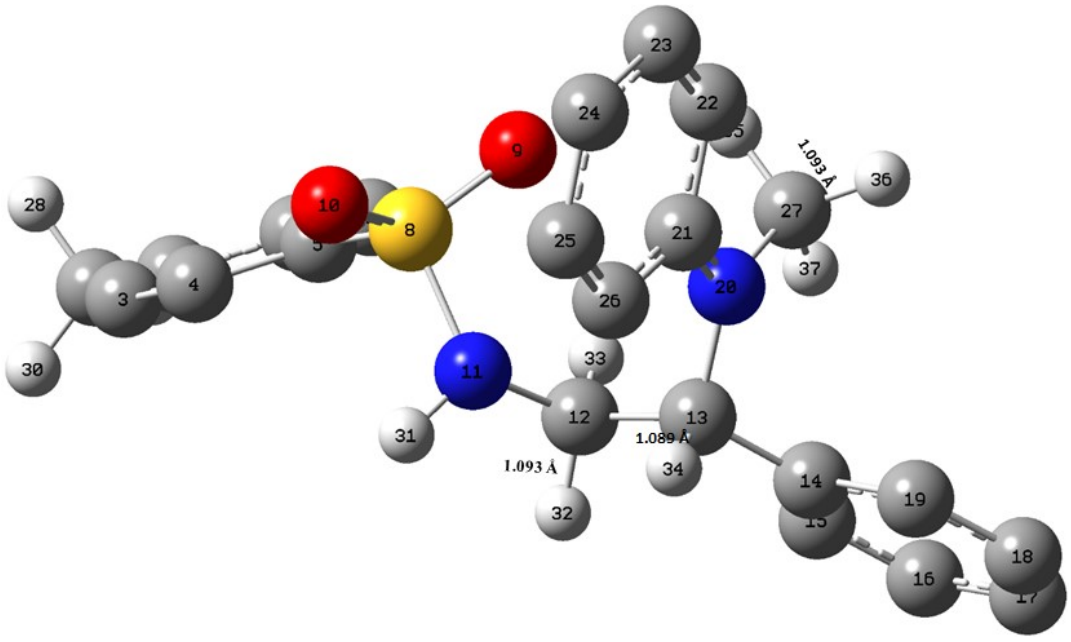

Figure S20: Optimized structure of intermediate I.

18. Apparent Quantum Yield (AQE) calculation:

The apparent quantum efficiency (AQE) of conversion of **3a** to **4a** was measured under the same photocatalytic reaction conditions, except for the incident light source. Instead of blue LED we used monochromatic light source. The AQE was determined by chemical actinometry[18-21] using monochromatic light of 460 nm and 436 nm wavelengths (These being the important emission peaks of the LED light source). At wavelengths 460 nm and 436 nm the quantum efficiencies of ferrioxalate decomposition are known ($\Phi_{436} = 1.01$ & $\Phi_{460} = 0.89$).[18]

(a) Determination of Photon flux at two different wavelengths (λ= 436 nm and λ= 460 nm):

A 0.15 M solution of ferrioxalate was prepared by dissolving 0.737 g of potassium ferrioxalate hydrate in 10 mL of 0.05 M H_2SO_4. A buffered solution of 1,10 phenanthroline was prepared by dissolving 50 mg of phenanthroline and 11.25 g of sodium acetate in 50 mL of 0.5M H_2SO_4. Both solutions were stored in the dark. To determine the photon flux of the spectrophotometer, 2 mL of the ferrioxalate solution was placed in a quartz cuvette and irradiated for 90 seconds at λ = 460 nm (emission slit width of 5 nm). After irradiation 0.35 mL of the 1,10 phenanthroline solution was added to it. The aluminium foil wrapped solution was then allowed to rest an hour for complete co-ordination of ferrous ion to phenanthroline. The absorbance of the solution was measured at 510 nm. The same procedure was repeated at monochromatic wavelength λ = 436 nm. A non-irradiated sample was also prepared and the absorbance at 510 nm was measured. The no. of moles of ferrous ion (Fe^{2+} ions) was calculated using equation 1.

$$Fe^{+2} = \frac{V.\Delta A}{l.\varepsilon} \qquad \text{.....(1)}$$

Where, V is the total volume of the solution after addition of phenanthroline (0.00235 L)

ΔA is the difference in absorbance at 510 nm between the irradiated and non-irradiated solutions.

l is the path length (1 cm)

ε is the molar absorptivity of the ferrioxalate solution at 510 nm (11,100 L mol^{-1} cm^{-1})

The photon flux of the spectrophotometer can be calculated using equation 2.

$$photon\ flux = \frac{mol\ Fe^{+2}}{\Phi\ .\ t.\ f} \qquad \text{..... (2)}$$

where, Φ = quantum yield for the ferrioxalate actinometer (1.01 for 0.15 M solution at λ= 436 nm , 0.89 for 0.15 M solution at λ= 460 nm)

The irradiation time, t = 90 seconds

The fraction of light absorbed at wavelength of applied monochromatic light source at λ= 436 nm and λ= 460 nm (f) are 0.997 and 0.993 respectively.

Therefore,

$$Photon\ flux\ (at\ 436\ nm) = \frac{5.14 \times 10^{-7}}{1.01\ \times 90 \times .0.997} = 5.72 \times 10^{-9}\ Es^{-1}$$

$$Photon\ flux\ (at\ 460\ nm) = \frac{4.60 \times 10^{-5}}{0.89\ \times 90 \times .0.993} = 5.81 \times 10^{-9} Es^{-1}$$

(b) Determination of AQE at two different wavelengths (λ= 436 nm and λ= 460 nm):

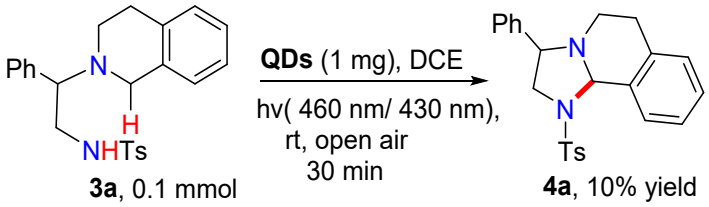

3a, 0.1 mmol **4a**, 10% yield

A cuvette was charged with 0.1 mmol (40 mg) of 3a and 1mg $CsPbBr_3$ QDs in 3 mL DCE as a solvent. A cuvette was then irradiated at two different wavelengths (λ= 436 nm and λ= 460 nm) for 30 minutes (1800 seconds). The yield of the product formation was determined by ^{1}H- NMR

spectroscopy using 0.12 mmol 1,3,5 trimethoxybenzene as an internal standard. The yield of the product at both wavelengths (λ= 436 nm and λ= 460 nm) was 10 % (~1× 10^{-5} mole).

The quantum yield was determined by using equation 3.

$$\Phi = \frac{mole\ product}{flux.\ t.f} \quad \text{..... (3)}$$

At λ= 436 nm,

$$\Phi = \frac{1 \times 10^{-5}}{5.72 \times 10^{-9} \times 1800 \times .0.99} = 0.98$$

At λ= 460 nm,

$$\Phi = \frac{1 \times 10^{-5}}{5.81 \times 10^{-9} \times 1800 \times .0.99} = 0.96$$

Table S3: Overview of the calculation of AQE at two different wavelengths (436 and 460 nm)

Monochromatic light source (wavelngth)	Total volume of the reaction solution (L)	Amount of Fe^{2+} (mol)	Photon Flux (Einstein s^{-1})	Product Yield (mol)	Reference quantum yield (Φ_r)	Apparent quantum yield (Φ)
436 nm	0.00235	5.14 x 10^{-7}	5.72 x 10^{-9}	1 x 10^{-5}	1.01	0.98
460 nm	0.00235	4.60 x 10^{-7}	5.81 x 10^{-9}	1 x 10^{-5}	0.89	0.96

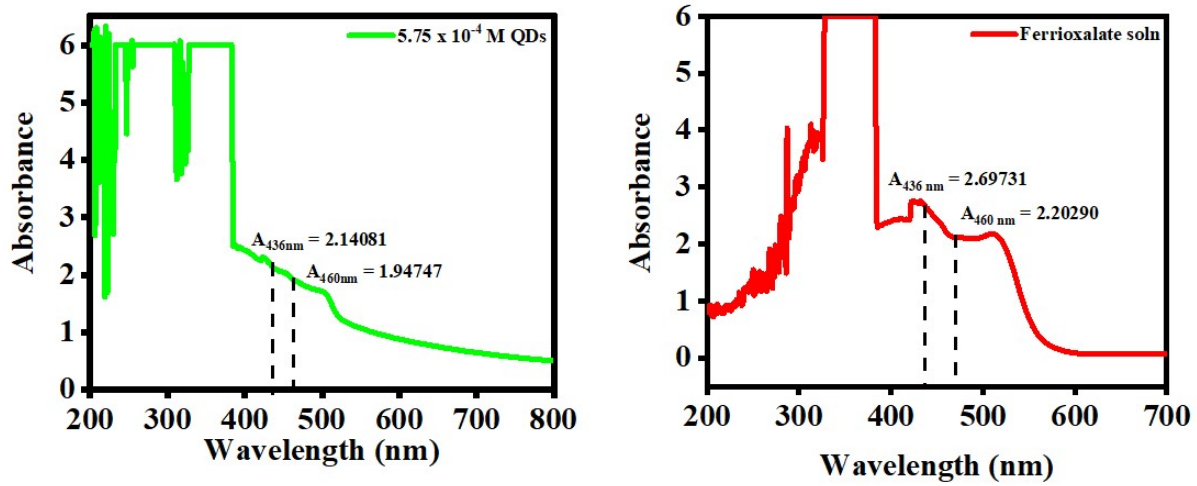

Figure S21: (a) Absorbance of 1mg $CsPbBr_3$ **QDs** dispersed in 3 mL DCE (5.75 × 10^{-5} M); (b) Absorbance of ferrioxalate actinometer solution.

19. NMR spectral data of products:

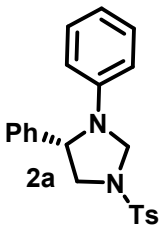

[1]. 3,4-diphenyl-1-tosylimidazolidine: Following a general procedure, $CsPbBr_3$ perovskite NCs (1 mg), **1a** (0.1 mmol) and 3 mL 1,2-dichloroethane solvent (DCE) were subjected to irradiation to afford the pure product **2a** (31.02 mg, 0.082 mmol) as a solid in 82% yield. ^{1}H NMR (400 MHz, $CDCl_3$) δ 7.73 (d, J = 8.2 Hz, 2H), 7.29- 7.25 (m, 5H), 7.17-7.13 (m, 4H), 6.77 (t, J = 7.32 Hz, 1H), 6.42 (d, J = 8.2 Hz, 2H), 5.08 (d, J = 5.88 Hz, 1H), 4.80 (d, J = 5.88 Hz, 1H), 4.57 (dd, J = 5.44 Hz, 7.04 Hz, 1H), 3.96 (dd, J = 7.44 Hz, 10.44 Hz, 1H), 3.50 (dd, J = 5.16 Hz, 10.40 Hz, 1H), 2.43 (s, 3H), ^{13}C{^{1}H} NMR (100 MHz, $CDCl_3$) δ 144.8, 144.3, 140.4, 132.7, 129.9, 129.1, 128.9, 127.8, 127.7, 125.9, 118.2, 113.06, 66.09, 61.4, 55.6, 21.6. **(*S*)-3,4-Diphenylimidazolidine (2a)**. 30 mg, yield 79%; HPLC analysis: > 99% ee [Daicel Chiralcel OD-H column], hexane: *i*PrOH = 90:10, flow rate= 1 mL/min, λ = 254 nm, t_R (retention time) = 30.63].

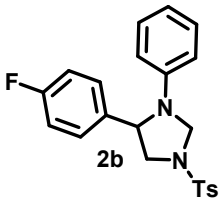

[2]. 4-(4-fluorophenyl)-3-phenyl-1-tosylimidazoline: Following a general procedure, $CsPbBr_3$ perovskite NCs (1 mg), **1b** (0.1 mmol) and 3 mL 1,2-dichloroethane solvent (DCE) were subjected to irradiation to afford the pure product **2b** (29.7 mg, 0.075 mmol) as a solid in 75% yield. ^{1}H NMR (400 MHz, $CDCl_3$) δ 7.71 (d, J = 8.08 Hz, 2H), 7.26(d, J= 7.96 Hz, 2H), 7.17-7.09 (m, 4H), 6.95 (t, J = 8.56 Hz, 2H), 6.77 (t, J = 7.32 Hz, 1H), 6.39 (d, J = 8.12 Hz, 2H), 5.06 (d, J = 5.84 Hz, 1H), 4.75 (d, J = 5.8 Hz, 1H), 4.56 (t, J = 6.64 Hz, 1H), 3.92 (dd, J = 7.4 Hz, 10.32 Hz, 1H), 3.47 (dd, J = 4.88 Hz, 10.4 Hz, 1H), 2.43 (s, 3H),^{13}C{^{1}H} NMR (100 MHz, $CDCl_3$) δ 163.4, 160.9, 144.6, 144.4, 136.2, 132.8, 129.9, 129.1, 127.8, 118.4, 115.6, 113.08, 65.9, 60.8, 55.5, 21.5.

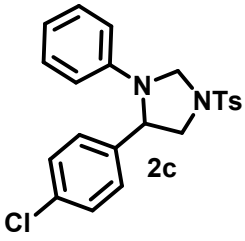

[3]. 4-(4-chlorophenyl)-3-phenyl-1-tosylimidazolidine: Following a general procedure, $CsPbBr_3$ perovskite NCs (1 mg), **1c** (0.1 mmol) and 3 mL 1,2-dichloroethane solvent (DCE) were subjected to irradiation to afford the pure product **2c** (30 mg, 0.073 mmol) as a solid in 73% yield. ^{1}H NMR (400 MHz, $CDCl_3$) δ 7.68 (d, J = 8.16 Hz, 2H), 7.28-7.20 (m, 4H), 7.15 (t, J = 7.92 Hz, 2H), 7.05 (d, J = 8.36 Hz, 2H), 6.77 (t, J = 7.32 Hz, 1H), 6.37 (d, J = 8.2 Hz, 2H), 5.05 (d, J = 5.92 Hz, 1H), 4.75 (d, J = 5.92 Hz, 1H), 4.55 (dd, J = 4.88, 7.2 Hz, 1H), 3.93 (dd, J = 7.4 Hz, 10.52 Hz, 1H), 3.48 (dd, J = 4.76 Hz, 10.52 Hz, 1H), 2.43 (s, 3H), ^{13}C{^{1}H} NMR (100 MHz, $CDCl_3$) δ 144.7, 144.6, 139.2, 133.5, 133.1,130, 129.4, 129.2, 127.9, 127.5, 118.7, 113.2, 66.1, 61.0, 55.6, 21.7.

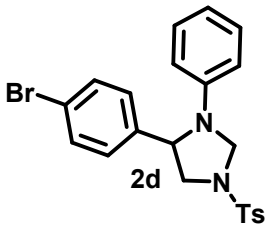

[4]. 4-(4-bromophenyl)-3-phenyl-1-tosylimidazoline: Following a general procedure, $CsPbBr_3$ perovskite NCs (1 mg), **1d** (0.1 mmol) and 3 mL 1,2-dichloroethane solvent (DCE) were subjected to irradiation to afford the pure product **2d** (32.5 mg, 0.071 mmol) as a solid in 71% yield. ^{1}H NMR (400 MHz, $CDCl_3$) δ 7.68 (d, J = 8.16 Hz, 2H), 7.36 (d, J= 8.36 Hz, 2H), 7.24 (d, J= 8.2 Hz, 2H), 7.15 (t, J = 8.16 Hz, 2H), 6.99 (d, J = 8.36 Hz, 2H), 6.77 (t, J = 7.36 Hz, 1H), 6.38 (d, J = 8.08 Hz, 2H), 5.06 (d, J = 5.96 Hz, 1H), 4.75 (d, J = 6 Hz, 1H), 4.54 (dd, J = 4.84, 7.2 Hz, 1H), 3.93 (dd, J = 7.4 Hz, 10.6 Hz, 1H), 3.48 (dd, J = 4.76

Hz, 10.56 Hz, 1H), 2.43 (s, 3H), $^{13}C\{^{1}H\}$ NMR (100 MHz, $CDCl_3$) δ 144.49, 144.45, 139.6, 132.9, 131.9, 129.8, 129.2, 127.7, 127.6, 121.45, 118.5, 113.05, 65.9, 60.9, 55.3, 21.5.

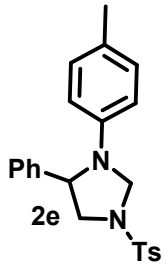

[5]. 4-Phenyl-3-(*p*-tolyl)-1-tosylimidazoidine: Following a general procedure, $CsPbBr_3$ perovskite NCs (1 mg), **1e** (0.1 mmol) and 3 mL 1,2-dichloroethane solvent (DCE) were subjected to irradiation to afford the pure product **2e** (29.4 mg, 0.075 mmol) as a solid in 75% yield. ^{1}H NMR (400 MHz, $CDCl_3$) δ 7.71 (d, J = 7.96 Hz, 2H), 7.26 (d, J = 8.68 Hz, 5H), 7.13 (d, J = 7.16 Hz, 2H), 6.95 (d, J = 8.2 Hz, 2H), 6.33 (d, J = 8.2 Hz, 2H), 5.06 (d, J = 5.72 Hz, 1H), 4.73 (d, J = 5.76 Hz, 1H), 4.54 (t, J = 6.32 Hz, 1H), 3.97-3.92(m, 1H), 3.44 (dd, J = 5.48 Hz, 10.28 Hz, 1H), 2.43 (s, 3H), 2.22 (s, 3H),$^{13}C\{^{1}H\}$ NMR (100 MHz, $CDCl_3$) δ 144.2, 142.7, 140.5, 132.9, 129.8, 129.6, 128.8, 127.8, 127.63, 127.61, 125.9, 113.3, 66.4, 61.7, 55.5, 21.5, 20.2.

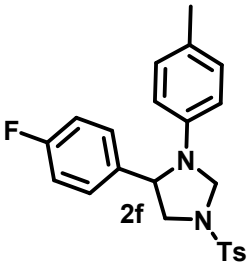

[6]. 4-(4-fluorophenyl)-3-(*p*-tolyl)-1-tosylimidazoline: Following a general procedure, $CsPbBr_3$ perovskite NCs (1 mg), **1f** (0.1 mmol) and 3 mL 1,2-dichloroethane solvent (DCE) were subjected to irradiation to afford the pure product **2f** (31.6 mg, 0.077 mmol) as a solid in 77% yield. ^{1}H NMR (400 MHz, $CDCl_3$) δ 7.71 (d, J = 8.12 Hz, 2H), 7.27 (d, J= 8.08 Hz, 2H), 7.11-7.07 (m, 2H), 6.97-6.91 (m, 4H), 6.32 (d, J = 8.32 Hz, 2H), 5.06 (d, J = 5.76 Hz, 1H), 4.69 (d, J = 5.76 Hz, 1H), 4.54 (t, J = 6.16 Hz, 1H), 3.91 (dd, J = 7.48 Hz, 10.32 Hz, 1H), 3.43 (dd, J = 5.16 Hz, 10.36 Hz, 1H), 2.43 (s, 3H), 2.22 (s, 3H), $^{13}C\{^{1}H\}$ NMR (100 MHz, $CDCl_3$) δ 163.3, 160.9, 144.3, 142.5, 136.2, 133, 129.8, 129.6, 127.8, 127.5, 115.8, 113.4, 66.3, 61, 55.5, 21.5, 20.2.

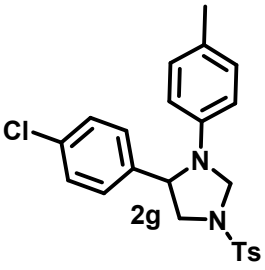

[7]. 4-(4-chlorophenyl)-3-(*p*-tolyl)-1-tosylimidazoline: Following a general procedure, $CsPbBr_3$ perovskite NCs (1 mg), **1g** (0.1 mmol) and 3 mL 1,2-dichloroethane solvent (DCE) were subjected to irradiation to afford the pure product **2g** (31.6 mg, 0.074 mmol) as a solid in 74% yield. ^{1}H NMR (400 MHz, $CDCl_3$) δ 7.68 (d, J = 8.24 Hz, 2H), 7.28-7.19 (m, 4H), 7.27 (d, J = 8.36 Hz, 2H), 6.95 (d, J = 8.2 Hz, 2H), 6.30 (d, J = 8.4 Hz, 2H),

5.05 (d, J = 8.4 Hz, 1H), 4.70 (d, J = 5.84 Hz, 1H), 4.54-4.51 (m, 1H), 3.95-3.90 (m, 1H), 3.44 (dd, J = 5.04 Hz, 10.48 Hz, 1H), 2.43 (s, 3H), 2.22 (s, 3H), $^{13}C\{^1H\}$ NMR (100 MHz, $CDCl_3$) δ 144.3, 142.4, 139.1, 133.3, 133.0, 129.8, 129.7, 128.9, 127.9, 127.7, 127.3, 113.3, 66.2, 61.1, 55.3, 21.5, 20.2.

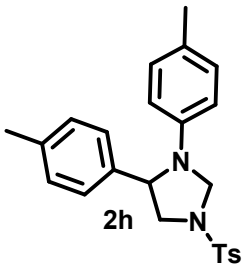

[8]. 3, 4-di-*p*-tolyl-1-tosylimidazoidine: Following a general procedure, $CsPbBr_3$ perovskite NCs (1 mg), **1h** (0.1 mmol) and 3 mL 1,2-dichloroethane solvent (DCE) were subjected to irradiation to afford the pure product **2h** (29.7 mg, 0.073 mmol) as a solid in 73% yield. ^1H NMR (400 MHz, $CDCl_3$) δ 7.70 (d, J = 8.2 Hz, 2H), 7.28-7.24 (m, 2H), 7.06-6.99 (m, 4H), 6.93 (d, J = 8.28 Hz, 2H), 6.32 (d, J = 8.4 Hz, 2H), 5.02 (d, J = 5.76 Hz, 1H), 4.71 (d, J = 5.8 Hz, 1H), 4.49 (t, J = 6.32 Hz, 1H), 3.91 (dd, J = 7.36 Hz, 10.24 Hz, 1H), 3.40 (dd, J = 5.6 Hz, 10.28 Hz, 1H), 2.42 (s, 3H), 2.31 (s, 3H), 2.21 (s, 3H), $^{13}C\{^1H\}$ NMR (100 MHz, $CDCl_3$) δ 144.1, 142.7, 137.4, 137.2, 133.03, 129.7, 129.57, 129.50, 125.8, 113.3, 66.4, 61.5, 55.6, 21.5, 21.06, 20.2.

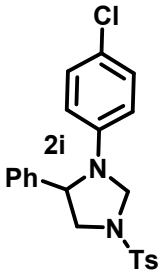

[**9**]. **3-(4-chlorophenyl)-4-Phenyl-1-tosylimidazoidine:** Following a general procedure, $CsPbBr_3$ perovskite NCs (1 mg), **1i** (0.1 mmol) and 3 mL 1,2-dichloroethane solvent (DCE) were subjected to irradiation to afford the pure product **2i** (29.8 mg, 0.072 mmol) as a solid in 72% yield. ^1H NMR (400 MHz, $CDCl_3$) δ 7.70 (d, J = 8.12 Hz, 2H), 7.27-7.24 (m, 5H), 7.11-7.05 (m, 4H), 6.28 (d, J = 8.88 Hz, 2H), 5.0 (d, J = 6.08 Hz, 1H), 4.77 (d, J = 6.12 Hz, 1H), 4.47 (t, J = 6.48 Hz, 1H), 3.98 (dd, J = 7.36, 10.6 Hz, 1H), 3.44 (dd, J = 5.56, 10.6 Hz, 1H), 2.42(s, 3H), $^{13}C\{^1H\}$ NMR (100 MHz, $CDCl_3$) δ 144.4, 143.3, 139.7, 132.7, 129.9, 129.0, 128.9, 127.89, 127.80, 125.85, 123.2, 114.1, 66.0, 61.5, 55.6, 21.5.

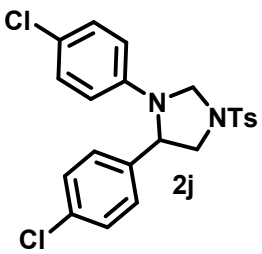

[10]. 3,4-bis(4-chlorophenyl)-1-tosylimidazolidine: Following a general procedure, $CsPbBr_3$ perovskite NCs (1 mg), **1j** (0.1 mmol) and 3 mL 1,2-dichloroethane solvent (DCE) were subjected to irradiation to afford the pure product **2j** (32.7 mg, 0.073 mmol) as a solid in 73% yield. ^1H NMR (400 MHz, $CDCl_3$) δ 7.67 (d, J = 8.12 Hz, 2H), 7.25-7.21 (m, 4H), 7.08 (d, J = 8.8 Hz, 2H), 7.02 (d,

J = 8.28 Hz, 2H), 6.27 (d, *J* = 8.84 Hz, 2H) 5.0 (d, *J* = 6.08 Hz, 1H), 4.73 (d, *J* = 6.12 Hz, 1H), 4.50-4.47 (m, 1H), 3.96 (dd, *J* = 8.16, 10.6 Hz, 1H), 3.44 (dd, *J* = 5.04, 10.8 Hz, 1H), 2.42 (s, 3H), $^{13}C\{^{1}H\}$ NMR (100 MHz, $CDCl_3$) δ 144.6, 143.3, 138.6, 133.8, 133.5, 130.1, 129.3, 129.2, 127.9, 127.4, 123.8, 114.3, 66.1, 61.2, 55.6, 21.8.

[11]. 4-Phenyl-3-(*m*-tolyl)-1-tosylimidazoidine: Following a general procedure, $CsPbBr_3$ perovskite NCs (1 mg), **1k** (0.1 mmol) and 3 mL 1,2-dichloroethane solvent (DCE) were subjected to irradiation to afford the pure product **2k** (29.0mg, 0.074 mmol) as a solid in 74% yield. ^{1}H NMR (400 MHz, $CDCl_3$) δ 7.73 (d, *J* = 8.12 Hz, 2H), 7.27 (d, *J* = 6.08 Hz, 5H), 7.17-7.15 (m, 2H), 7.03 (d, *J* = 7.84 Hz, 1H), 6.60 (d, *J* = 7.36 Hz,1H), 6.27-6.20 (m, 2H), 5.06 (d, *J* = 5.84 Hz, 1H), 4.78 (d, *J* = 5.8 Hz, 1H), 4.60-4.57 (m, 1H), 3.93 (dd, *J* = 7.48, 10.28 Hz, 1H), 3.49 (dd, *J* = 5.08, 10.28 Hz, 1H), 2.43 (s, 3H), 2.26 (s, 3H), $^{13}C\{^{1}H\}$ NMR (100 MHz, $CDCl_3$) δ 144.8, 144.3, 140.6, 138.9, 132.7, 129.9, 128.9, 128.8, 127.8, 127.6, 125.9, 119.2, 113.7, 110.3, 66.1, 61.4, 55.5, 21.7, 21.6.

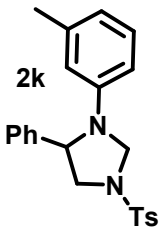

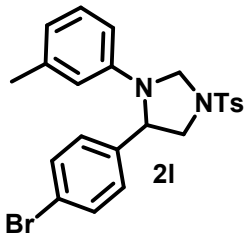

[12]. 4-(4-bromophenyl)-3-(*m*-tolyl)-1-tosyllimidazolidine: Following a general procedure, $CsPbBr_3$ perovskite NCs (1 mg), **1l** (0.1 mmol) and 3 mL 1,2-dichloroethane solvent (DCE) were subjected to irradiation to afford the pure product **2l** (35.3 mg, 0.075 mmol) as a solid in 75% yield. ^{1}H NMR (400 MHz, $CDCl_3$) δ 7.67 (d, *J* = 8.20 Hz, 2H), 7.36 (d, *J* = 8.32 Hz, 2H), 7.28-7.23 (m, 2H), 7.04-6.96 (m, 3H), 6.60 (d, *J* = 7.48 Hz, 1H),, 6.21-6.15 (m, 2H), 5.04 (d, *J* = 5.88 Hz, 1H), 4.73 (d, *J* = 5.92 Hz, 1H), 4.56-4.53 (m, 1H), 3.90 (dd, *J* = 7.44, 10.52 Hz, 1H), 3.47 (dd, *J* = 4.60, 10.48 Hz, 1H), 2.43 (s, 3H), 2.24 (s, 3H), $^{13}C\{^{1}H\}$ NMR (100 MHz, $CDCl_3$) δ 144.5, 144.3, 139.7, 139.1, 131.9, 129.8, 129.1, 127.7, 127.6, 121.4, 119.5, 113.7, 110.3, 65.9, 60.9, 55.2, 21.7, 21.6.

[13]. 3-phenyl-1-tosyl-1,2,3,5,6,10b-hexahydroimidazo(2,1-a)isoquinoline: Following a general procedure, $CsPbBr_3$ perovskite NCs (1 mg), **3a** (0.1 mmol) and 3 mL 1,2-dichloroethane solvent (DCE) were subjected to irradiation to afford the pure product **4a** (33.2 mg, 0.082 mmol) as a solid in 82% yield. ^{1}H NMR (400 MHz, $CDCl_3$) δ 7.99 (d, *J* = 7.72 Hz, 1H), 7.87 (d, *J* = 8.2 Hz, 2H), 7.42 (d, *J*= 8.12Hz,

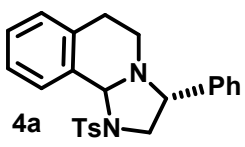

2H), 7.36 (t, *J* = 7.56 Hz, 1H), 7.29-7.21 (m, 4H), 7.09 (d, *J* = 7.56 Hz, 1H), 6.91-6.89 (m, 2H), 5.97 (s, 1H), 4.13 (t, *J* = 8.12 Hz, 1H), 3.72-3.70 (m, 1H), 3.21 (t, *J* = 9.44 Hz, 1H), 3.17-3.10 (m, 1H), 2.98-2.90 (m, 1H), 2.77 (dd, *J* = 5.44 Hz, 13.76 Hz, 1H), 2.56 (s, 3H), 2.4 (dd, *J* = 4.44 Hz, 16.88 Hz, 1H), $^{13}C\{^{1}H\}$ NMR (100 MHz, $CDCl_3$) δ 143.8, 138.7, 134.8, 134.1, 133.9, 129.7, 129.03, 128.6, 128.4, 128.1, 127.56, 127.52, 127.04, 76.3, 60.7, 55.5, 41.4, 21.6, 21.3. **(3R)-3-phenyl-1-tosyl-1,2,3,4,5,6,10b-hexahydroimidazo[2,1-a]isoquinoline 4a'**. 32.5 mg, yield 80%; HPLC analysis: > 99% ee [Daicel Chiralcel OD-H column], hexane : *i*PrOH = 90:10, flow rate= 1 mL/min, λ = 254 nm, t_R (retention time) = 9.88].

[14].3-(4-chlorophenyl)-1-tosyl-1,2,3,5,6,10b-hexahydroimidazo(2,1-a)isoquinoline:

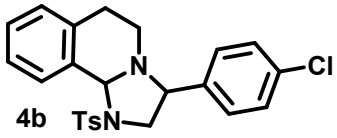

Following a general procedure, $CsPbBr_3$ perovskite NCs (1 mg), **3b** (0.1 mmol) and 3 mL 1,2-dichloroethane solvent (DCE) were subjected to irradiation to afford the pure product **4b** (29.4 mg, 0.067 mmol) as a solid in 67% yield. ^{1}H NMR (400 MHz, $CDCl_3$) δ 7.95 (d, *J* = 7.72 Hz, 1H), 7.84 (d, *J* = 8.2 Hz, 2H), 7.41 (d, *J*= 8.12 Hz, 2H), 7.34 (t, *J* = 7.4 Hz, 1H), 7.26 (t, *J*= 7.4 Hz, 1H), 7.19 (d, *J* = 8.36 Hz, 2H), 7.08 (d, *J* = 7.56 Hz, 1H), 6.80 (d, *J* = 8.44 Hz, 2H), 5.96 (s, 1H), 4.09 (t, *J* = 8.08 Hz, 1H), 3.69 (dd, *J* = 7.6, 10.32 Hz, 1H), 3.17-3.09 (m, 2H), 2.95-2.86 (m, 1H), 2.72 (dd, *J* = 4.88, 14.08 Hz, 1H), 2.55 (s, 3H), 2.42 (dd, *J* = 4.44 Hz, 17.08 Hz, 1H), $^{13}C\{^{1}H\}$ NMR (100 MHz, $CDCl_3$) δ 143.9, 137.4, 134.5, 134.06, 133.8, 133.7, 129.7, 128.9, 128.7, 128.4, 128.3, 127.6, 127.09, 76.3, 60.1, 55.2, 41.4, 21.6, 21.2.

[15]. 3-(*p*-tolyl)-1-tosyl-1,2,3,5,6,10b-hexahydroimidazo(2,1-a)isoquinoline: Following a general procedure, $CsPbBr_3$ perovskite NCs (1 mg), **3c** (0.1 mmol) and 3 mL 1,2-dichloroethane solvent (DCE) were subjected to irradiation to afford the pure product **4c** (33.9 mg, 0.081 mmol) as a solid in 81% yield. ^{1}H NMR (400 MHz, $CDCl_3$) δ 7.95 (d, *J* = 7.72 Hz, 1H), 7.87 (d, *J* = 8.16 Hz, 2H), 7.42 (d, *J*= 8.04 Hz, 2H), 7.35 (t, *J* = 7.4 Hz, 1H), 7.28-7.25 (m, 1H), 7.09- 7.04 (m, 3H), 6.80 (d, *J* = 7.92 Hz, 2H), 5.95 (s, 1H), 4.09 (t, *J* = 8.12 Hz, 1H), 3.69 (dd, *J* = 7.4, 9.96 Hz, 1H), 3.18 (t, *J* = 9.56 Hz, 1H), 3.14-3.08 (m, 1H), 2.97-2.88 (m, 1H), 2.76 (dd, *J* = 5.04, 14.08 Hz, 1H), 2.56 (s, 3H), 2.40 (dd, *J* = 4.40 Hz, 17.08 Hz, 1H), $^{13}C\{^{1}H\}$ NMR (100 MHz, $CDCl_3$) δ 144.0, 138.1, 135.6, 135.02, 134.2, 134.1, 129.9, 129.5, 129.2, 128.6, 127.7, 127.6, 127.2, 76.5, 60.6, 55.7, 41.5, 21.8, 21.5, 21.3.

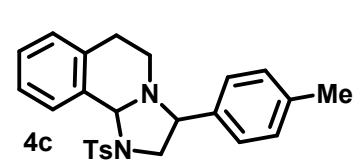

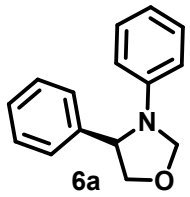

[16]. 3,4 diphenyloxazolidine: Following a general procedure, $CsPbBr_3$ perovskite NCs (1 mg), **5a** (0.1 mmol) and 3 mL 1,2-dichloroethane solvent (DCE) were subjected to irradiation to afford the pure product **6a** (16.2 mg, 0.072 mmol) as a solid in 72% yield. ^{1}H NMR (400 MHz, $CDCl_3$) δ 7.55- 7.45 (m, 5H), 7.38 (t, J = 7.56 Hz, 2H), 6.96 (d, J = 7.2 Hz, 1H), 6.69 (d, J = 8.12 Hz, 2H), 5.50 (d, J = 1.52 Hz, 1H), 5.20 (d, J = 1.4 Hz, 1H), 4.86 (dd, J = 4.48, 6.48 Hz, 1H), 4.54 (t, J = 7.92 Hz, 1H), 4.15 (dd, J = 4.32, 8.40 Hz, 1H), ^{13}C{^{1}H} NMR (100 MHz, $CDCl_3$) δ 145.2, 141.7, 129.5, 129.1, 127.8, 126.4, 117.9, 113, 82.9, 75.8, 61.8. **(*S*)-3,4-Diphenyloxazolidine 6a'**. 16 mg, yield 71%; HPLC analysis: > 99% ee [Daicel Chiralcel OD-H column], hexane : *i*PrOH = 90:10, flow rate= 1 mL/min, λ = 254 nm, t_R (retention time) = 5.76 min (major) and 10.6 min (minor)].

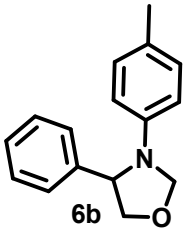

[17]. 4-phenyl-3-(*p*-tolyl)oxazolidine: Following a general procedure, $CsPbBr_3$ perovskite NCs (1 mg), **5b** (0.1 mmol) and 3 mL 1,2-dichloroethane solvent (DCE) were subjected to irradiation to afford the pure product **6b** (18.2 mg, 0.076 mmol) as a solid in 76% yield. ^{1}H NMR (400 MHz, $CDCl_3$) δ 7.48- 7.39 (m, 5H), 7.13-7.11 (m, 2H), 6.56-6.53 (m, 2H), 5.43 (d, J = 1.96 Hz, 1H), 5.12 (d, J = 1.96 Hz, 1H), 4.77-4.78 (m, 1H), 4.50 (t, J = 7.0 Hz, 1H), 4.09-4.05 (m, 1H), 2.37 (s, 3H), ^{13}C{^{1}H} NMR (100 MHz, $CDCl_3$) δ 143.1, 141.7, 129.8, 128.9, 127.6, 126.9, 126.3, 113.0, 83.2, 75.7, 62.04, 20.4.

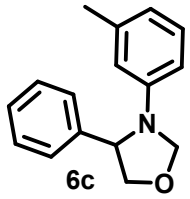

[18]. 4-phenyl-3-(*m*-tolyl)oxazolidine: Following a general procedure, $CsPbBr_3$ perovskite NCs (1 mg), **5c** (0.1 mmol) and 3 mL 1,2-dichloroethane solvent (DCE) were subjected to irradiation to afford the pure product **6c** (17.94 mg, 0.075 mmol) as a solid in 75% yield. ^{1}H NMR (400 MHz, $CDCl_3$) δ 7.59- 7.47 (m, 6H), 7.30 (t, J = 7.76 Hz, 1H), 6.83 (d, J = 7.44 Hz, 1H), 6.57-6.53 (m, 2H), 5.53 (d, J = 2.24 Hz, 1H), 5.22 (d, J = 2.2 Hz, 1H), 4.88 (dd, J = 4.28, 6.72 Hz, 1H), 4.55 (t, J = 8.12 Hz, 1H), 4.15 (dd, J = 4.2, 8.36 Hz, 1H), 2.50 (s, 3H), ^{13}C{^{1}H} NMR (100 MHz, $CDCl_3$) δ 145.3, 141.9, 139.1, 129.4, 129.05, 127.7, 126.4, 118.9, 113.6, 110.3, 83.0, 61.8, 22.04.

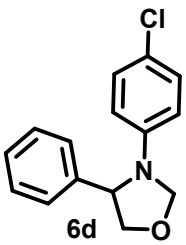

[19]. 4-phenyl-3-(*m*-tolyl)oxazolidine: Following a general procedure, $CsPbBr_3$ perovskite NCs (1 mg), **5d** (0.1 mmol) and 3 mL 1,2-dichloroethane solvent (DCE) were subjected

to irradiation to afford the pure product **6d** (18.1 mg, 0.07 mmol) as a solid in 70% yield. ^{1}H NMR (400 MHz, $CDCl_3$) δ 7.39- 7.28 (m, 5H), 7.13 (d, J = 8.84 Hz, 2H), 6.40 (d, J = 8.84 Hz, 2H), 5.30 (d, J = 2.20 Hz, 1H), 5.01 (d, J = 2.20 Hz, 1H), 4.67 (dd, J = 4.68, 6.60 Hz, 1H), 4.45- 4.42 (m, 1H), 3.98 (dd, J = 4.52, 8.44 Hz, 1H), ^{13}C{^{1}H} NMR (100 MHz, $CDCl_3$) δ 143.4, 140.8, 129.0, 127.7, 126.1, 122.6, 113.8, 82.7, 75.8, 61.7, 29.7.

20. HPLC chromatograms

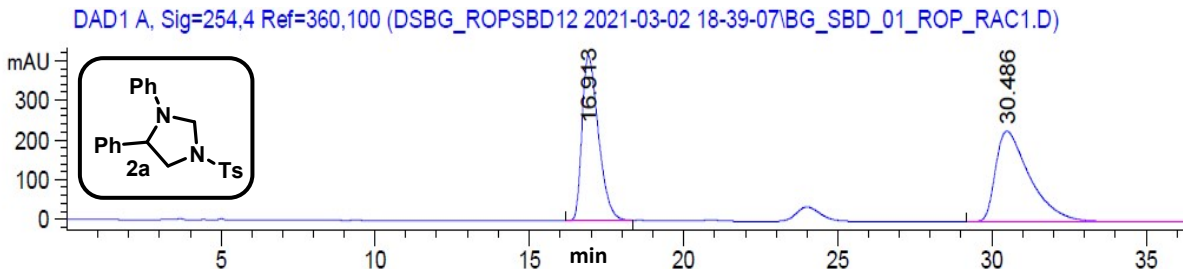

Peak	Retention Time(min)	Type	Area (%)
1	16.916	BV	43.78
2	30.486	BBA	49.80

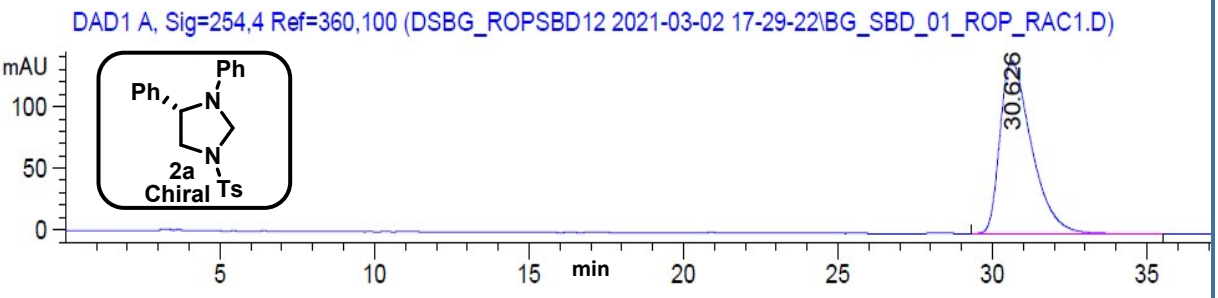

Peak	Retention Time (min)	Type	Area (%)
1	30.626	BB	99.99

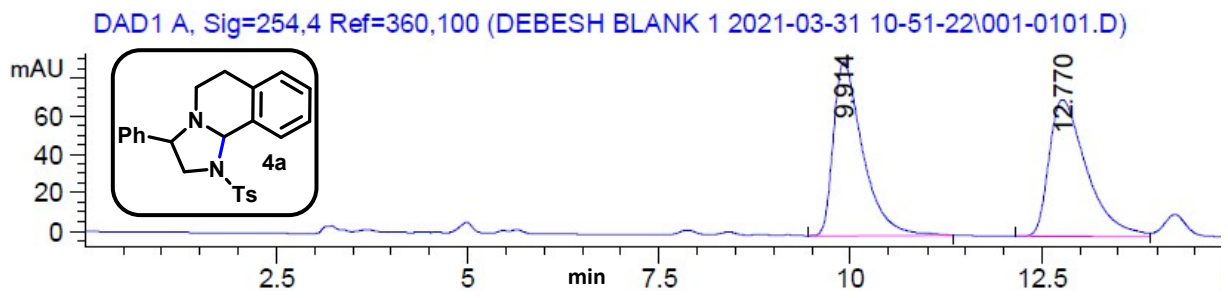

Peak	Retention Time(min)	Type	Area (%)
1	9.914	BB	45.45
2	12.77	BV	45.90

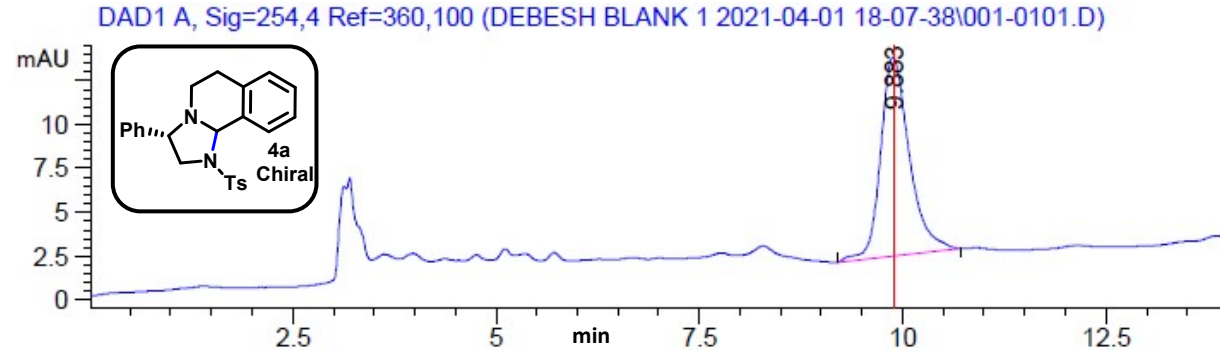

Peak	Retention Time(min)	Type	Area (%)
1	9.883	BB	99.99%

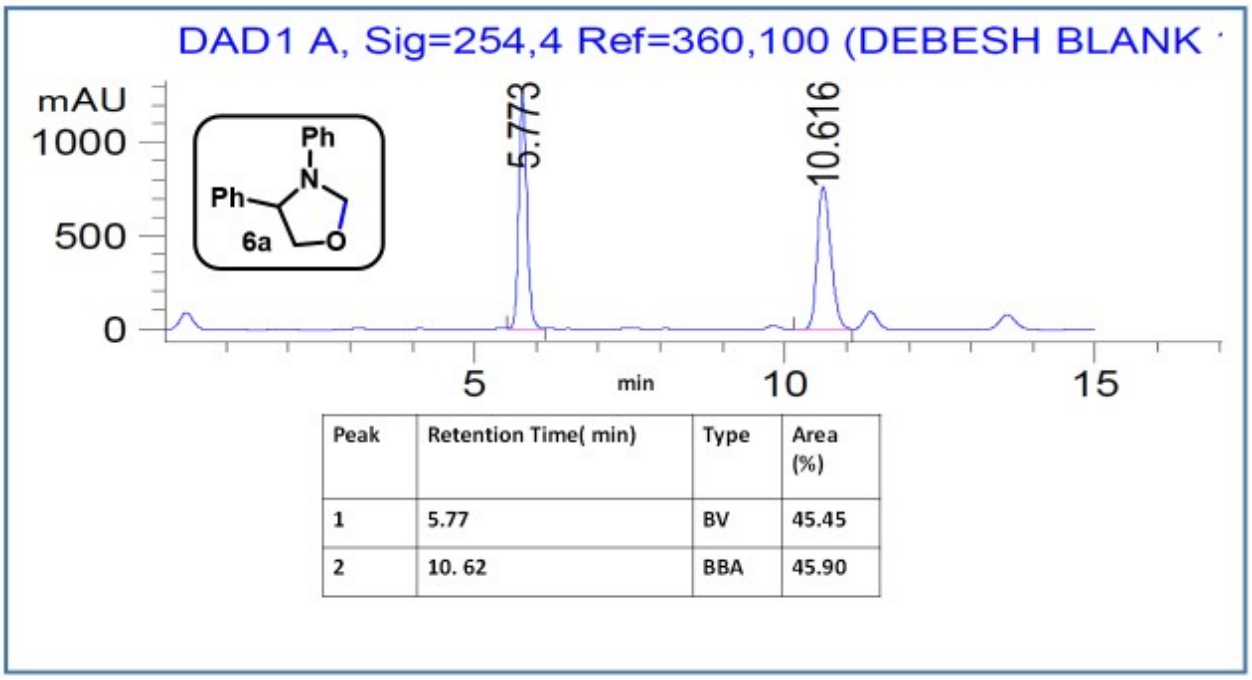

Peak	Retention Time(min)	Type	Area (%)
1	5.77	BV	45.45
2	10. 62	BBA	45.90

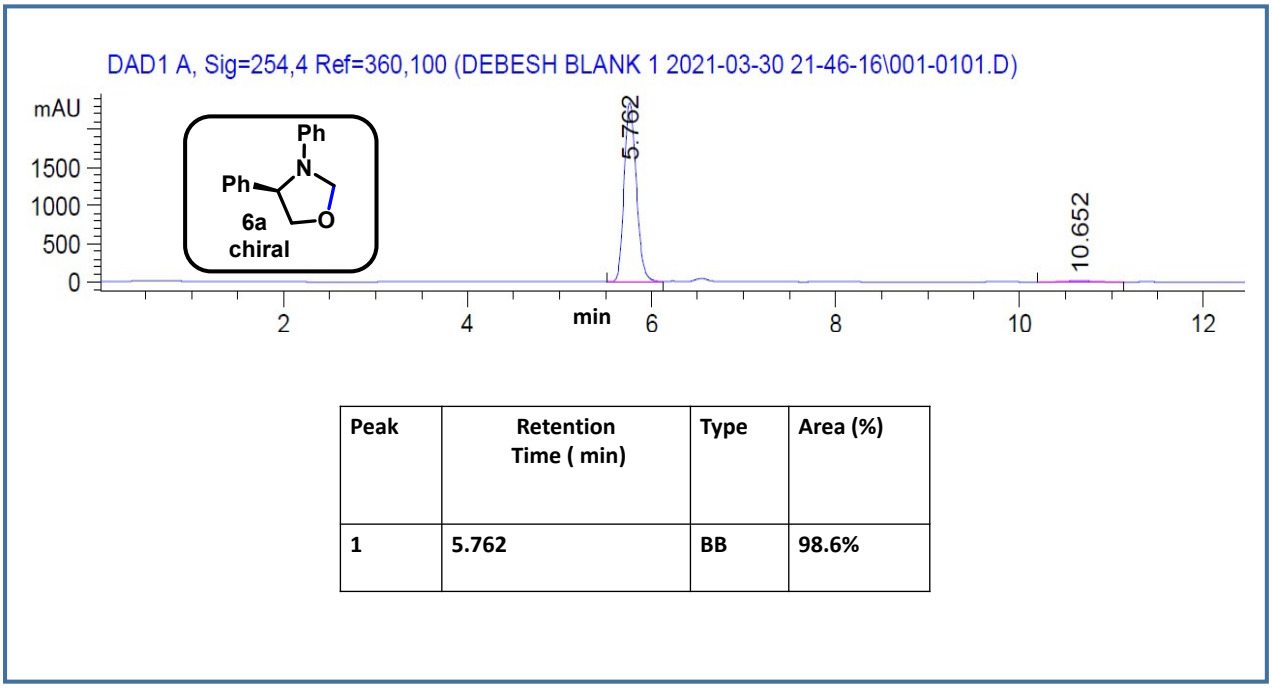

Peak	Retention Time (min)	Type	Area (%)
1	5.762	BB	98.6%

21. Copies of NMR and CMR spectra of products:

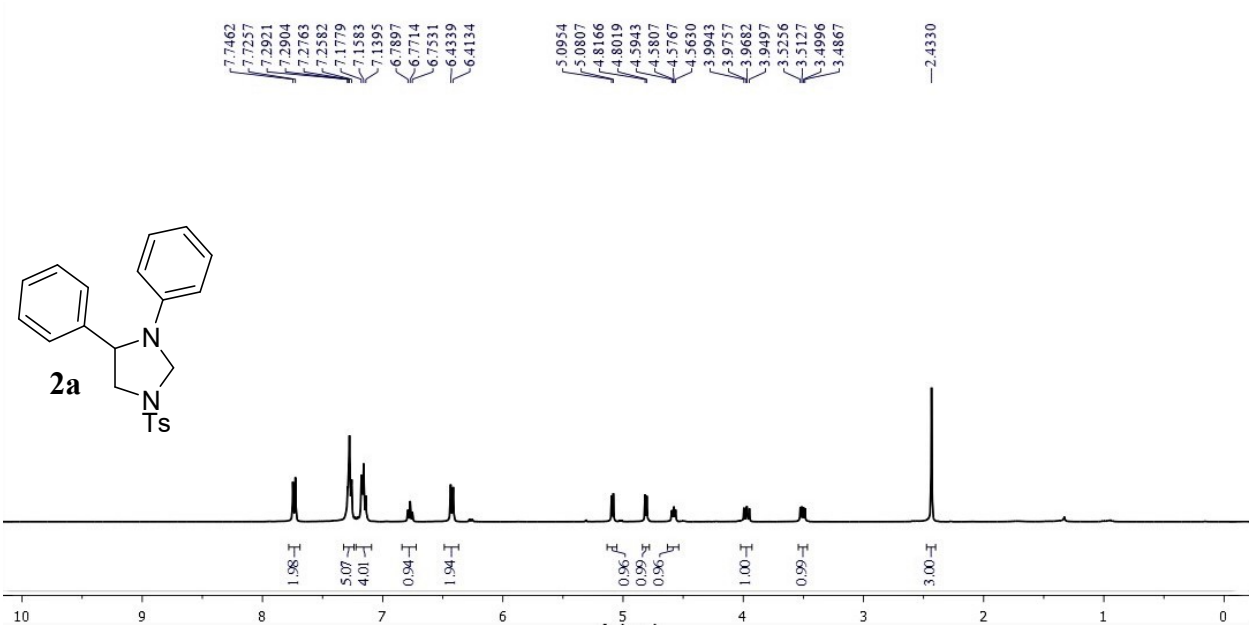

Figure S22. ^{1}H NMR of **2a** (400 MHz, $CDCl_3$)

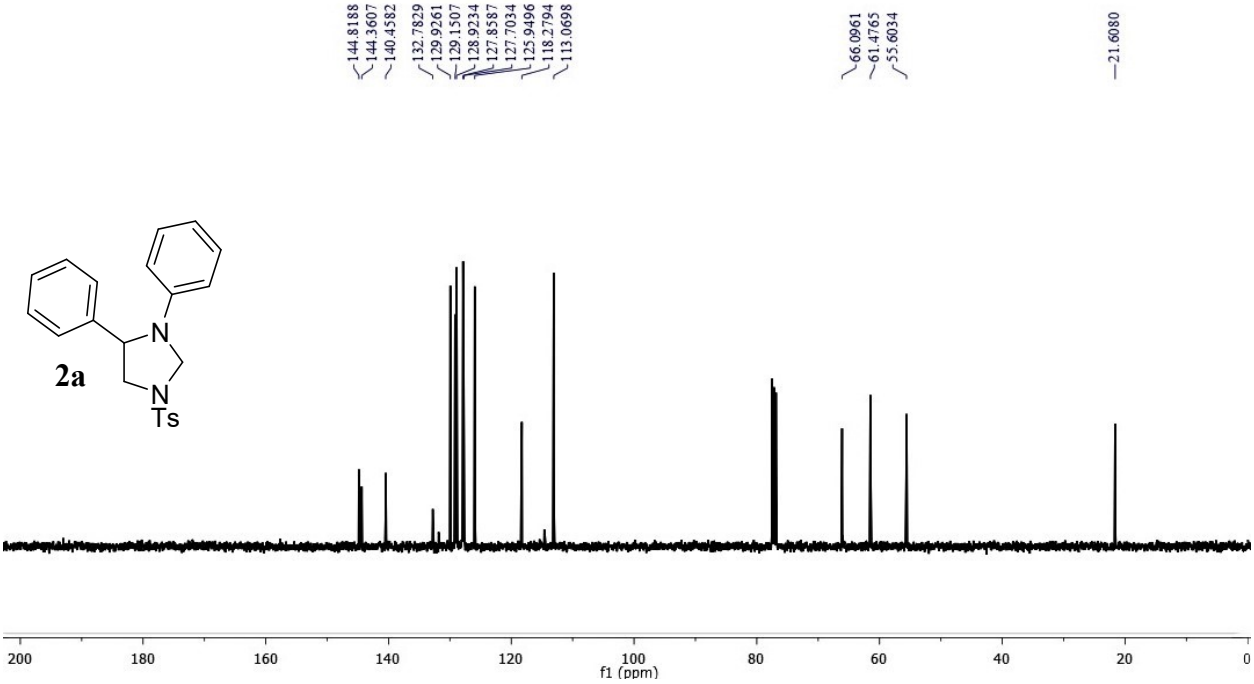

Figure S23. $^{13}C\{^{1}H\}$ NMR of **2a** (100 MHz, $CDCl_3$)

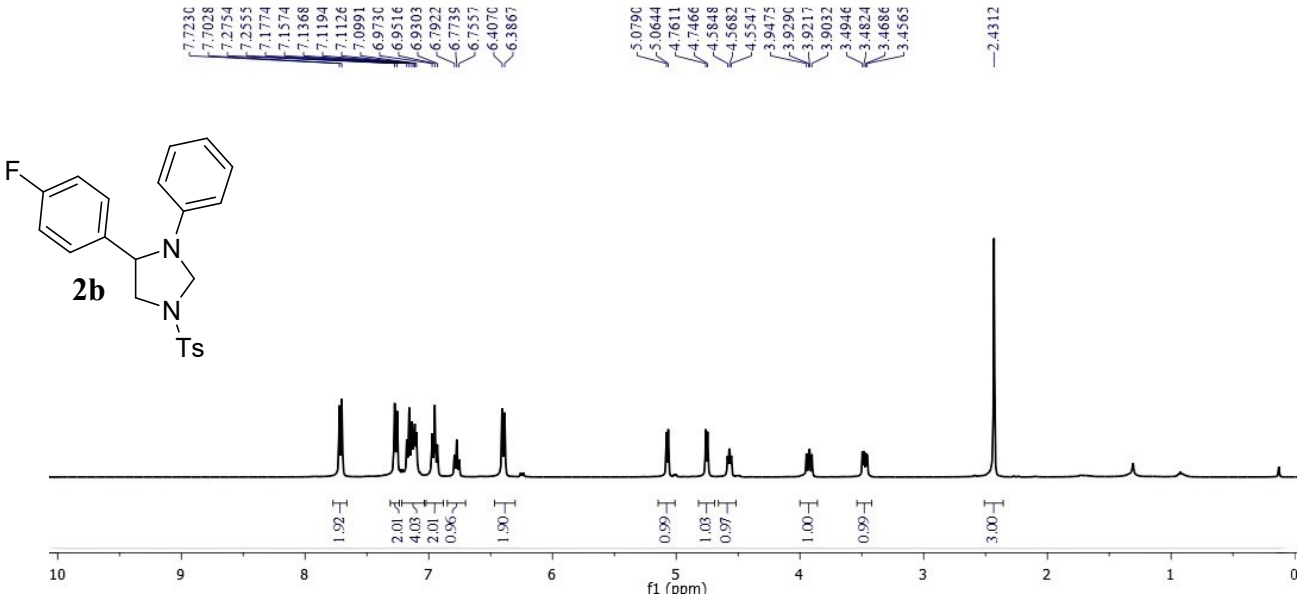

Figure S24. ^{1}H NMR of **2b** (400 MHz, $CDCl_3$)

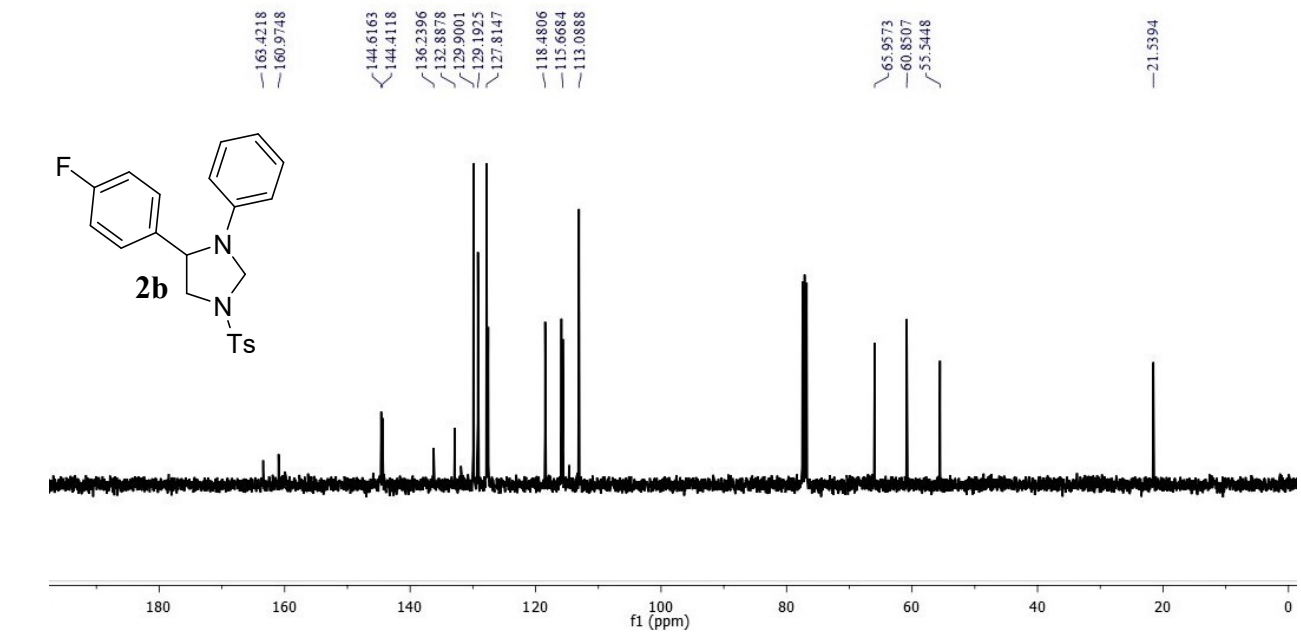

Figure S25. $^{13}C\{^{1}H\}$ NMR of **2b** (100 MHz, $CDCl_3$)

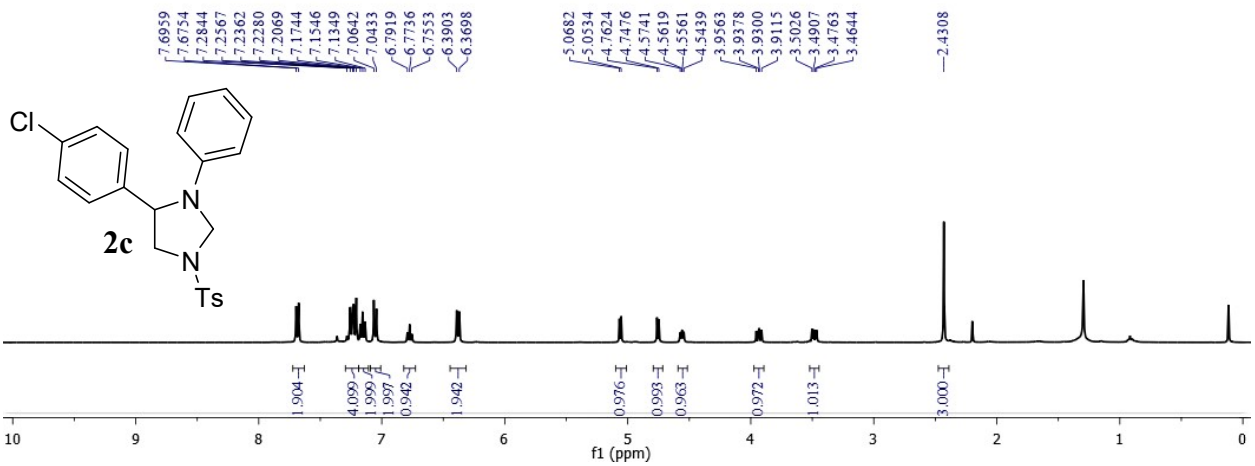

Figure S26. ^{1}H NMR of **2c** (400 MHz, $CDCl_3$)

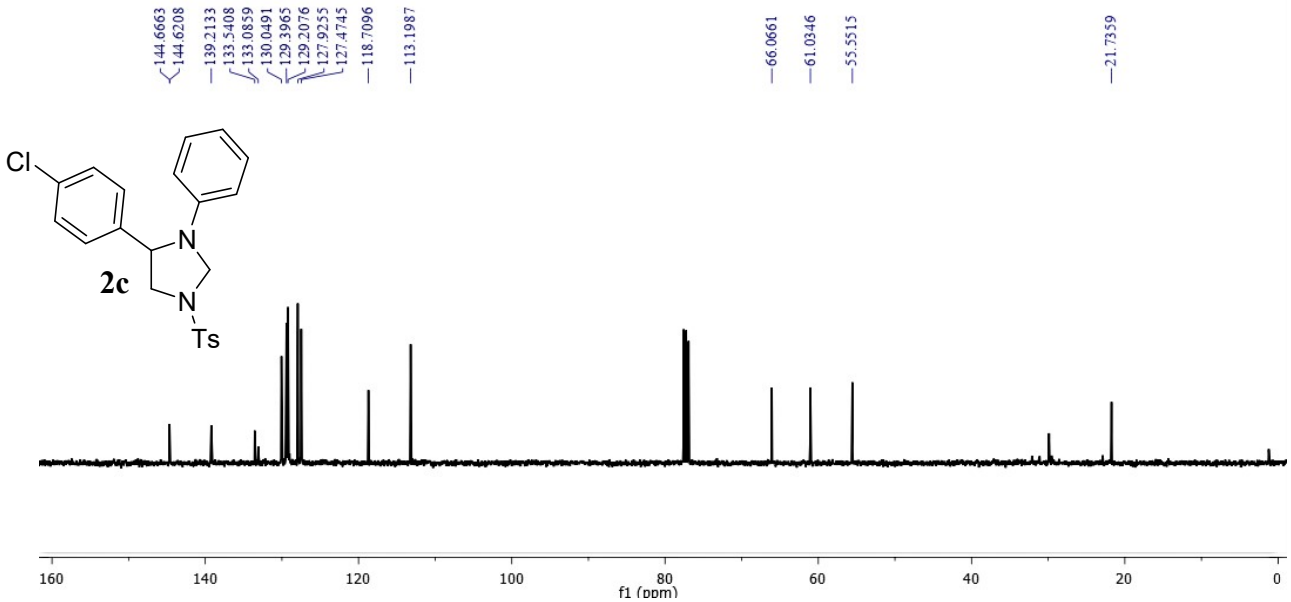

Figure S27. $^{13}C\{^{1}H\}$ NMR of **2c** (100 MHz, $CDCl_3$)

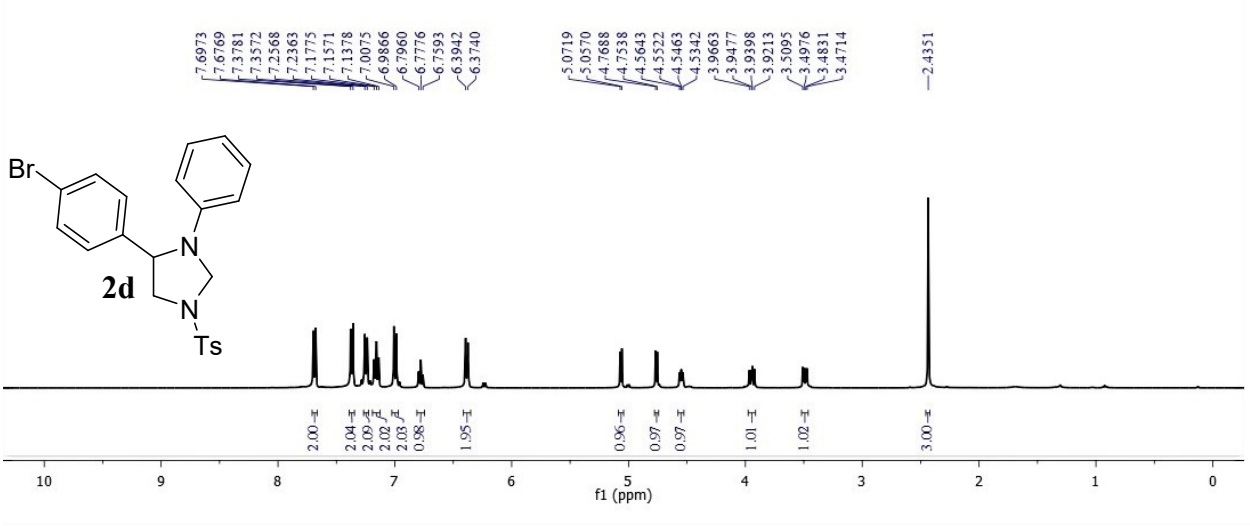

Figure S28. ^{1}H NMR of **2d** (400 MHz, $CDCl_3$)

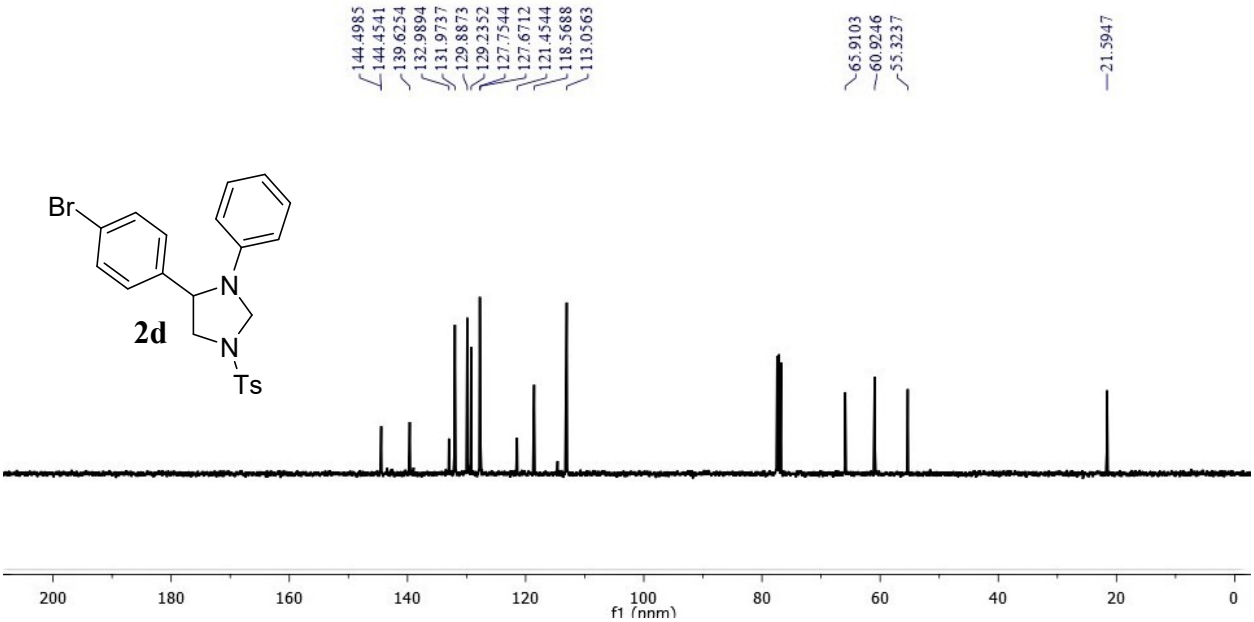

Figure S29. $^{13}C\{^{1}H\}$ NMR of **2d** (100 MHz, $CDCl_3$)

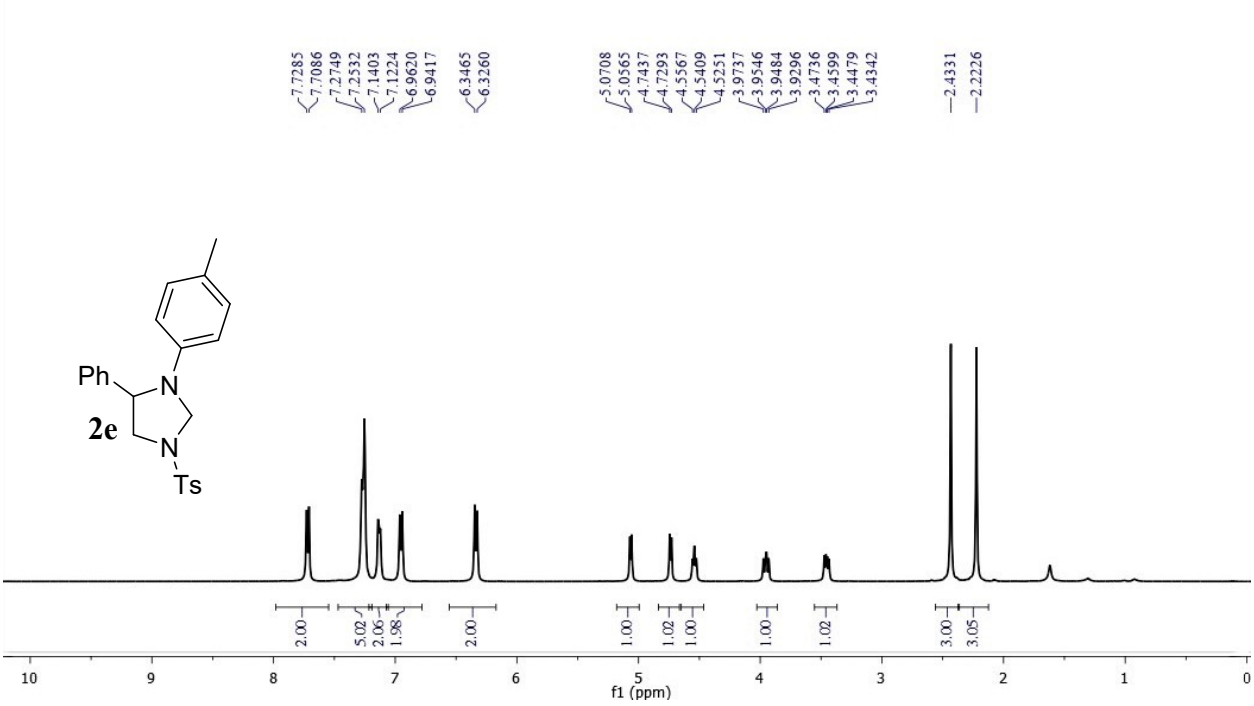

Figure S30. ^{1}H NMR of **2e** (400 MHz, $CDCl_3$)

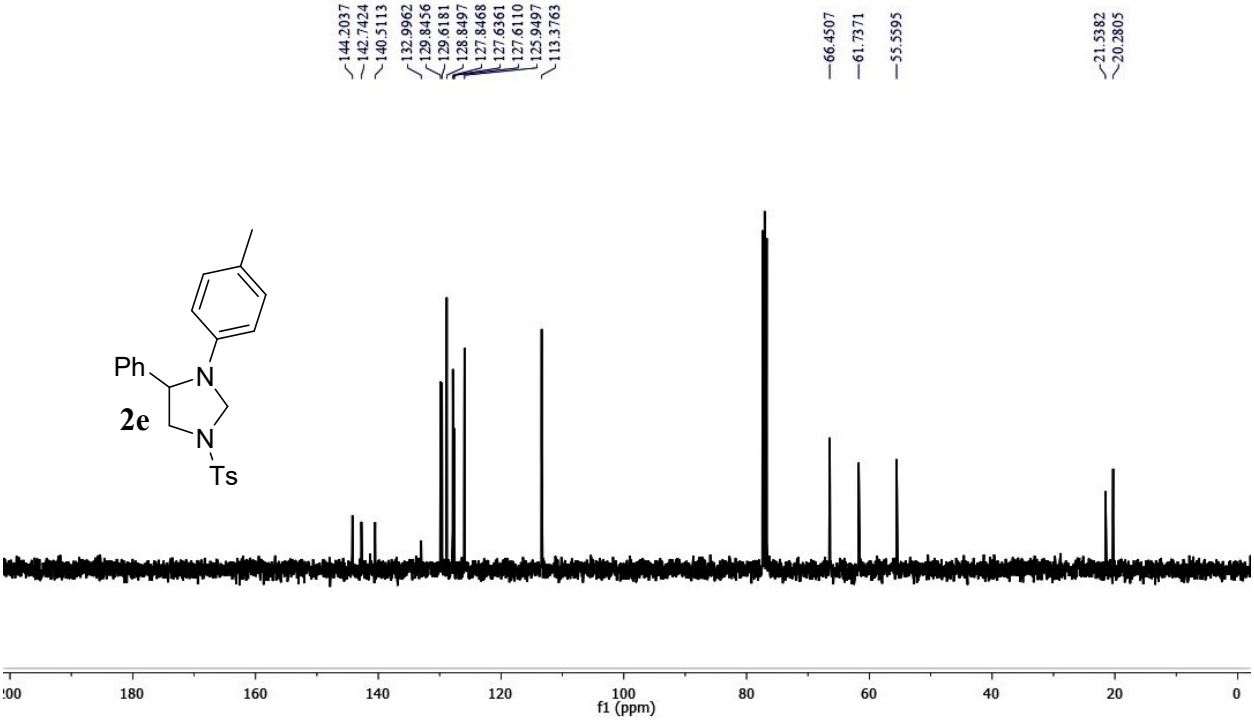

Figure S31. $^{13}C\{^{1}H\}$ NMR of **2e** (100 MHz, $CDCl_3$)

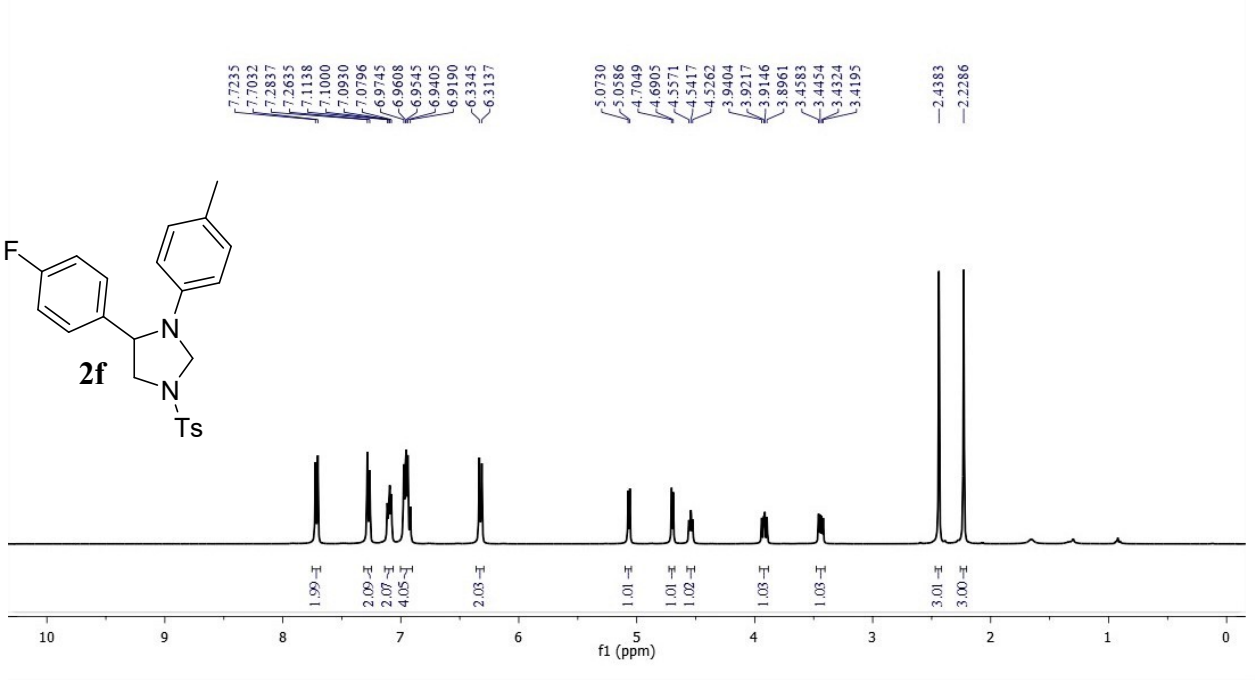

Figure S32. ^{1}H NMR of **2f** (400 MHz, $CDCl_3$)

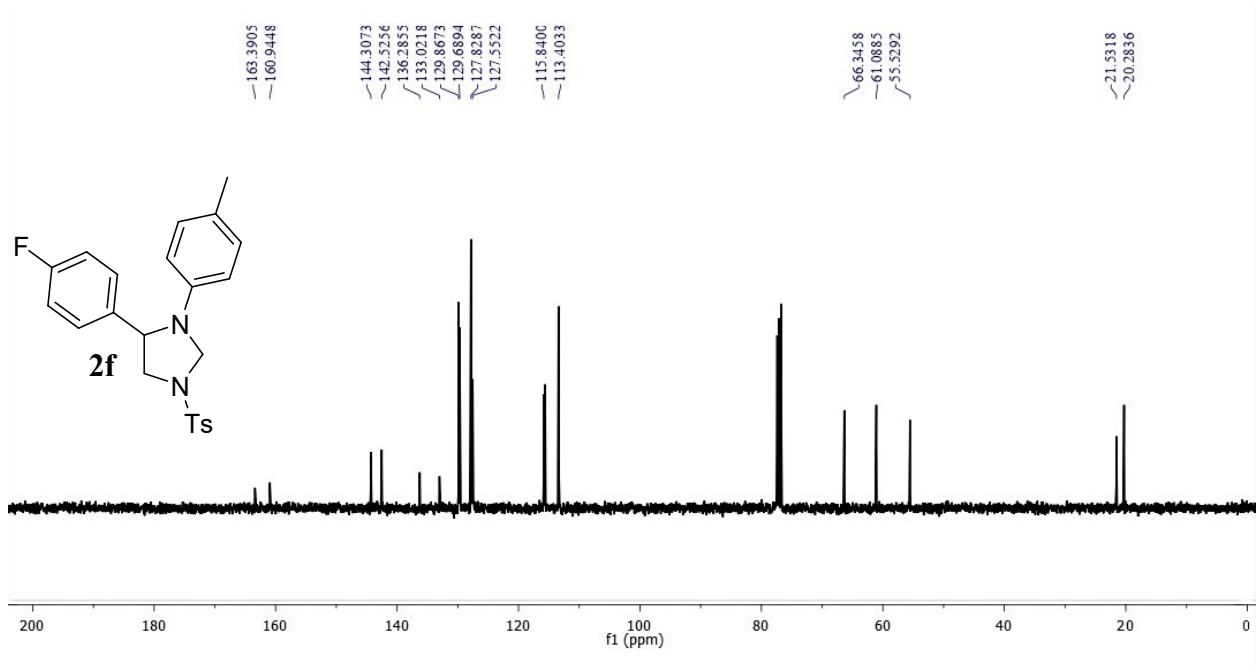

Figure S33. $^{13}C\{^{1}H\}$ NMR of **2f** (100 MHz, $CDCl_3$)

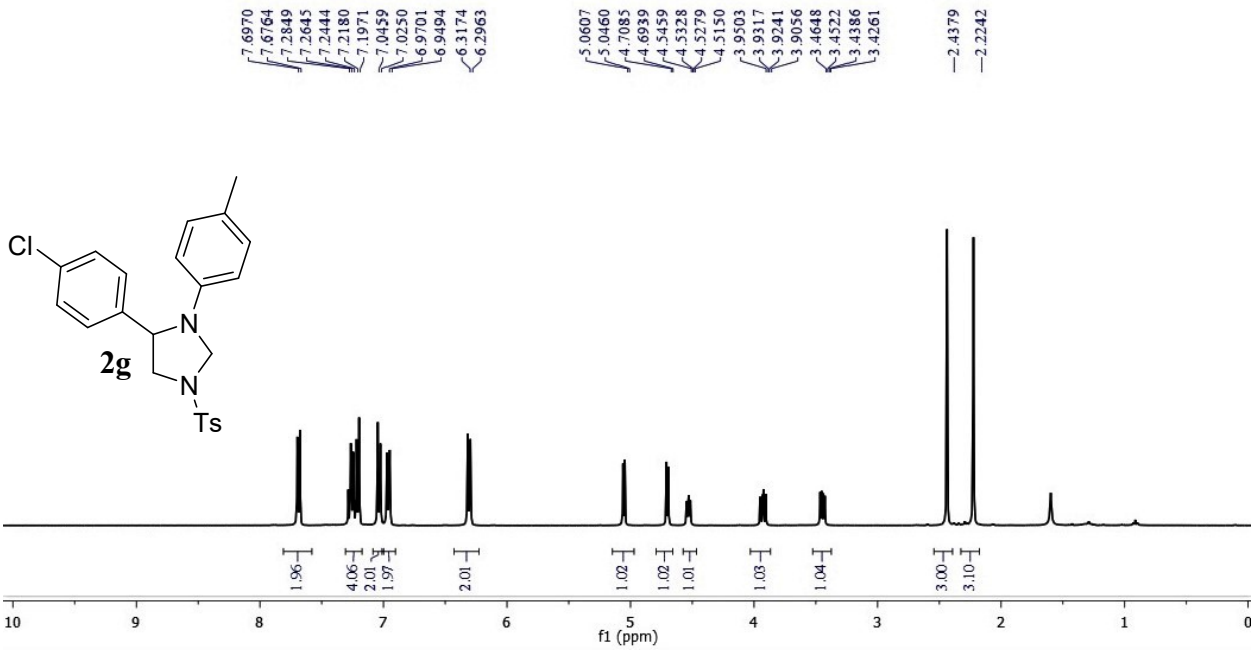

Figure S34. ^{1}H NMR of **2g** (400 MHz, $CDCl_3$)

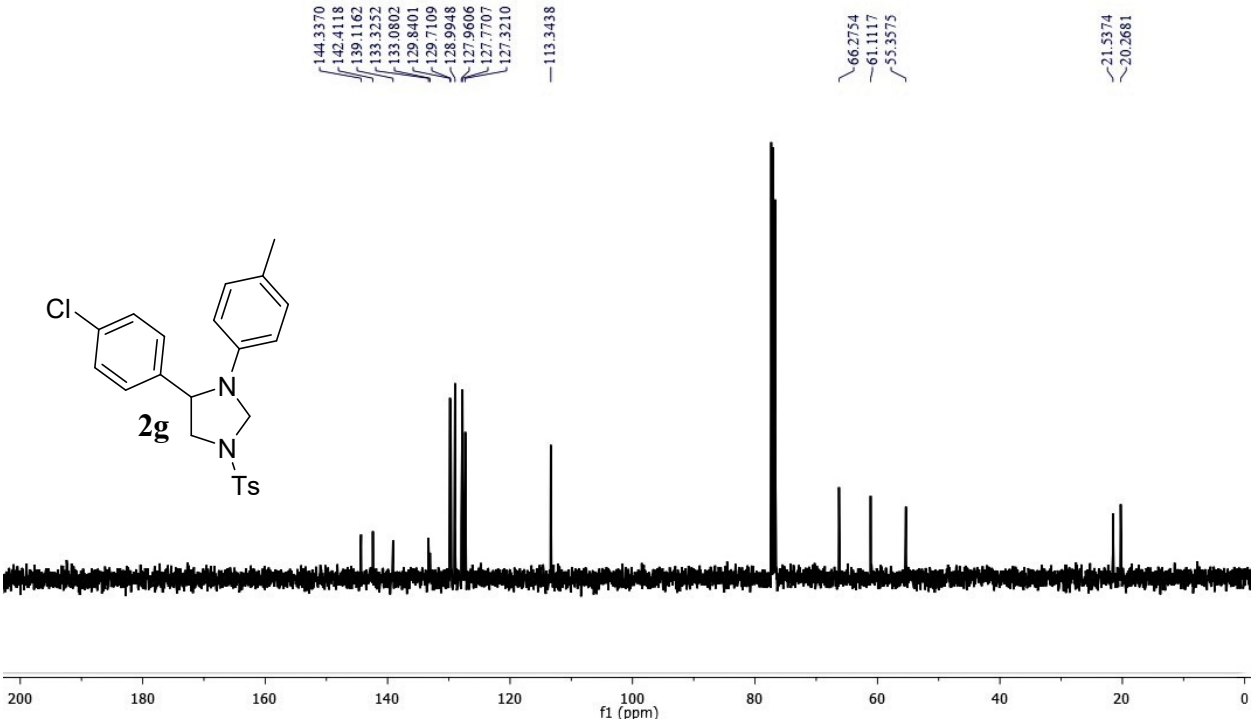

Figure S35. $^{13}C\{^{1}H\}$ NMR of **2g** (100 MHz, $CDCl_3$)

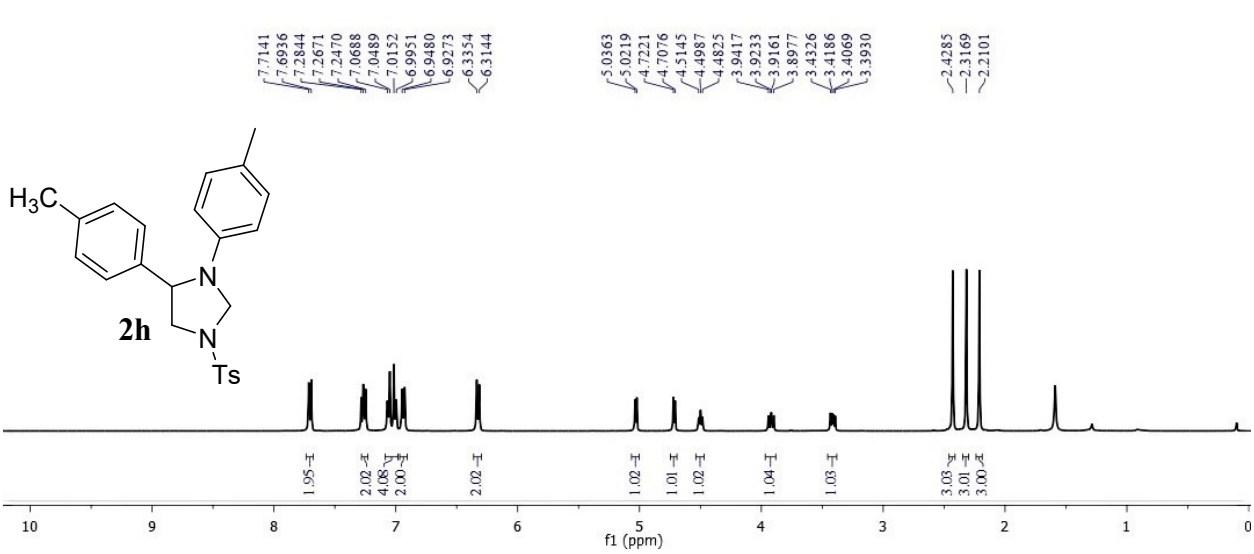

Figure S36. ^{1}H NMR of **2h** (400 MHz, $CDCl_3$)

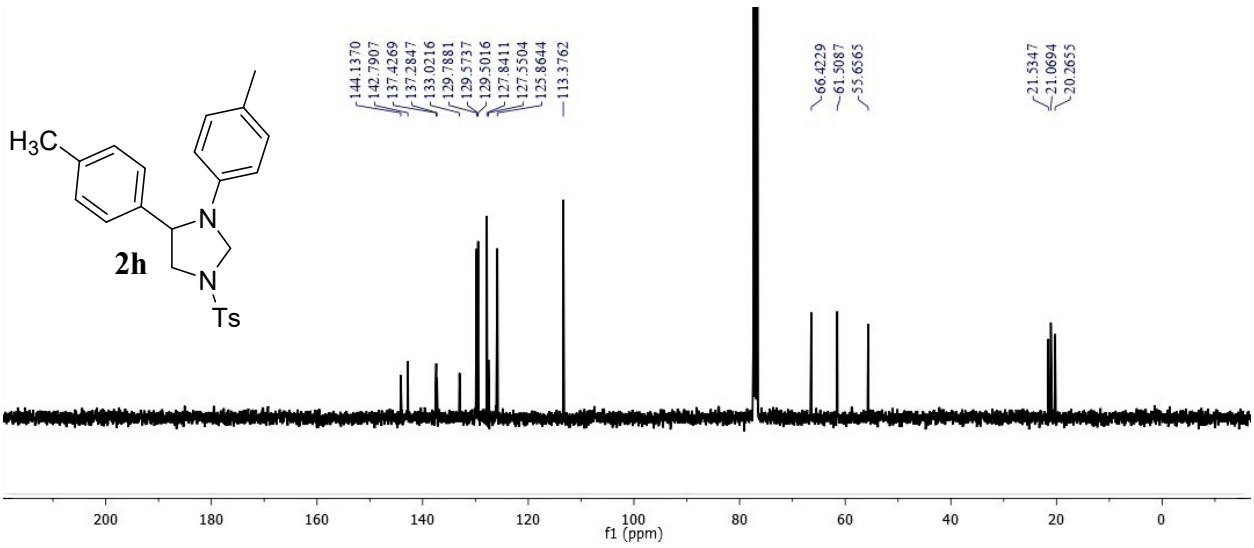

Figure S37. $^{13}C\{^{1}H\}$ NMR of **2h** (100 MHz, $CDCl_3$)

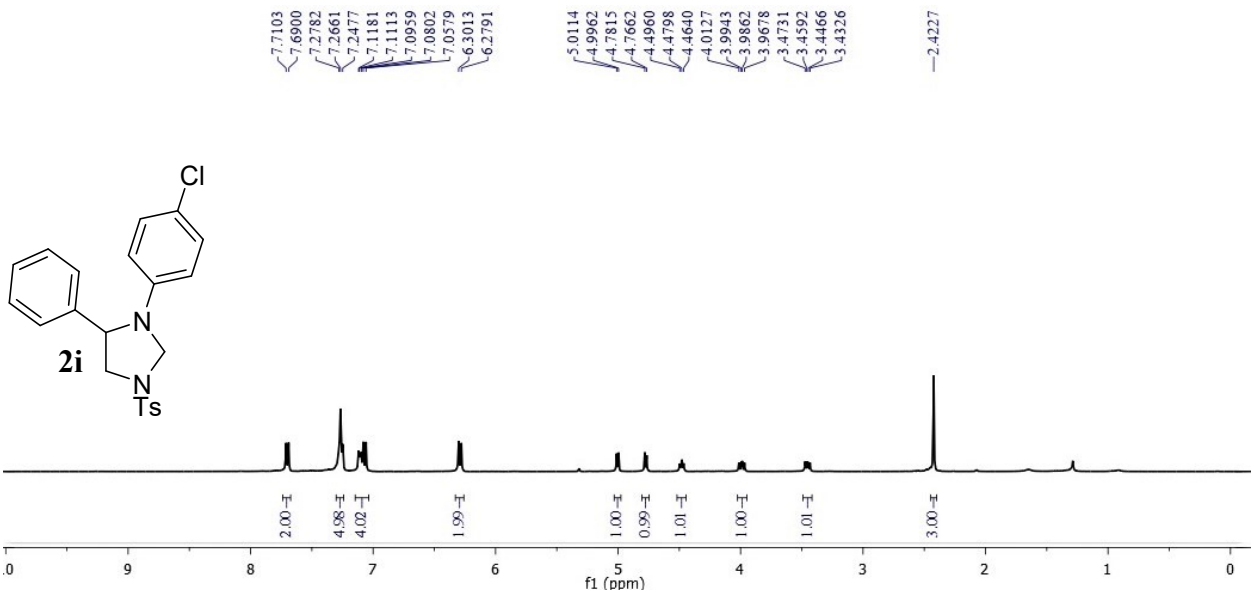

Figure S38. ^{1}H NMR of **2i** (400 MHz, $CDCl_3$)

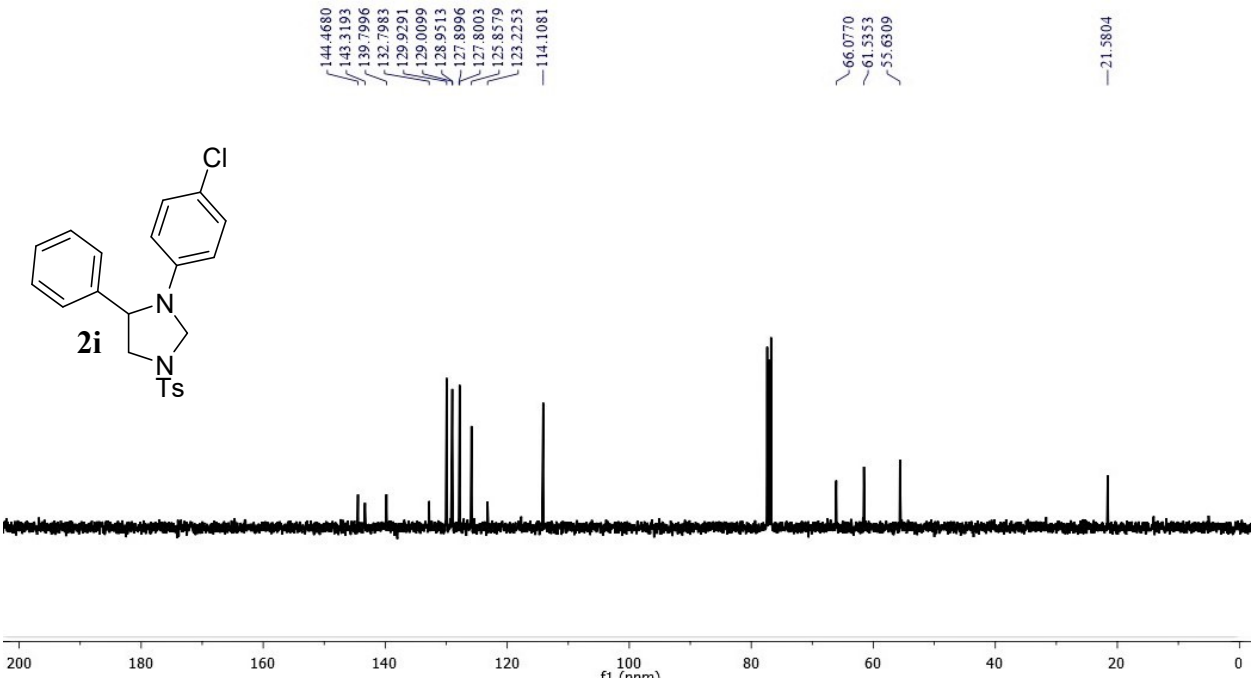

Figure S39. $^{13}C\{^{1}H\}$ NMR of **2i** (100 MHz, $CDCl_3$)

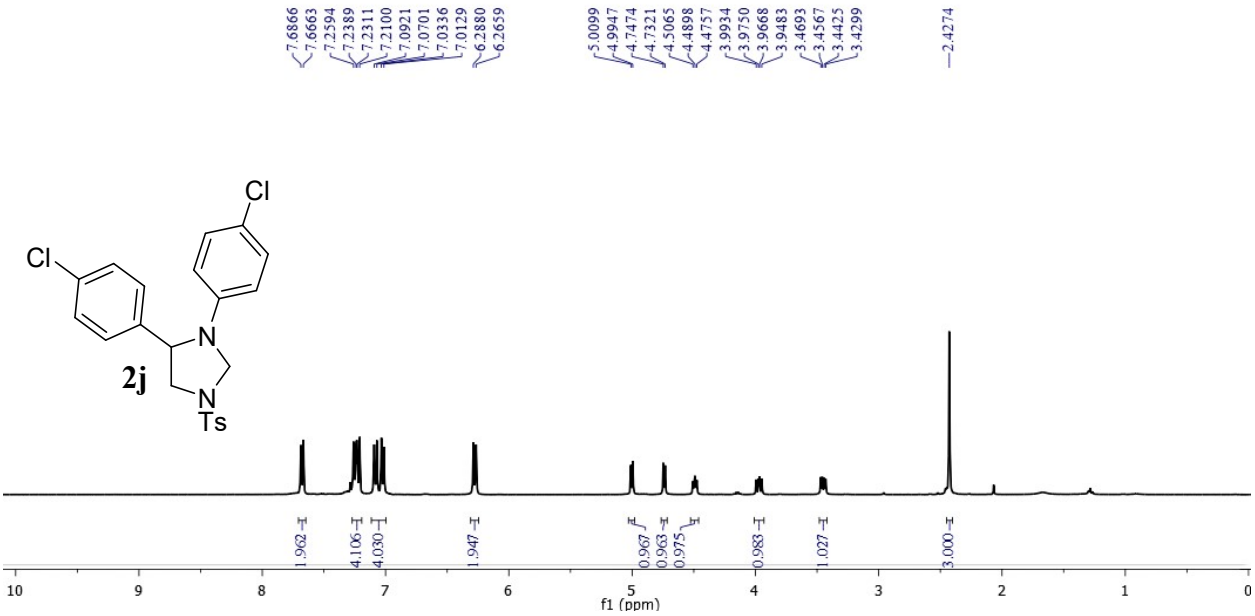

Figure S40. $^{13}C\{^{1}H\}$ NMR of **2j** (100 MHz, $CDCl_3$)

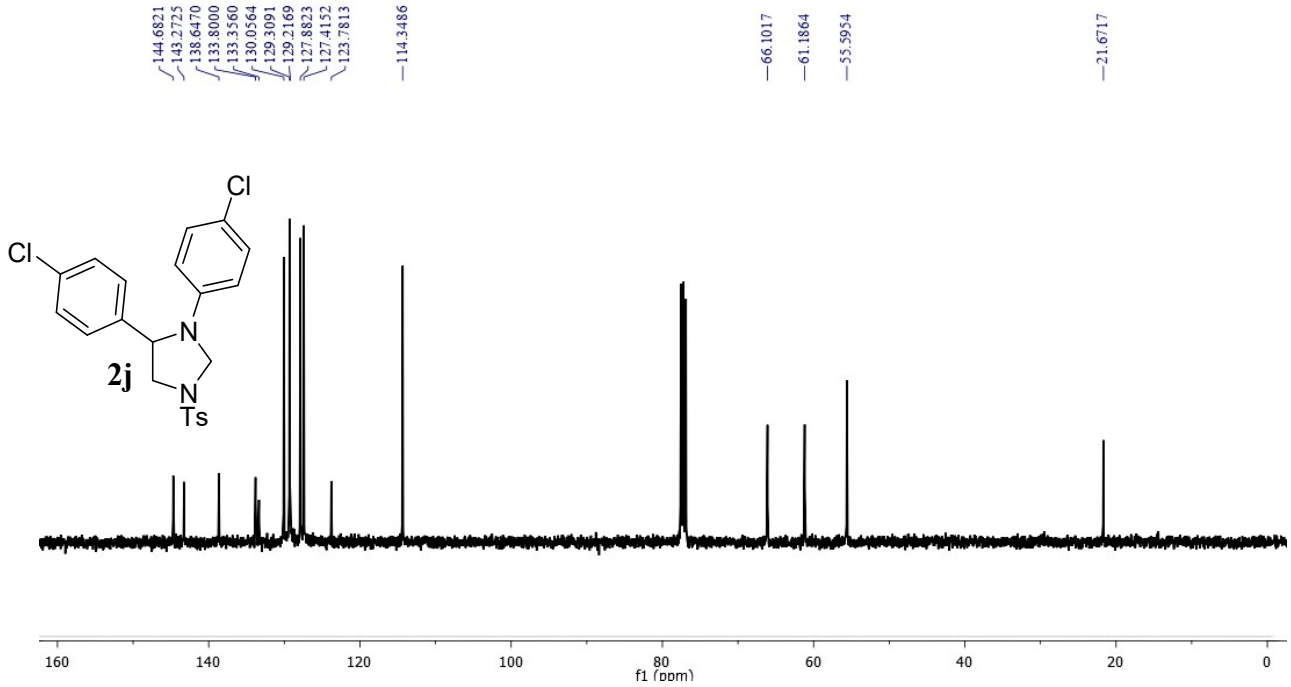

Figure S41. $^{13}C\{^{1}H\}$ NMR of **2j** (100 MHz, $CDCl_3$)

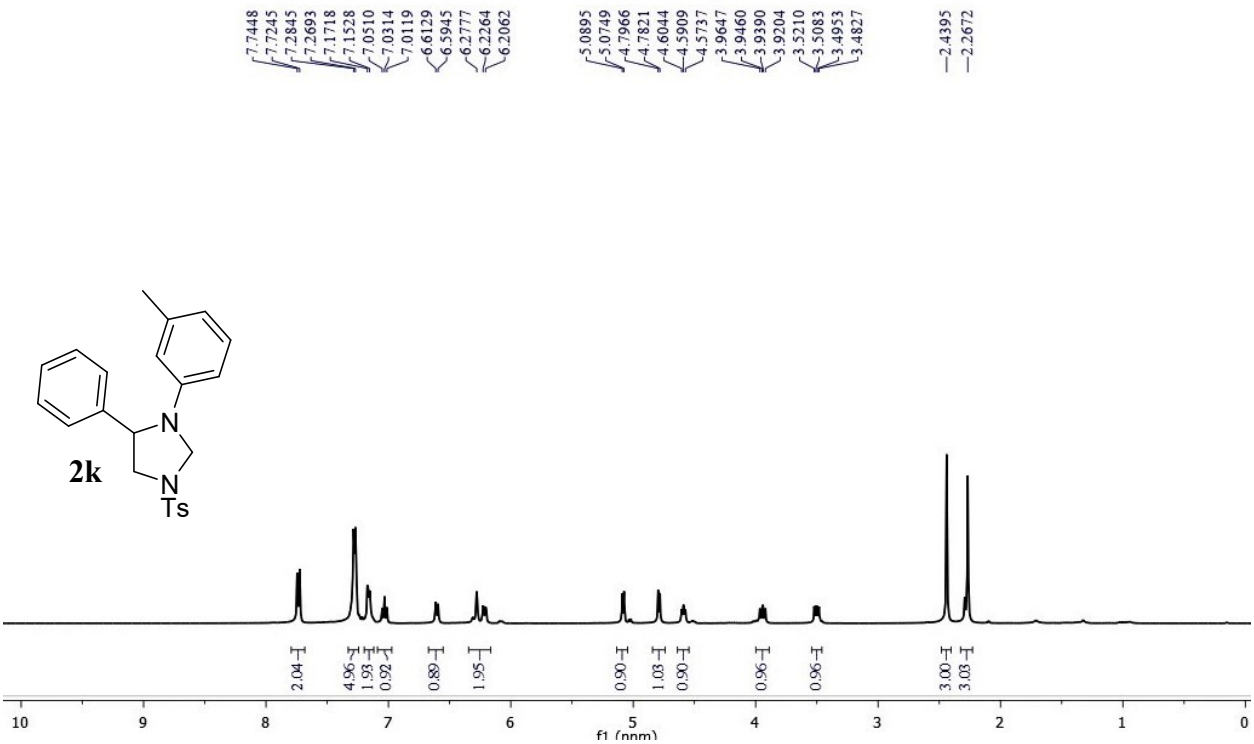

Figure S42. ^{1}H NMR of **2k** (400 MHz, $CDCl_3$)

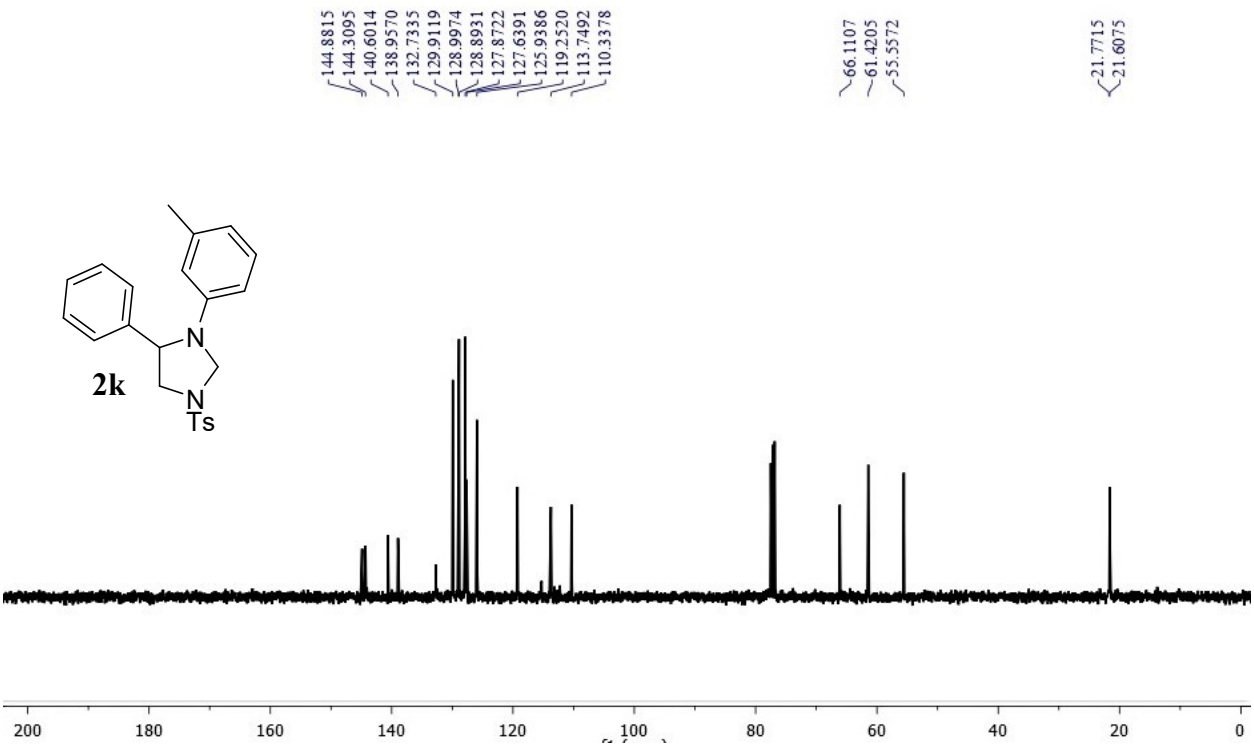

Figure S43. $^{13}C\{^{1}H\}$ NMR of **2k** (100 MHz, $CDCl_3$)

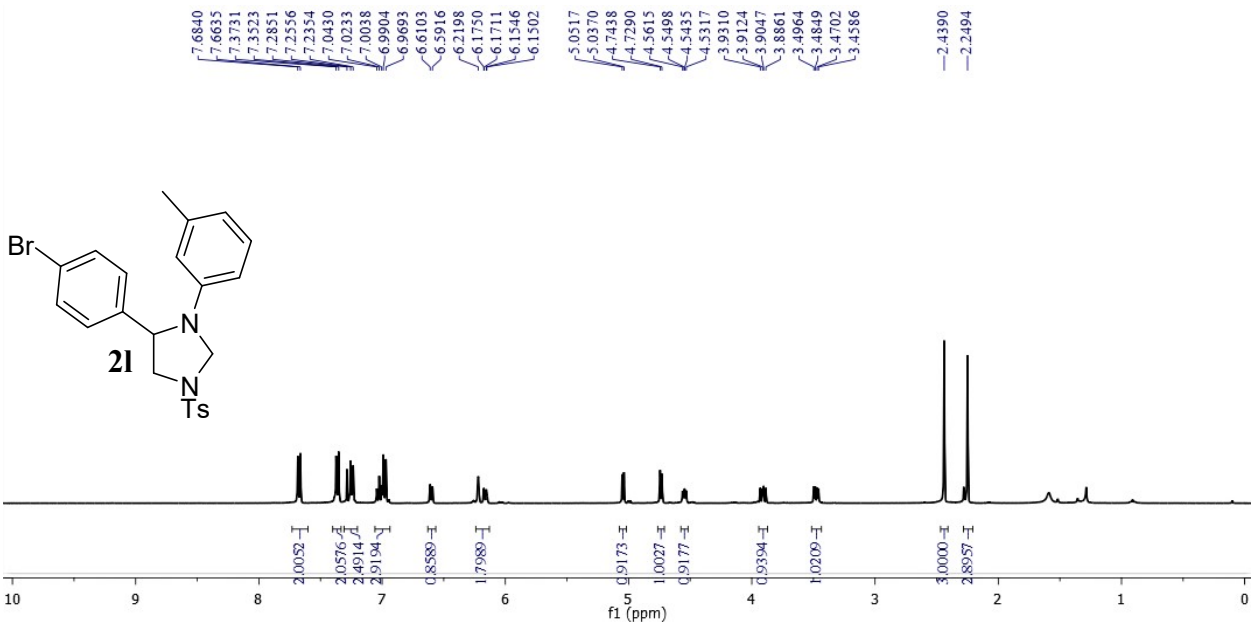

Figure S44. ^{1}H NMR of **2l** (400 MHz, $CDCl_3$)

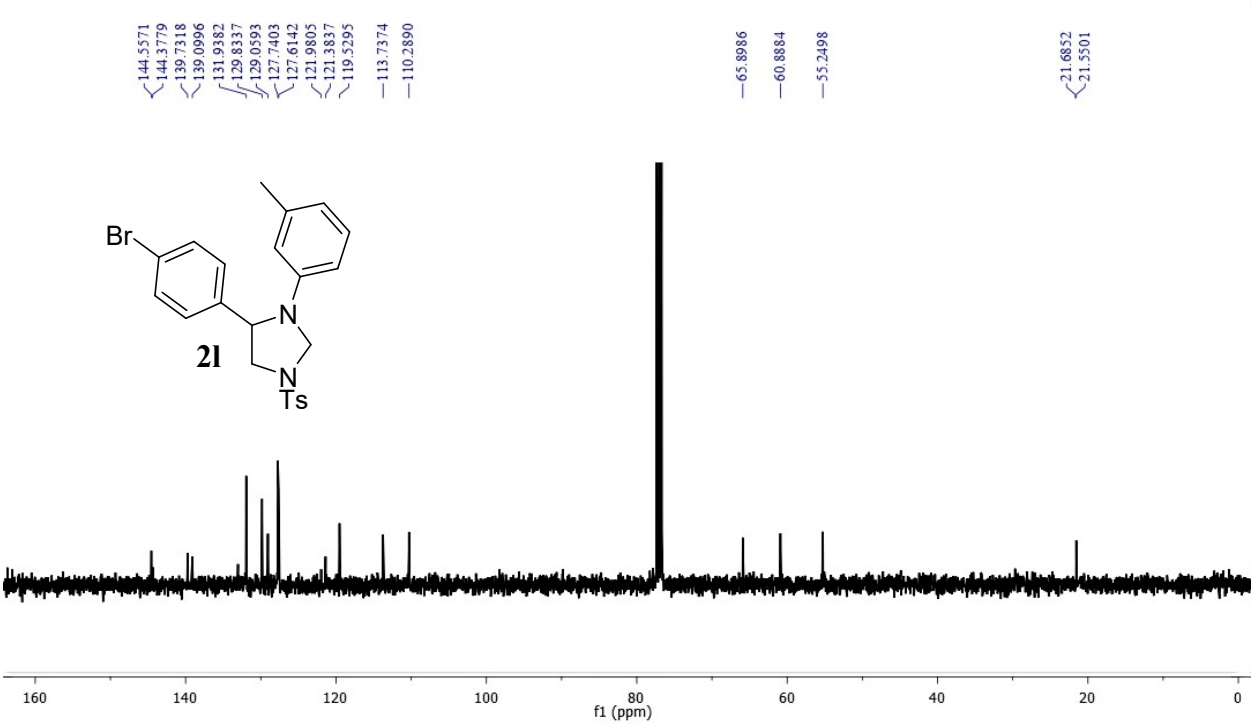

Figure S45. $^{13}C\{^{1}H\}$ NMR of **2l** (100 MHz, $CDCl_3$)

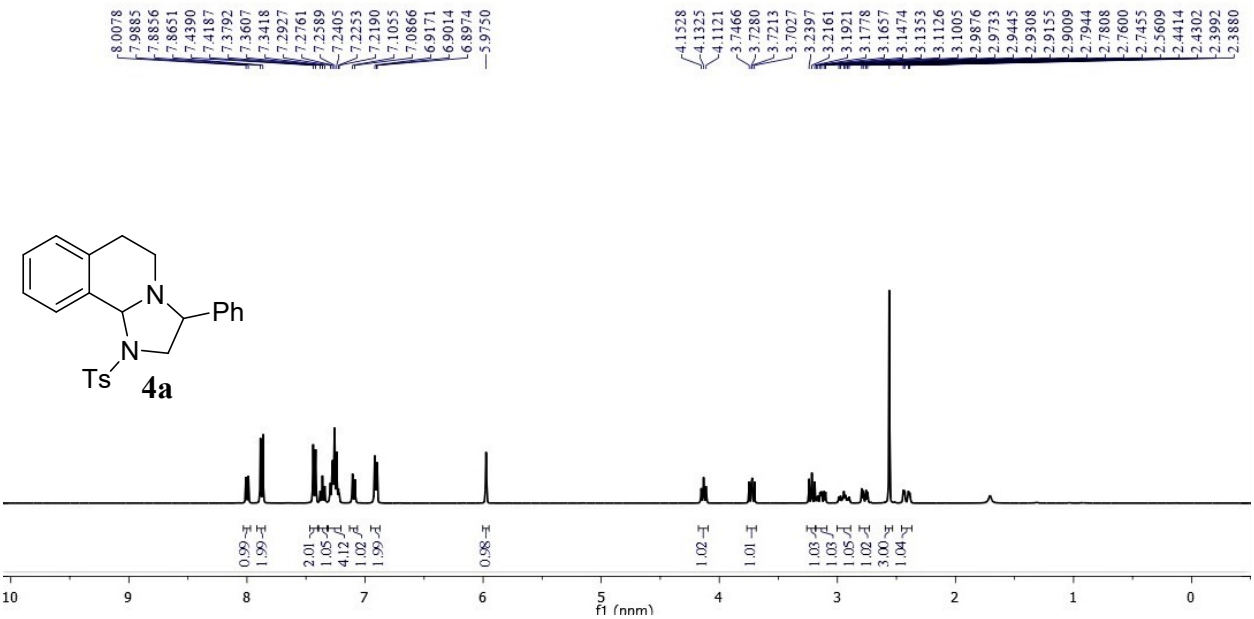

Figure S46. ^{1}H NMR of **4a** (400 MHz, $CDCl_3$)

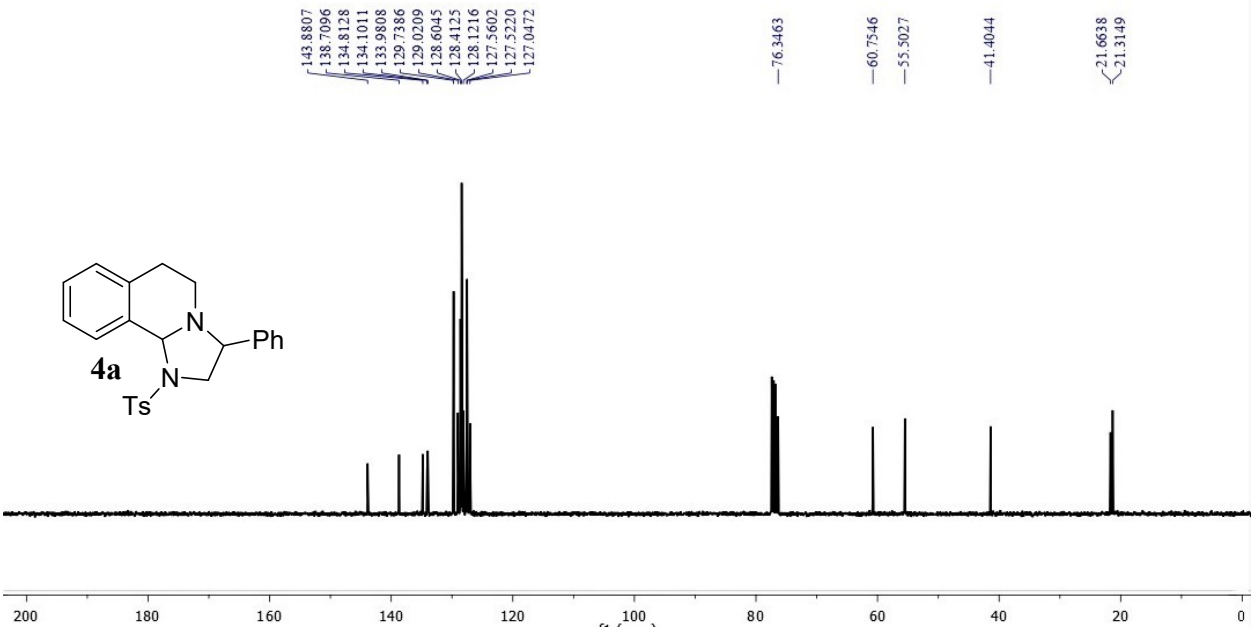

Figure S47. $^{13}C\{^{1}H\}$ NMR of **4a** (100 MHz, $CDCl_3$)

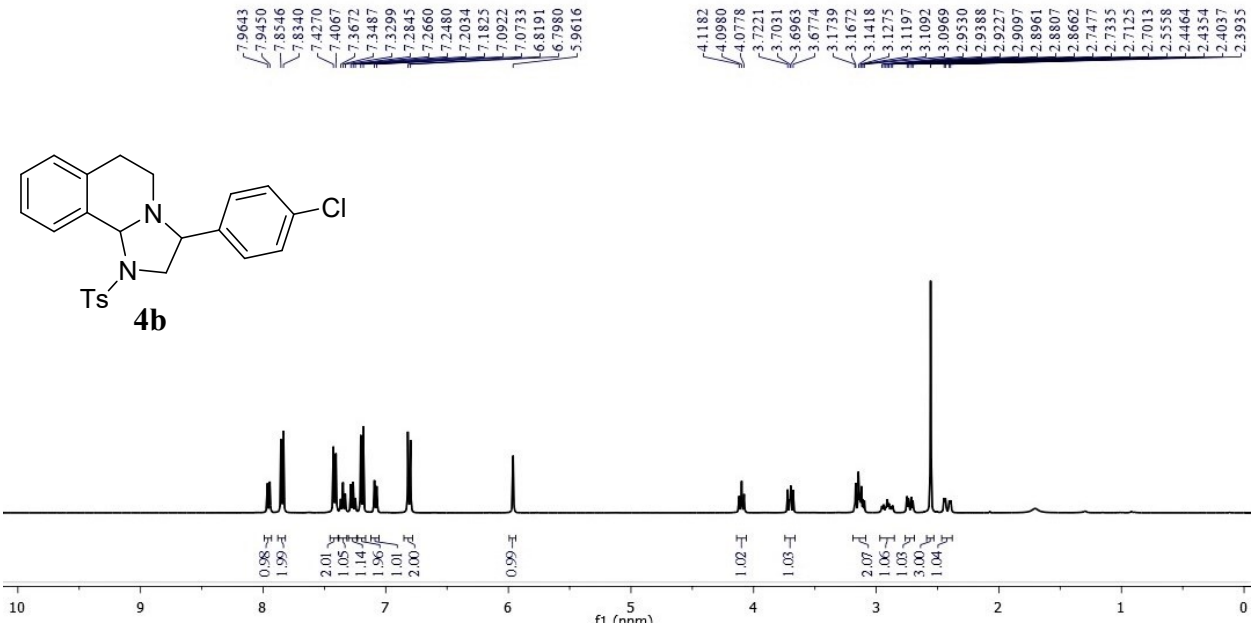

Figure S48. ^{1}H NMR of **4b** (400 MHz, $CDCl_3$)

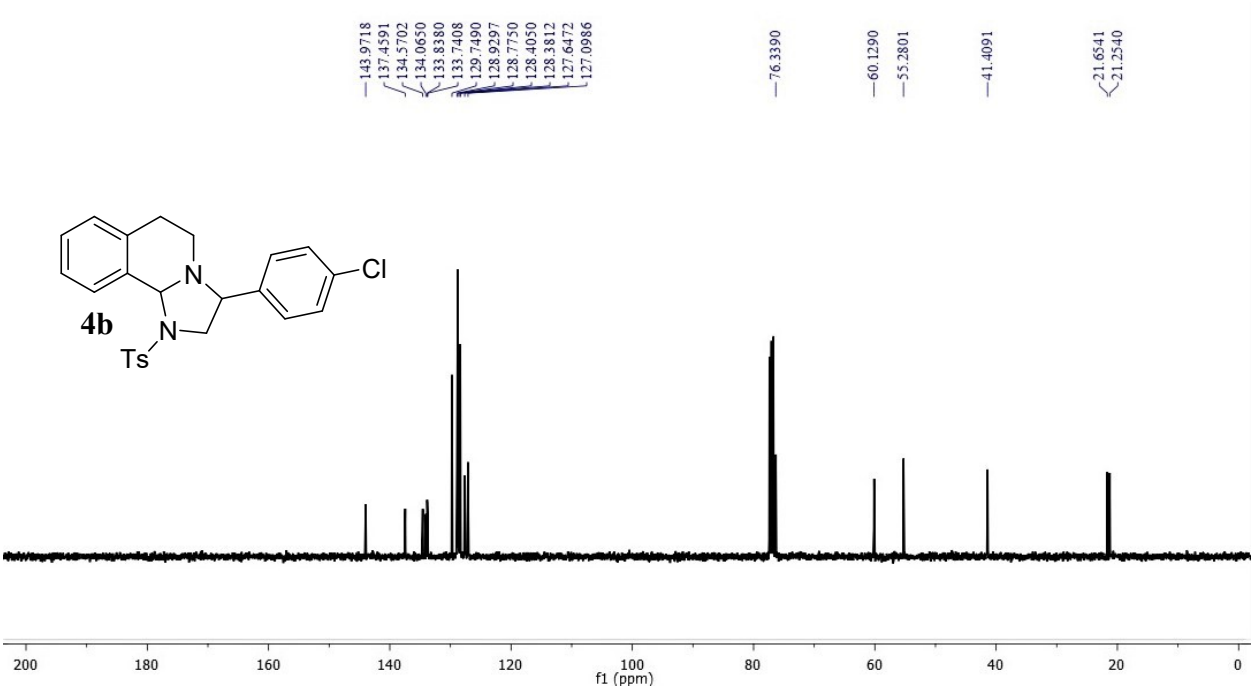

Figure S49. $^{13}C\{^{1}H\}$ NMR of **4b** (100 MHz, $CDCl_3$)

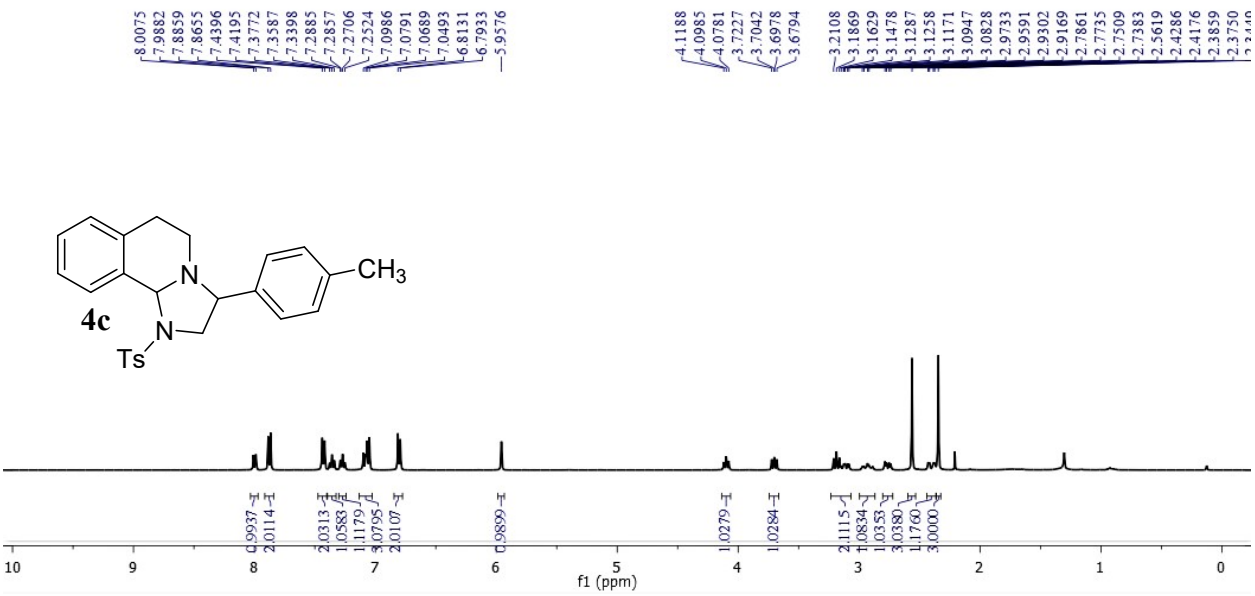

Figure S50. ^{1}H NMR of **4c** (400 MHz, $CDCl_3$)

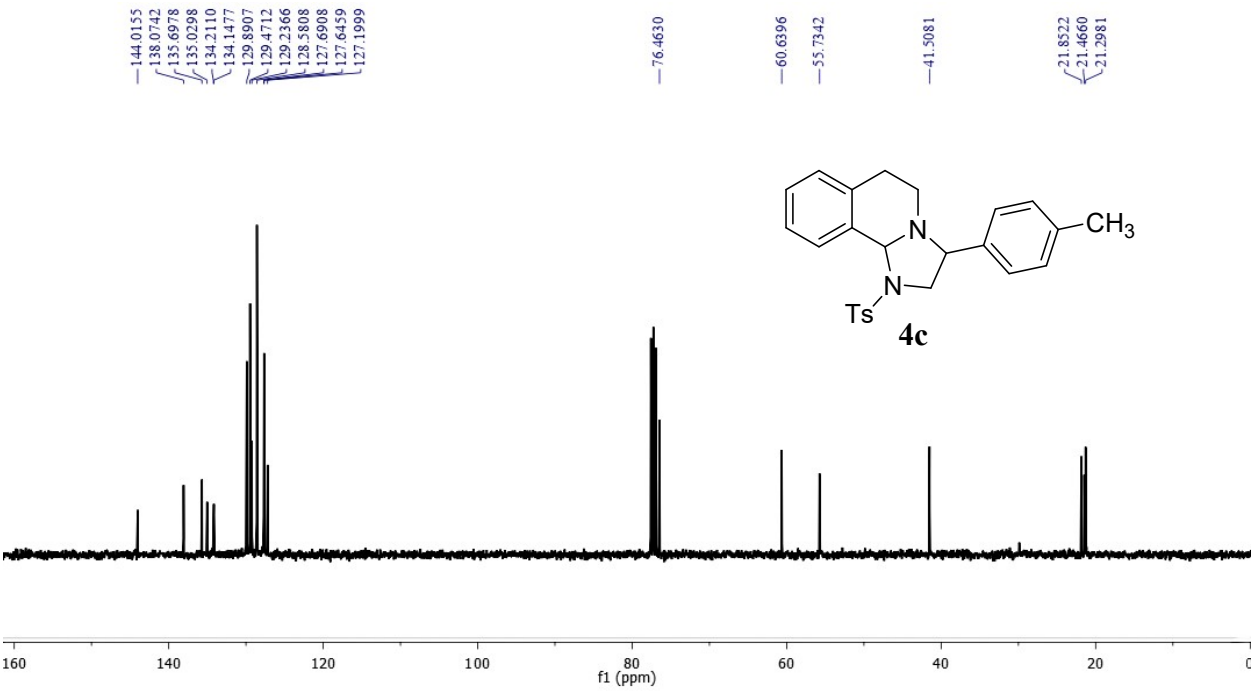

Figure S51. $^{13}C\{^{1}H\}$ NMR of **4c** (100 MHz, $CDCl_3$)

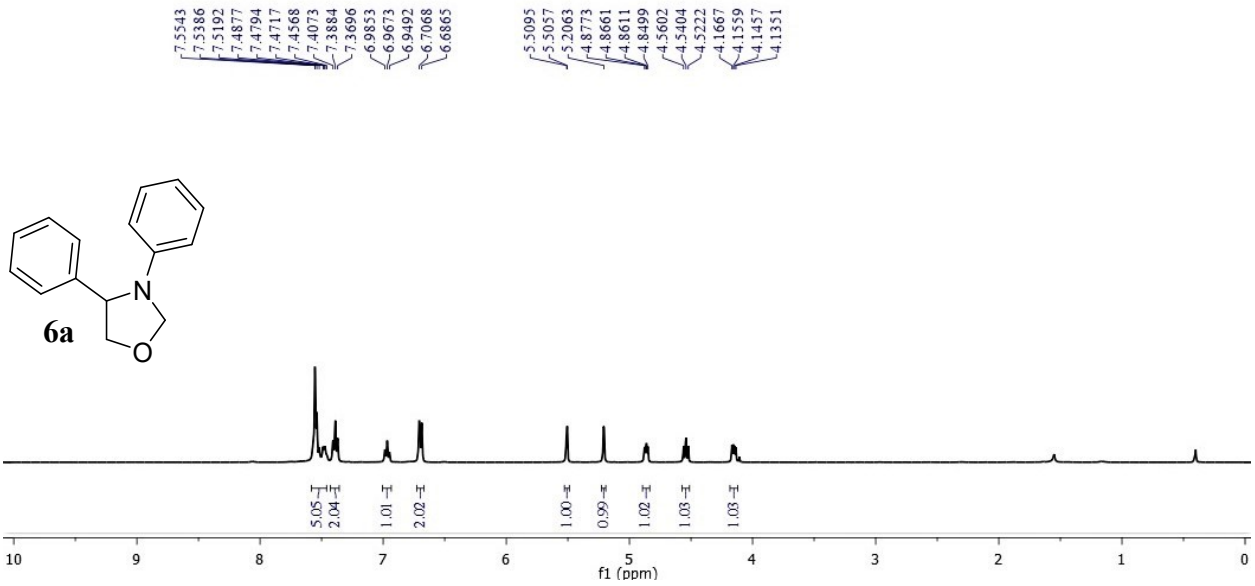

Figure S52. ^{1}H NMR of **6a** (400 MHz, $CDCl_3$)

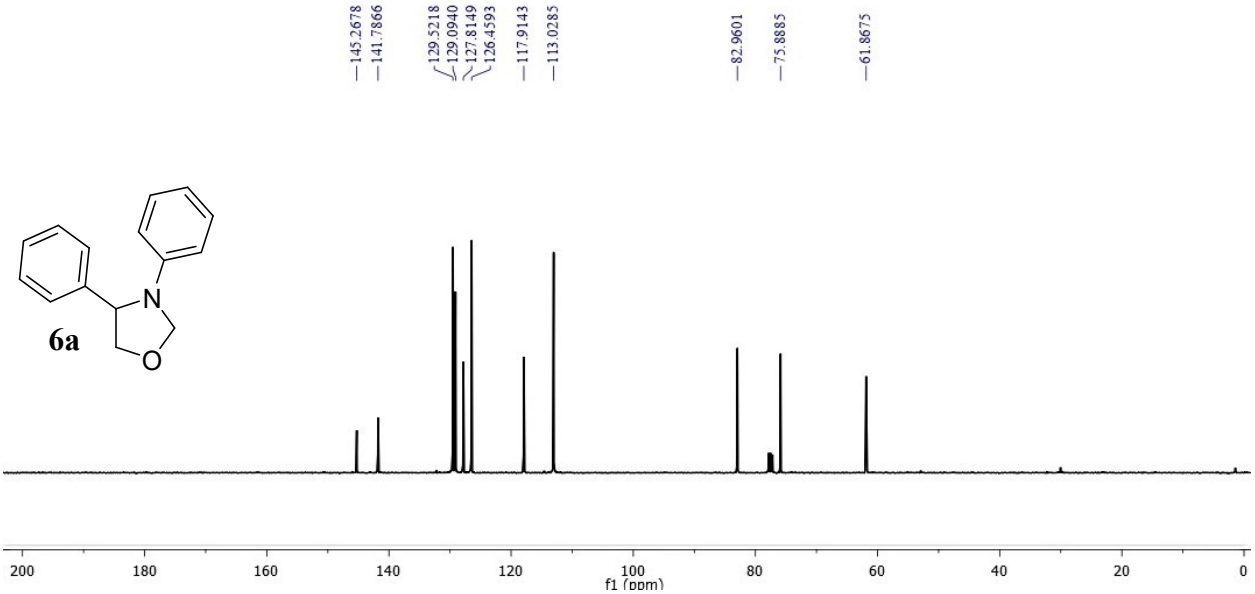

Figure S53. ^{13}C{^{1}H} NMR of **6a** (100 MHz, $CDCl_3$)

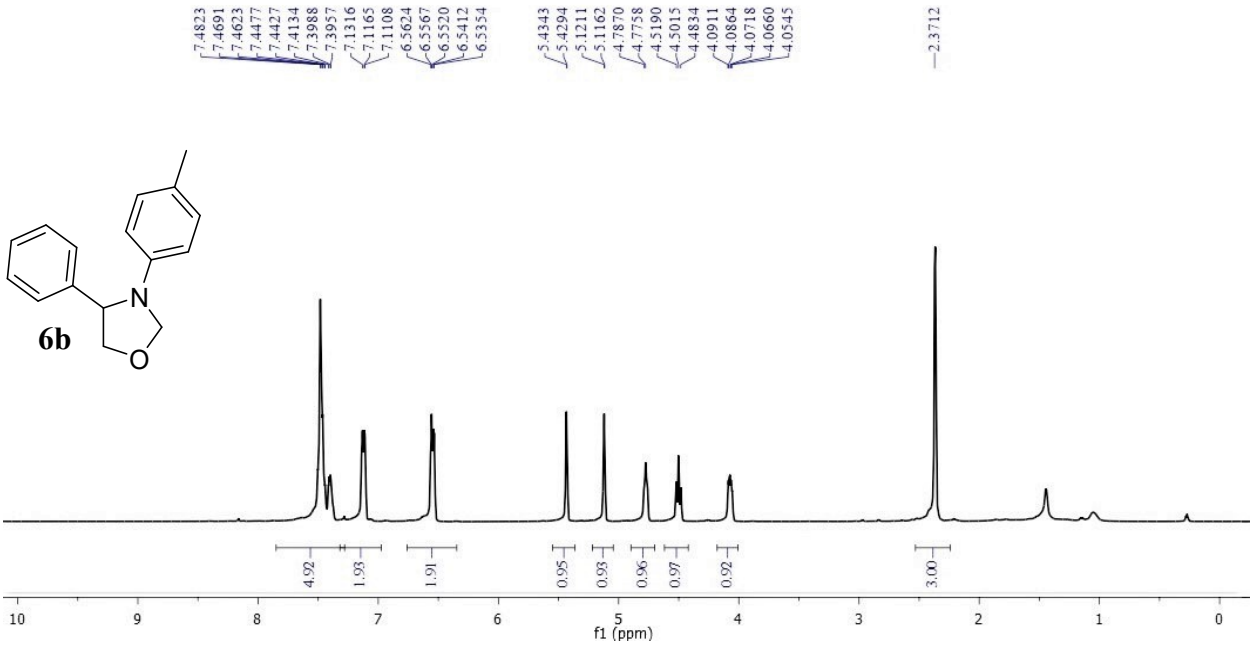

Figure S54. ^{1}H NMR of **6b** (400 MHz, $CDCl_3$)

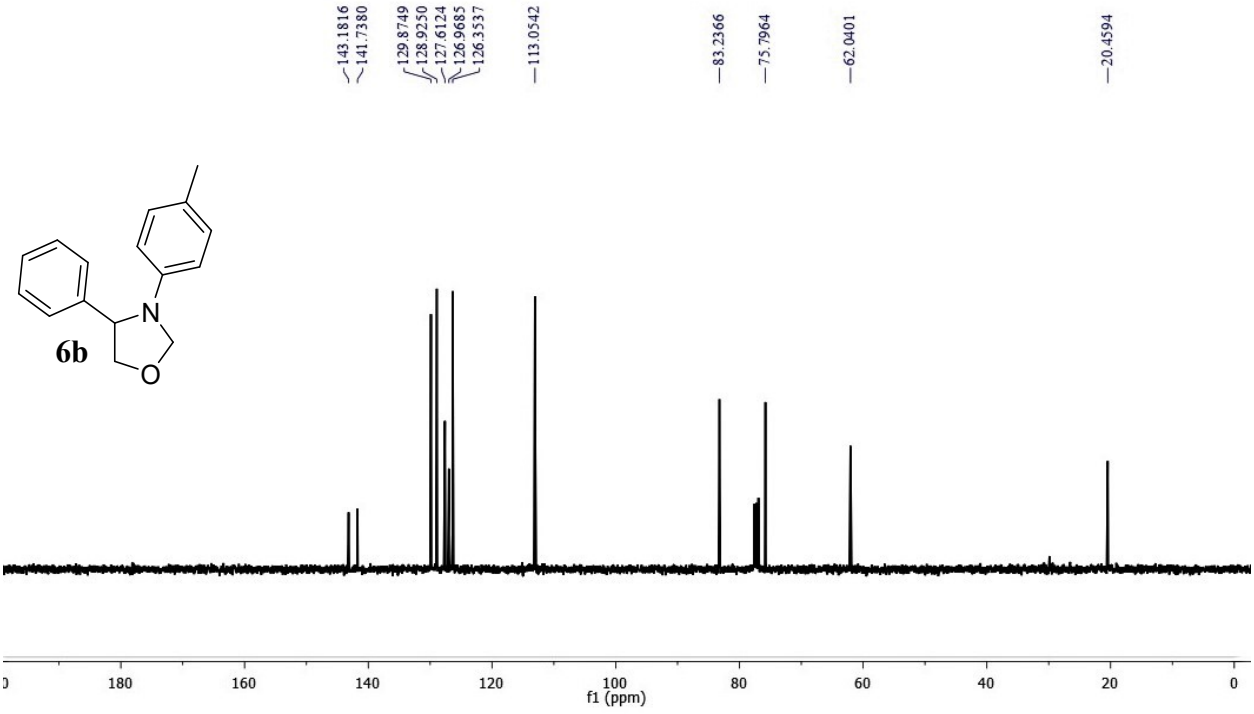

Figure S55. $^{13}C\{^{1}H\}$ NMR of **6b** (100 MHz, $CDCl_3$)

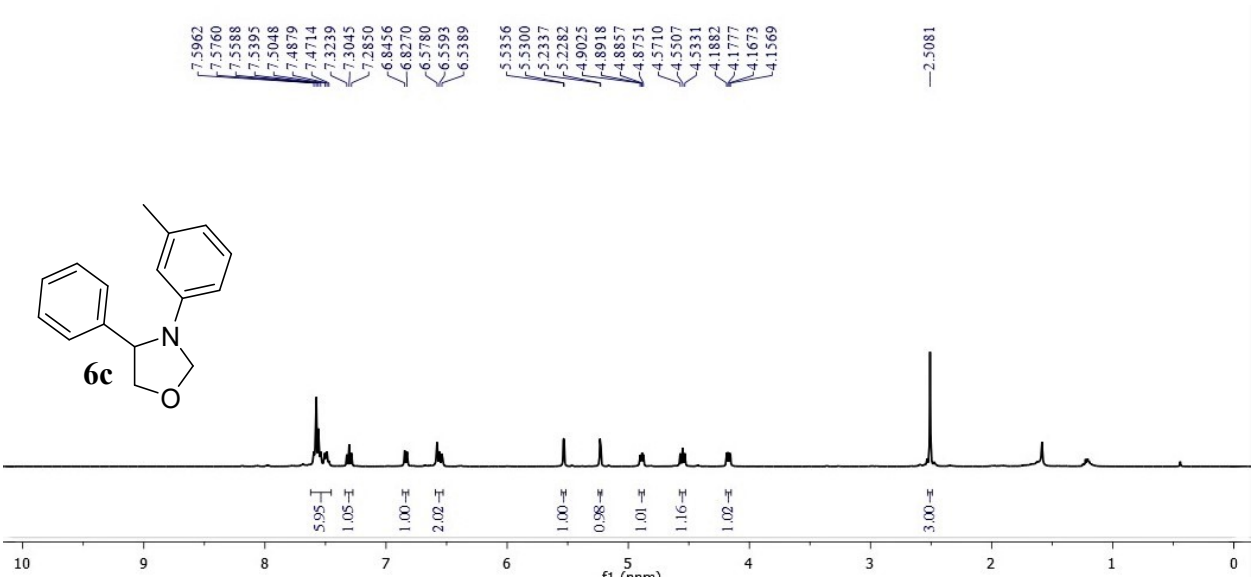

Figure S56. ^{1}H NMR of **6c** (400 MHz, $CDCl_3$)

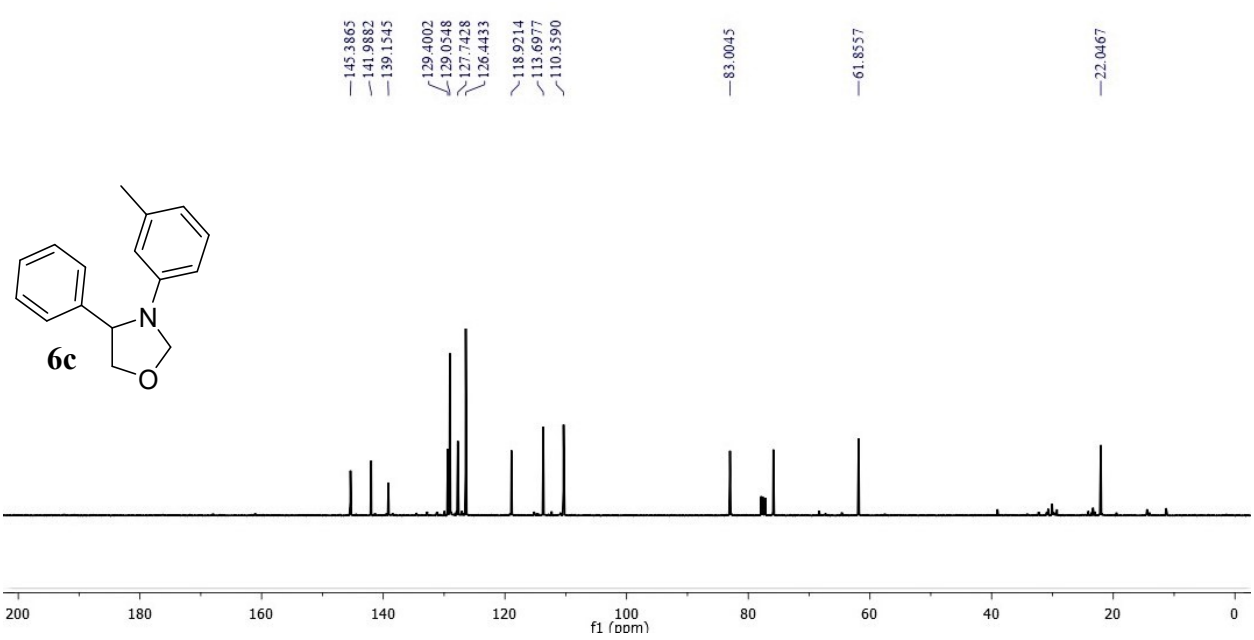

Figure S57. $^{13}C\{^{1}H\}$ NMR of **6c** (100 MHz, $CDCl_3$)

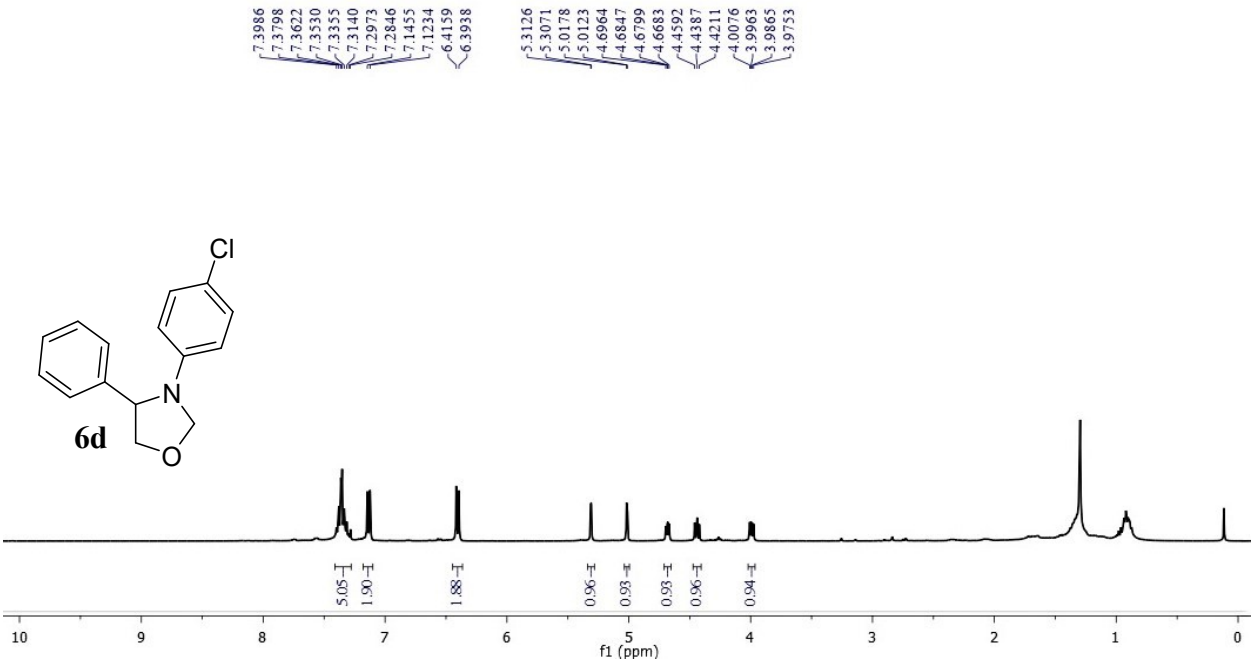

Figure S58. ^{1}H NMR of **6d** (400 MHz, $CDCl_3$)

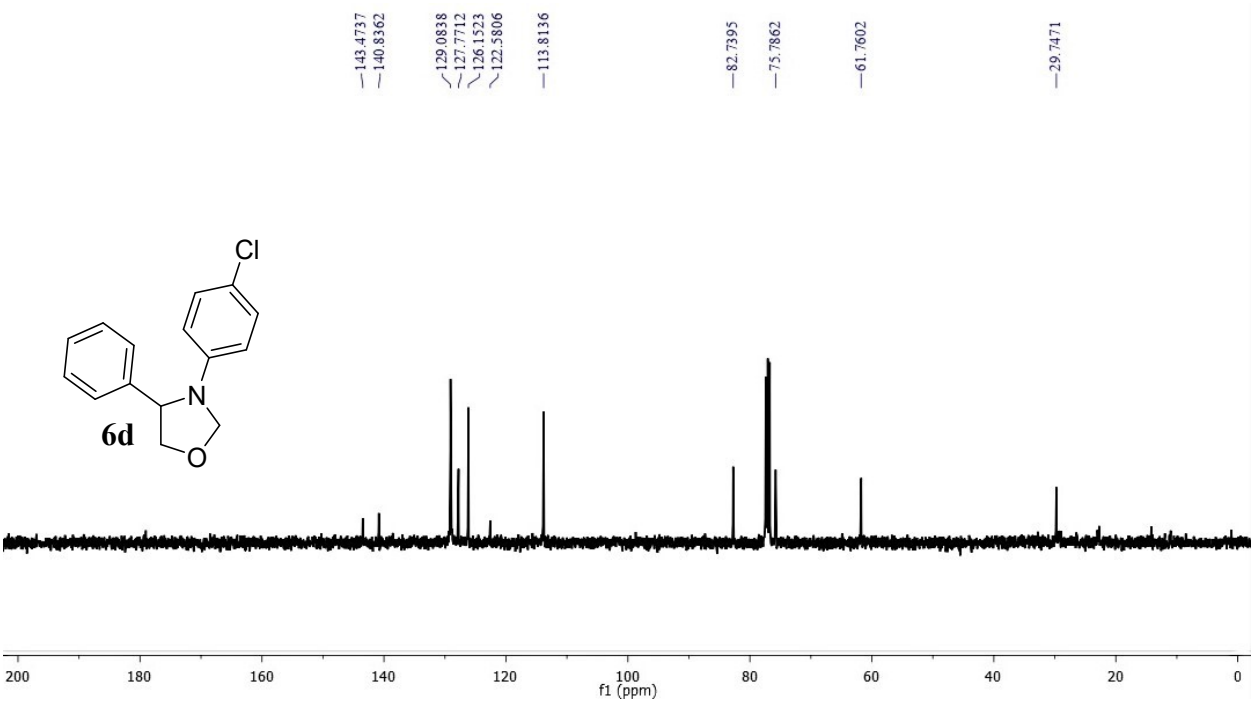

Figure S59. $^{13}C\{^{1}H\}$ NMR of **6d** (100 MHz, $CDCl_3$)

22. Single Crystal Data of 2j:

Compound reference	**2j**
Chemical formula	$C_{22}H_{20}Cl_2N_2O_2S$
Chemical formula weight	447.36
Crystal system	Monoclinic
a/Å	23.213(5)
b/Å	6.0771(2)
c/Å	30.525(6)
α/°	90
β/°	151.09(5)
γ/°	90
Unit cell volume/Å^3	2082.0(18)
Temperature/K	293(2)
Space group	*P*21/c
No. of formula units per unit cell, *Z*	4
No. Of independent reflections	6932
No. of reflections measured	3163
Cell measurement theta min	70.74
Cell measurement theta max	3.906
R_{int}	0.0499
Final R_1 values ($I > 2\sigma(I)$)	0.0585
Final $wR(F^2)$ values ($I > 2\sigma(I)$)	0.1673
Final R_1 values (all data)	0.0690
Final $wR(F^2)$ values (all data)	0.1886
Goodness of fit on F^2	1.039
CCDC depository number	2153616

23. References:

(1) Sengoden, M.; Bhowmick, A.; Punniyamurthy, T. Stereospecific Copper-Catalyzed Domino Ring Opening and Sp3 C−H Functionalization of Activated Aziridines with N-Alkylanilines. *Org. Lett.* **2017**, *19*, 158–161.

(2) Vijay, M.; Kumar, S. V.; Satheesh, V.; Ananthappan, P.; Srivastava, H. K.; Ellairaja, S.; Vasantha, V. S.; Punniyamurthy, T. Stereospecific Assembly of Fused Imidazolidines via Tandem Ring Opening/Oxidative Amination of Aziridines with Cyclic Secondary Amines Using Photoredox Catalysis. *Org. Lett.* **2019**, *21*, 7649–7654.

(3) Satheesh, V.; Vivek Kumar, S.; Punniyamurthy, T. Expedient Stereospecific Co-Catalyzed Tandem C-N and C-O Bond Formation of: N -Methylanilines with Styrene Oxides. *Chem. Commun.* **2018**, *54*, 11813–11816.

(4) Fujisue, C.; Kadoya, T.; Higashino, T.; Sato, R.; Kawamoto, T.; Mori, T. Air-Stable Ambipolar Organic Transistors Based on Charge-Transfer Complexes Containing Dibenzopyrrolopyrrole. *RSC Adv.* **2016**, *6*, 53345–53350.

(5) Tang, M. L.; Reichardt, A. D.; Wei, P.; Bao, Z. Correlating Carrier Type with Frontier Molecular Orbital Functionalized Acene Derivatives. *J. Am. Chem. Soc.* **2009**, *131*, 5264–5273.

(6) Wang, W.; Zhao, N.; Geng, Y.; Cui, S.; Hauser, J.; Decurtins, S.; Liu, S.-X. A Highly Sensitive TTF-Functionalised Probe for the Determination of Physiological Thiols and Its Application in Tumor Cells. *RSC Adv.* **2014**, *4*, 32639–32642.

(7) Paul, S.; Samanta, A. N-Bromosuccinimide as Bromide Precursor for Direct Synthesis of Stable and Highly Luminescent Green-Emitting Perovskite Nanocrystals. *ACS Energy Lett.* **2020**, *5*, 64–69.

(8) Pradhan, S.; Bhujel, D.; Gurung, B.; Sharma, D.; Basel, S.; Rasaily, S.; Thapa, S.; Borthakur, S.; Ling, W. L.; Saikia, L.; et al. Stable Lead-Halide Perovskite Quantum Dots as Efficient Visible Light Photocatalysts for Organic Transformations. *Nanoscale Adv.* **2021**, *3*, 1464–1472.

(9) Luiz, F. C. L.; Garcia, L. S. Fluorescence Studies of Gold (III) -Norfloxacin Complexes

in Aqueous Solutions. *J Fluoresc* **2011**, *21*, 1933–1940.

(10) Hayyan, M.; Hashim, M. A.; Alnashef, I. M. Superoxide Ion: Generation and Chemical Implications. *Chem. Rev.* **2016**, *116*, 3029–3085.

(11) Zhang, Y.; Zhang, N.; Tang, Z. R.; Xu, Y. J. Transforming CdS into an Efficient Visible Light Photocatalyst for Selective Oxidation of Saturated Primary C-H Bonds under Ambient Conditions. *Chem. Sci.* **2012**, *3*, 2812–2822.

(12) Huang, W.; Ma, B. C.; Lu, H.; Li, R.; Wang, L.; Landfester, K.; Zhang, K. A. I. Visible-Light-Promoted Selective Oxidation of Alcohols Using a Covalent Triazine Framework. *ACS Catal.* **2017**, *7*, 5438–5442.

(13) Ding, X.; Zhao, K.; Zhang, L. Enhanced Photocatalytic Removal of Sodium Pentachlorophenate with Self-Doped Bi2WO6 under Visible Light by Generating More Superoxide Ions. *Environ. Sci. Technol.* **2014**, *48*, 5823–5831.

(14) Fónagy, O.; Szabó-Bárdos, E.; Horváth, O. 1,4-Benzoquinone and 1,4-Hydroquinone Based Determination of Electron and Superoxide Radical Formed in Heterogeneous Photocatalytic Systems. *J. Photochem. Photobiol. A Chem.* **2021**, *407*, 113057.

(15) Zhang, M.; Li, Z.; Xin, X.; Zhang, J.; Feng, Y.; Lv, H. Selective Valorization of 5-Hydroxymethylfurfural to 2,5- Diformylfuran Using Atmospheric O2 and MAPbBr3 Perovskite under Visible Light. *ACS Catal.* **2020**, *10*, 14793–14800.

(16) Zhao, Y.; Truhlar, D. G. The M06 Suite of Density Functionals for Main Group Thermochemistry, Thermochemical Kinetics, Noncovalent Interactions, Excited States, and Transition Elements: Two New Functionals and Systematic Testing of Four M06-Class Functionals and 12 Other Function. *Theor. Chem. Acc.* **2008**, *120*, 215–241.

(17) Zhao, Y.; Truhlar, D. G. The M06 Suite of Density Functionals for Main Group Thermochemistry, Thermochemical Kinetics, Noncovalent Interactions, Excited States, and Transition Elements: Two New Functionals and Systematic Testing of Four M06-Class Functionals and 12 Other Function. *Theor. Chem. Acc.* **2008**, *120*, 215–241

(18) Hatchard, C. G.; Parker, C. A. A New Sensitive Chemical Actinometer - II. Potassium Ferrioxalate as a Standard Chemical Actinometer. *Proc. R. Soc. London. Ser. A. Math. Phys. Sci.* **1956**, *235*, 518–536.

(19) Cismesia, M. A.; Yoon, T. P. Characterizing Chain Processes in Visible Light Photoredox Catalysis. *Chem. Sci.* **2015**, *6*, 5426–5434.

(20) Rabani, J.; Mamane, H.; Pousty, D.; Bolton, J. R. Practical Chemical Actinometry—A Review. *Photochem. Photobiol.* **2021**, *97* (5), 873–902.

(21) Rai, P.; Maji, K.; Maji, B. Photoredox/Cobalt Dual Catalysis for Visible-Light-Mediated Alkene-Alkyne Coupling. *Org. Lett.* **2019**, *21*, 3755–3759.